BIO-FUNCTIONALIZED PEG-MALEIMIDE HYDROGEL FOR VASCULARIZATION OF TRANSPLANTED PANCREATIC ISLETS

A Dissertation
Presented to
The Academic Faculty

by

Edward A. Phelps

In Partial Fulfillment
of the Requirements for the Degree
Doctor of Philosophy in Bioengineering in the
Woodruff School of Mechanical Engineering

Georgia Institute of Technology
December 2011

BIO-FUNCTIONALIZED PEG-MALEIMIDE HYDROGEL FOR VASCULARIZATION OF TRANSPLANTED PANCREATIC ISLETS

Approved by:

Dr. Andrés García, Advisor
School of Mechanical Engineering
Georgia Institute of Technology

Dr. Athanassios Sambanis
School of Chemical & Biomolecular
Engineering
Georgia Institute of Technology

Dr. Niren Murthy
School of Biomedical Engineering
Georgia Institute of Technology

Dr. W. Robert Taylor
Division of Cardiology
Emory University

Dr. Johnna Temenoff
School of Biomedical Engineering
Georgia Institute of Technology

Dr. Peter Thulé
Division of Endocrinology &
Metabolism
Emory University

Date Approved: Oct. 31, 2011

To my family, for their love and support

ACKNOWLEDGEMENTS

The support of colleagues, collaborators, friends, and family has been essential to the completion of this dissertation. But as all things go in science, the work is never completed, new findings always lead to more questions and I feel honored to pass the torch of this body of work on to new students who will build on what we have learned.

I would like to start by thanking my faculty advisor Andrés García. Andrés's support, friendship, and unwavering enthusiasm have kept me marching forward despite days of failed experiments and negative results. Andrés has been a great listener, a tireless motivator, and, above all else, a fountain of knowledgeable ways to fix my screw ups. There will always be a tube of silicon vacuum grease in my desk drawer for emergency repairs. Andrés, thank you for your sincere encouragement, belief in my abilities, and reminding me to enjoy myself! You are the best advisor any Ph.D. student could ever wish for.

Thank you to the members of my thesis committee for their personal support, professional dedication, and scientific enthusiasm for this project. Peter Thulé who provided the medical expertise on diabetes and developed the transplantation procedure, I will never forget our long days spent doing rat surgeries. W. R. Taylor who enlightened me to the mysteries and difficulties of therapeutic vascularization, provided critical expertise for all of my *in vivo* work, and constantly came up with new and awesome ways to use our materials. Niren Murthy who guided me in developing the engineered hydrogels and helped me to turn the corner at a difficult stage in our efforts. Thanks to Johnna Temenoff for always being there to play ideas back and forth and insights into hydrogel technologies and biomaterials. And thanks to Athanassios Sambanis for his valuable expertise in tissue engineering, islet physiology, transplantation, and diabetes models.

I would also like to especially thank Laura O'Farrell, our veterinarian, for consultation on countless protocols and procedures, her knowledge and compassion for research has been tremendously important. Marc Levenston my undergraduate research advisor, and John Connelly my graduate student mentor, I thank for taking in a naïve college kid and shaping me into an able researcher.

To the members of the Garcia Lab, past and present: Charlie Gersbach, my undergraduate TA, was my inspiration to join the world of research. Kellie Templeman, who gave my rats CPR, can wave a magic wand to make shipments of HBSS appear in 30 seconds, and crack jokes about Old Gregg, I relied heavily on her professionalism, sense of humor, and friendship. Thanks to Jenn Phillips and Kristen Michael for being models of success and excellence for me to aspire to. Tim Petrie, AKA Dr. Fantastic, I am in awe of his powers of chaos, destruction, and sheer genius. He took me under his wing, showed me the ropes in the lab, and made sure I understood how to properly enjoy conferences in Amsterdam and midnight western-blotting alike. Thanks to Abbey Wojtowicz, a good mentor and my inspiration to save all of my great results as "Cover of Nature.jpg". Sean Coyer, my City Chase Urban Adventure National Championship race buddy, is the only man with whom I will ever go skydiving, wrestle a gator, stand on a street corner covered in body paint, or get chased by homeless zombies. Thanks to Dave Dumbauld, an example of the importance for attending to details, doing things the right way, and who taught me the secret code to mislabeling solution bottles to make Dr. Fantastic afraid to steal them. Ted Lee, a man who can deplete grant funds on sexy equipment faster than he drives through his parking deck, taught me that if I can't afford the best one I don't want it. Nduka Enemchukwu and Rachel Whitmire who joined the lab at the same time as me, we have been through every stumble and hurdle together. Thanks Rachel for sympathizing with my latest complaints over morning coffee. Nduka, who has the biggest heart of any person I've ever met, I admire his compassion and patience for people. Asha Shekaran, who packs the more talent per inch in everything she

endeavors from conditional genetic knockouts, to shotgun shooting, to billiards, she is definitely on the zombie apocalypse squad. Thanks to my undergraduate student Ricky Rath, for teaching me how to be a mentor and being my guinea pig! Special thanks to Jay Sy, Vince Fiore, Joel Boerckel, and Natalia Landazuri for awesome research collaborations. Thanks to all the other Garcia Lab members: Ram Selvam, Ankur Singh, Imen Hannachi, Susan Lehman, Amy Cheng, Apoorva Kalasuramath, Stacie Gutowski and other IBB community members who have made this experience so special and who continue to ensure the Lair of Inefficiency never becomes the Lair of Insufficiency.

My path to taking on a Ph.D. dissertation was anything but an accident. I was guided and shaped and encouraged by my loving and wonderful family and I thank them for everything they have done. I want to thank my grandfather, Pharo Phelps, the first member of my family to earn a doctorate, and whose encouragement, teaching, and love was instrumental in starting me on this path. I feel so lucky to have spent the time together that we did and I wish that he could be here to celebrate this moment. My mother who packed my lunches, washed my clothes, read me books, made sure I did my homework, and made me play outside. She gave me a wonderful childhood and her continued love and support are so important to me. My father who taught me to love the outdoors and always encouraged my interests in engineering and science. My brother Michael, who's partnered with me in all my outdoor adventures, I couldn't imagine going through this process without him to blow off some steam with on the weekends. Thanks to Grandma Nancy and Grandpa Don whose timely shipments of baked treats and holiday greeting cards always made exam times a little less painful. Uncle John for his guidance on how to best invest my grad student living stipend and helping me with my job search. Aunt Rachel for being an all around awesome aunt and inspiring me with your entrepreneurship capabilities. Grandma Lois for encouraging my love of reading and cooking from an early age. Aunt Jenny and Uncle Frank for fostering my interests in medicine and doing something to make a difference for other people.

TABLE OF CONTENTS

LIST OF FIGURES

Page

LIST OF SYMBOLS AND ABBREVIATIONS

AFM	atomic force microscopy
A-PEG-GPQ-PEG-A	MMP-degradable PEG-DA macromer
A-PEG-RGD	PEG-acrylate functionalized RGD adhesive ligand
A-PEG-VEGF	PEG-acrylate functionalized VEGF
BMP-2	bone morphogenetic protein-2
CAM	chorioallantoic membrane
DMEM	dulbecco's modified eagle medium
DTT	dithiothreitol
ECM	extracellular matrix
EDTA	ethylenediaminetetraacetic acid
ELISA	enzyme-linked immunosorbent assay
EPC	endothelial progenitor cells
FBS	fetal bovine serum
FGF	fibroblast growth factor
FITC-PEG-MAL	linear fluorescein labeled PEG-maleimide
G-CSF	granulocyte colony stimulating factor

GFP	green fluorescent protein
GPQ	peptide sequence GPQGIWGQK
H&E	hematoxylin and eosin
HEPES	(4-(2-hydroxyethyl)-1-piperazineethanesulfonic acid)
hEST	human embryonic stem cells
HGF	hepatocyte growth factor
HIF-1	hypoxia-inducible factor 1
HIF-1	hypoxia-inducible factor-1
HUVEC	human umbilical vein endothelial cells
IBMIR	instant blood-mediated inflammatory reaction
ICG	indocyanine green dye
ICG-VEGF	ICG-labeled VEGF
IEQ	islet equivalents
IP	intraperitoneal
IV	intravenous
LDPI	laser doppler perfusion imaging
MCP-1	monocyte chemoattractant protein-1
MEF	mouse embryonic fibroblasts

MMP	matrix metalloproteinase
MSC	mesenchymal stem cells
MTS	(3-(4,5-dimethylthiazol-2-yl)-5-(3-carboxymethoxyphenyl)-2-(4-sulfophenyl)-2H-tetrazolium
NO	nitric oxide
PBS	phosphate buffered saline
PCL	poly-caprolactone
PDGF	platelet-derived growth factor
PEG	polyethylene glycol
PEG-4A	4-arm PEG-acrylate
PEG-4MAL	4-arm PEG-maleimide
PEG-4VS	4-arm PEG-vinyl sulfone
PEG-DA	linear PEG-diacrylate
PGC-1α	peroxisome-proliferator-activated receptor-γ coactivator-1α
Q_m	equilibrium mass swelling ratio
RGD	peptide sequence GRGDSPC
ROI	region of interest
SDS-PAGE	sodium dodecyl sulfate polyacrylamide gel electrophoresis

STZ streptozotocin

T1DM Type 1 diabetes mellitus

TEA triethanolamine

VEGF vascular endothelial growth factor A

VEGF-750 alexa-fluor 750 labeled VEGF

VPM peptide sequence GCRDVPMSMRGGDRCG

SUMMARY

Type 1 diabetes affects one in every 400-600 children and adolescents in the US. Standard therapy with exogenous insulin is burdensome, associated with a significant risk of dangerous hypoglycemia, and only partially efficacious in preventing the long term complications of diabetes. Pancreatic islet transplantation has emerged as a promising therapy for type 1 diabetes. However, this cell-based therapy is significantly limited by inadequate islet supply (more than one donor pancreas is needed per recipient), instant blood-mediated inflammatory reaction, and loss of islet viability/function during isolation and following implantation. In particular, inadequate revascularization of transplanted islets results in reduced islet viability, function, and engraftment. Delivery of pro-vascularization factors has been shown to improve vascularization and islet function, but these strategies are hindered by insufficient and/or complex release pharmacokinetics and inadequate delivery matrices as well as technical and safety considerations. We hypothesized that controlled presentation of angiogenic cues within a bioartificial matrix could enhance the vascularization, viability, and function of transplanted islets. The primary objective of this dissertation was to enhance allogenic islet engraftment, survival and function by utilizing synthetic hydrogels as engineered delivery matrices. Polyethylene glycol (PEG)-maleimide hydrogels presenting cell adhesive motifs and vascular endothelial growth factor (VEGF) were designed to support islet activities and promote vascularization in vivo. We analyzed the material properties and cytocompatibility of these engineered materials, islet engraftment in an allo-transplantation model, and glycemic control in diabetic subjects. The rationale for this project is to establish novel biomaterial strategies for islet delivery that support islet viability and function via the induction of local vascularization.

CHAPTER 1

SPECIFIC AIMS

Pancreatic islet transplantation has emerged as a promising strategy for the treatment of Type 1 diabetes. However, cell-based transplantation therapies are limited by inadequate blood supply and loss of viability/function following implantation resulting in incomplete or transient regeneration. Additionally, the scarce availability of islet donors significantly limits this potential therapy where two or more donors are required for each recipient due to low levels of engraftment and viability.

The objective of this project is to enhance allogenic islet engraftment, survival, and function through the use of engineered synthetic hydrogels that present cell adhesive cues and angiogenic factors. My hypothesis is that pancreatic islets encapsulated in vascular-inductive matrices will exhibit improved viability and endocrine function compared to non-encapsulated pancreatic islets or islets transplanted in non-vascularizing matrices. Additionally, we hypothesize that improved islet vascularization and viability will translate to improved glycemic control in diabetic animal recipients. The objective will be accomplished through completion of the following aims:

1: Engineering of bio-functionalized PEG-maleimide hydrogel to support pancreatic islet encapsulation

We have succeeded in producing protease-degradable PEG hydrogels presenting cell-adhesive domains and angiogenic growth factors using a novel crosslinking moiety. We show that these maleimide cross-linked gels exhibit improved crosslinking and cyto-compatibility characteristics compared to several types of previously published PEG hydrogels. These materials promote encapsulated islet survival and endocrine function in vitro as measured by insulin production, Live/Dead staining, and metabolic

1

measurements. In addition, encapsulated islets respond to gels with tethered growth factor and adhesive ligands by extending endothelial cells sprouts into the surrounding matrix.

2: In vivo vascularization potential of engineered PEG-maleimide hydrogel and islet grafting in healthy rats

We hypothesized that engineered constructs exhibiting protease degradable sites, cell adhesion ligands, and vascular-inductive growth factors will become highly vascularized. Our objective was to connect encapsulated pancreatic islets with invading vasculature to enhance islet transplant engraftment and function. In our assessment of islet engraftment and vascularization through histology/immunohistochemistry as well as microCT imaging and quantitative analysis of implant vasculature we observed that degradable hydrogels incorporating bioactive ligands and growth factors resulted in improved islet survival and re-vascularization of the intra-islet capillary bed over non-vascularizing hydrogels or islets transplanted in control alginate gels.

3: Transplantation of hydrogel-encapsulated pancreatic islets in a rat model of type-1 diabetes

We hypothesized that enhanced islet vascularization and survival from engineered hydrogels would translate into improved glycemic control and a possible return to normoglycemia in STZ-induced diabetic rats over islets transplanted alone or through the hepatic portal system. We monitored diabetic rats receiving islet transplants for weight gain/loss, blood glucose, circulating insulin levels, and response to a glucose bolus challenge in multiple trials. We observed moderately significant changes in weight gain, fasting blood glucose levels, and response to a glucose challenge.

Project Significance

      The research completed for this thesis is highly innovative because it developed a fully synthetic bioactive material that can be precisely tailored for controlled, on-demand release of angiogenic factors. This approach is entirely different from other hydrogel encapsulation or cell-delivery vehicles that attempt to achieve immuno-isolation or rely on poorly controlled growth factor release. The novel innovation strategy of the completed work lies in both the on-demand availability of the growth factor that is only released as the matrix degrades, the tailorability of the individual bioactive components, and a novel crosslinking reaction that occurs rapidly enough for *in vivo* delivery while maintaining an mild non-toxic environment for incorporation of encapsulated islet cells.
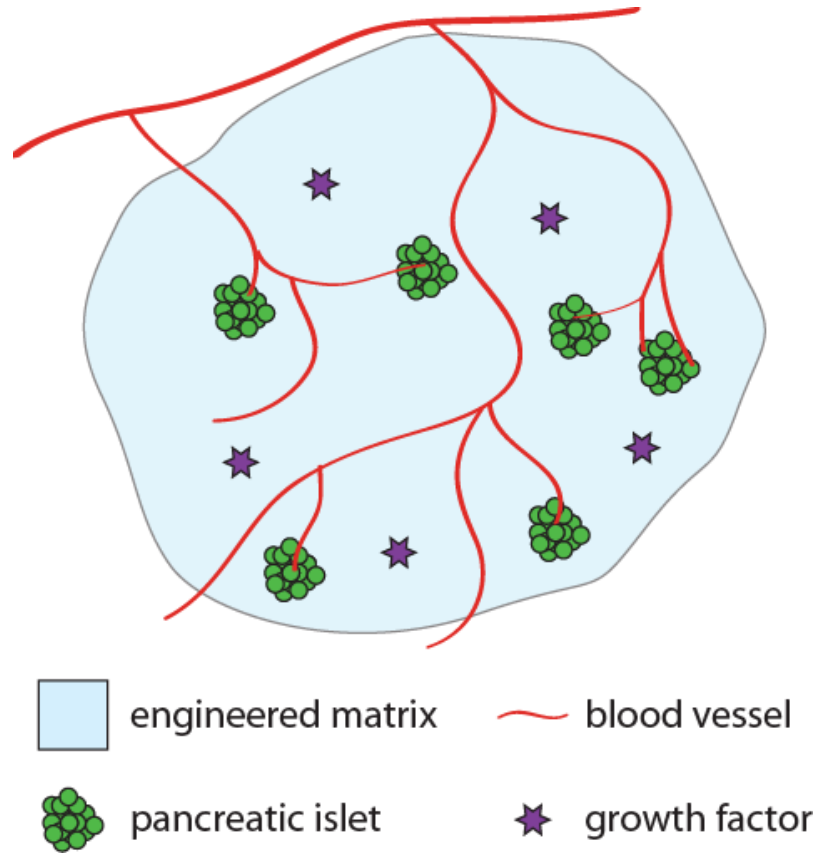
Figure 1.1 Engineered matrix for re-vascularization of transplanted islets concept illustrating blood vessels growing into a delivery matrix, attracted by growth factors, and providing nutrients and oxygen to encapsulated islets.

CHAPTER 2

LITERATURE REVIEW [*]

Vascularization in regenerative medicine

Introduction

The ability to exploit angiogenesis and vascularization as a therapeutic strategy will be of enormous benefit to a wide range of medical and tissue engineering applications. Angiogenic growth factor and cell-based therapies have thus far failed to produce a robust healing response in clinical trials for a variety of ischemic diseases, while engineered tissue substitutes are size-limited by a lack of vascularization. Recent advances focus on better regulation of growth factor delivery and attempts to better mimic natural processes by delivering combinations of multiple growth factors, cells, and bioactive materials in the right spatial and temporal setting. A number of disease states are related to reduced vascular perfusion and could be treated with pro-vascularization strategies. Peripheral vascular disease, ischemic heart disease, wound healing, and cell and tissue transplantation are just a few examples that would greatly benefit from pro-angiogenic therapies. Aging patients also suffer from slower healing responses, especially after surgery and during fracture repair [1]. Pro-angiogenic therapy is likely to improve the healing response of elderly patients in many situations. While research in the field of tissue engineering has been active for several decades, there are still relatively

---

[*] adapted from:

Phelps, E.A., and Garcia, A.J. Update on therapeutic vascularization strategies, Regen. Med. 2009 4(1):65-80

Phelps, E.A., and Garcia, A.J. Engineering more than a cell: vascularization strategies in tissue engineering. Curr. Opin. Biotechnol. 2010 21(5):705-9

few effective clinical implementations of tissue engineering technology. Clinical use of engineered tissues and tissue substitutes is largely limited to avascular or thin tissue types such as cartilage, bladder, and skin. Great progress has been attained in the development of a variety of engineered tissue types that function on a small scale *in vitro*, but these ultimately suffer from a lack of vascular perfusion when scaled up to a size relevant for implantation and disease treatment. Researchers have been working hard to overcome this limitation and are developing a number of innovative strategies for vascularizing engineered tissues.

Human trials in therapeutic vascularization have had limited success to date despite promising results in animals with experimentally induced ischemia [2]. Most therapeutic clinical trials have focused on delivery of a single gene or growth factor, commonly various isoforms of vascular endothelial growth factor (VEGF) or fibroblast growth factor (FGF), as discussed in detail in several review articles [3-7]. Cell transplantation therapy has also been tested clinically to treat myocardial and peripheral ischemia with promising results, reviewed in [5, 7-10]. The FDA has designated the primary endpoint for approval of a post-myocardial infarction angiogenic agent as an improvement in exercise performance. Several clinical trials have shown angiogenic therapy to alleviate certain secondary symptoms such as chest pain, but failed to show a significant difference in exercise performance. Part of the reason for this lack of enhanced performance is a strong placebo effect in control groups and difficulty in selecting an ideal patient cohort [11]. However, the results of Phase I and II trials also indicate that pro-angiogenic gene and protein therapy is generally safe and feasible. Critics have expressed a number of concerns for pro-angiogenic therapy including the potential for triggering growth of latent tumors, increasing the risk for retinopathy, and promotion or destabilization of atherosclerotic plaques. In studies to date, none of these potential issues has been noted to be above baseline for the study population. Some less serious side effects associated with administration of VEGF and FGF-2 include

hypotension, vascular leakage, transient tissue edema, and renal insufficiency. Clinicians continue to express optimism for the future of pro-angiogenic therapy and a number of promising new strategies are currently under investigation. At present, a large focus of clinical and preclinical studies is focused on identifying the ideal angiogenic agent (or combination therapy), delivery strategy, and dosing regimen.

Review of Angiogenesis Mechanisms

The formation of the vascular network is a finely tuned and complex process controlled by the signaling balance between integrins, angiopoietins, chemokines, junctional molecules, oxygen sensors, endogenous inhibitors, and many others [12]. Several excellent review articles give a detailed description of the mechanisms of angiogenesis [13-15]. There are three main mechanisms of new blood vessel growth in adults: sprouting angiogenesis, arteriogenesis, and vasculogenesis. Sprouting angiogenesis is the best understood and most common mechanism and involves the growth of new microvasculature and capillary beds, usually driven naturally in adults by hypoxia or wound healing but is also activated in the growth of tumors. Oxygen in tissue is monitored by hypoxia-inducible factor-1 (HIF-1), composing of alpha and beta subunits. The HIF-1β subunit is relatively stable while the HIF-1α subunit is targeted for rapid degradation by the oxygen sensitive von Hippel-Lindau pathway. At low oxygen levels HIF-1α degradation is impaired, leading to increased HIF-1 heterodimerization, DNA binding, and transcription of pro-angiogenic genes. HIF-independent pathways also exist. For example, peroxisome-proliferator-activated receptor-γ coactivator-1α (PGC-1α), a major regulator of mitochondrial function in response to exercise or low-nutrient environments, is able to exert strong control over the vascular endothelial growth factor gene and induce angiogenesis [16].

In sprouting angiogenesis, new blood vessels are formed by sprouting and migration from existing capillaries. A growth factor gradient initiates endothelial cell

activation. Migrating endothelial cells lead the growth of a new sprouting vessel by degrading the basement membrane and laying down a provisional extracellular matrix. Endothelial cells proliferate and form connections to neighboring vessels, develop lumens, and split existing vessels though a process known as intussusception, and remove extra branches in a process known as quiescence [17]. An intricate process of sprouting, branching, intussusception, and regression plays out to shape the ultimate pattern of a growing capillary plexus. Following tubule formation, newly formed vessels are sealed by formation of endothelial cell-cell junctions and stabilized by addition of mural cells or pericytes and smooth muscle cells. Sprouting vessels grow down gradients of VEGF and other factors, led by an endothelial tip cell, that is tuned to a variety of positive and negative signals coming from the surrounding matrix and other cells. The process of sprouting angiogenesis is illustrated in Figure 2.1. This process appears to be driven in a very similar way to neuron guidance, and many of the neural guidance proteins are being discovered to play pivotal roles in vascular morphogenesis [17-19]. The four major families of guidance proteins in neural and vascular sprouting are semaphorins, ephrins, slits, and netrins, along with their associated receptors. The regulation of neural and vascular guidance is a fascinating field of study, but is outside the focus of this review.
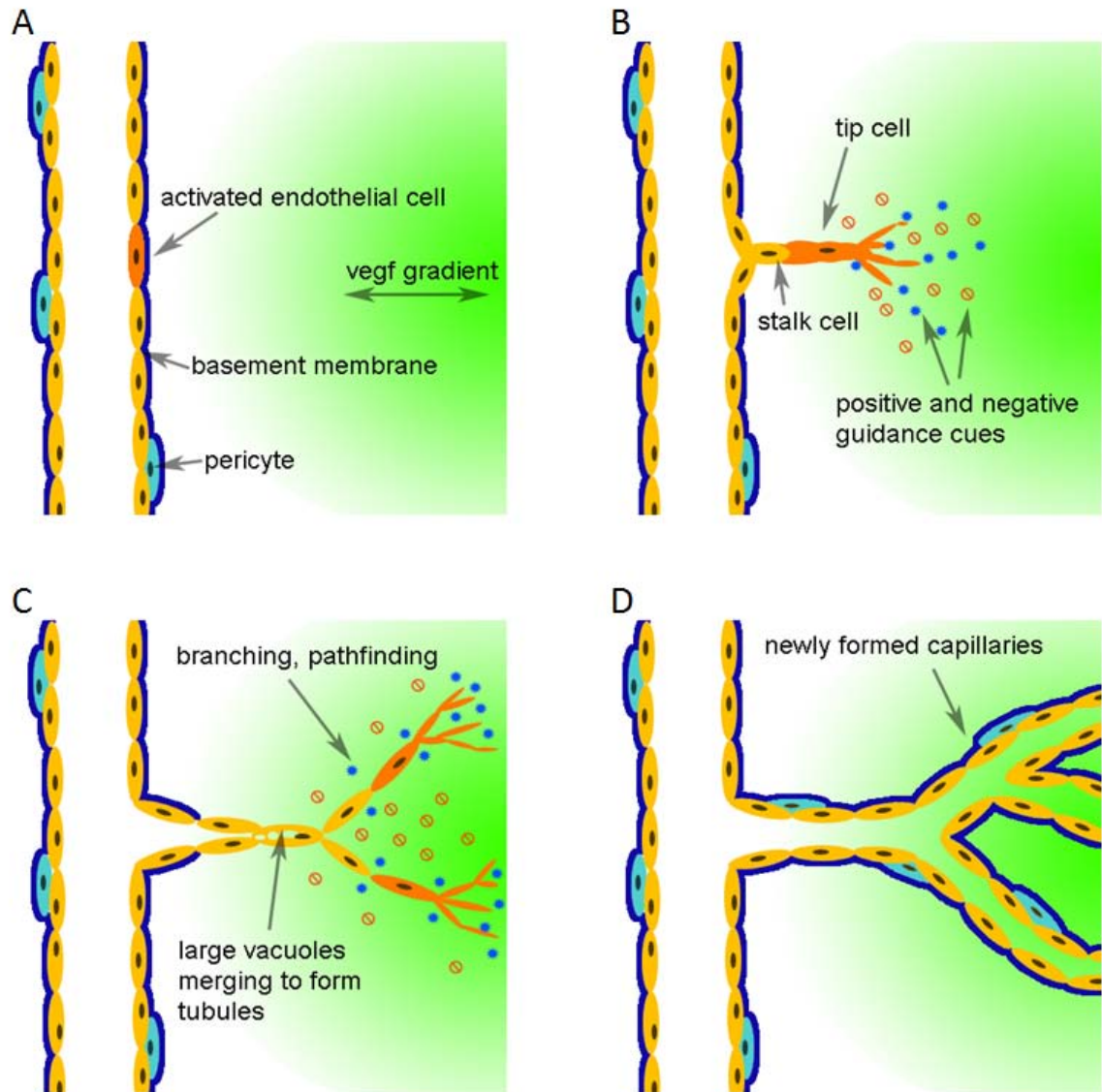
Figure 2.1 Mechanisms of sprouting angiogenesis. (A) Endothelial cell is activated in response to a growth factor gradient, tip cell is selected. (B) Tip cell degrades basement membrane and migrates down gradient, following positive and negative guidance cues in the matrix, stalk cells form behind leading tip cell. (C) Guidance cues control pathfinding and morphogenesis, large vacuoles form in stalk cells and merge to make tubules. (D) Recruitment of pericytes and deposition of basement memebrane stabilizes newly formed endothelial tubules.

The VEGF family of growth factors has been identified as critically important to angiogenesis and comprises several isoforms. VEGF-A (commonly referred to as simply VEGF) is a potent stimulator of endothelial cell mitogenesis, cell migration, vasodilation, and a mediator of microvascular permeability. Placental growth factor (PlGF), another potent VEGF isoform is capable of stimulating angiogenesis and collateral vessel growth while avoiding side effects common to VEGF such as edema and hypotension [20]. While being a strong vascular stimulator, VEGF signaling primarily serves to drive expansion of the capillary bed, and it appears that VEGF administered alone has limited ability to induce the growth of larger vessels. Long-duration exposure is necessary to produce stable microvasculature that does not resorb after withdrawal of the VEGF stimulus [21]. Because VEGF-driven angiogenesis does not consistently result in formation of functional, stable vasculature, VEGF therapy alone may not be the ideal treatment for increasing blood perfusion to an ischemic tissue [3, 22]. Administration of additional supporting growth factors such as FGF-2, angiopoeitins, PlGF, or PDGF [22] at the appropriate time point help to stabilize newly formed endothelial tubules by recruiting pericytes and smooth muscle cells, perhaps resulting in a more predictable therapeutic response.

In contrast to ischemia-induced angiogenesis, arteriogenesis usually occurs proximally to the ischemic tissue and is often linked to atherosclerosis when it occurs naturally in adults, although the specific mechanisms are less well understood. Mechanical stresses at the site of arterial stenosis activate endothelial cells [23], upregulating expression of the monocyte chemoattractant protein-1 (MCP-1), FGF, PDGF, VEGF, MMP, cell-adhesion molecules, and nitric oxide (NO). This mixture of factors promotes inflammatory and remodeling responses. MCP-1 attracts monocytes that enter the vessel wall and differentiate to macrophages, producing inflammatory cytokines such as TNF-α. Studies of hindlimb ischemia in animals indicate that arteriogenesis is more likely to occur by widening of existing vessels rather than

formation of new vessels [24], although this has not been confirmed for all situations. The process of arteriogenesis has the ability to increase blood flow to distal tissues 20-30 times [11], a much larger volume of flow than possible by microvascular expansion. A few large vessels are capable of delivering a much larger volume of blood than many small high-resistance capillaries according to the Poiseuille's law [25], and as such, therapeutic vascularization should aim to develop these larger collateral vessels. At the same time, capillary formation cannot be ignored as it is crucial to improving oxygenation and gas exchange at the cellular level in ischemic tissues [25], and it may prove true that stimulation of both capillaries and collateral vessels is required for the best healing response.

Vasculogenesis, once believed to only occur in the developing embryo, refers to the *de novo* generation of new vessels from the migration and differentiation of endothelial progenitor cells found in the bone marrow and in circulation. Vasculogenesis in adults has been an area of intense study and controversy in the recent literature with conflicting studies published as to the sourcing and contribution of progenitors in the growth of new vessels. Some evidence indicates that progenitor cells do not directly contribute to the endothelium and are located only perivascularly [26]. Nevertheless, a growing body of preclinical [27] and clinical trials [28, 29] indicates that transplantation of blood-derived or bone marrow-derived progenitor cells beneficially affects cardiac function after myocardial infarction as well as promotes neovascularization in ischemic tissue. An increasingly well-characterized cell population expressing CD34 as well as other markers and considered to include a hematopoietic cell population is known as endothelial progenitor cells or EPCs. These endothelial progenitors have the ability to home to sites of neovascularization and differentiate into endothelial cells [30].

Growth Factor Delivery

The early phase I and II human clinical trials with VEGF, FGF, and hepatocyte growth factor (HGF) were promising, but larger randomized placebo-controlled trials failed to show significant benefits in the approved end-points. One of the proposed problems associated with the limited success of early clinical trials is insufficient delivery or dosing of growth factors due to a short half life in the body. Bolus injection of soluble growth factor, either systemically or locally administered by one of the classical delivery methods including intra-arterial administration, systemic administration (intravenous), and direct intramuscular injection, results in a rapidly depleted, poorly controlled delivery with the resulting vascular growth often disorganized, poorly functional, and transient. New studies are aimed at developing a better understanding of the specific concentration ranges, gradients, and exposure duration to elicit a more controlled angiogenic response.

The dosage response of VEGF is highly sensitive: low doses result in increased vascular permeability and overdoses result in hemangioma formation [31] and fatal vascular leakage [31]. Most research shows that sustained stimulation with a high level of VEGF is required for formation of stable vasculature *in vivo [32]*, but optimal dosing schedules remain unproven [33]. Researchers are investigating ways to regulate the exposure time [34] and local delivery dosage of angiogenic growth factors as well as optimize safe and effective dosages for use in humans. In mice, VEGF dosages of 150 ng per day delivered by osmotic pump consistently induced high degrees of vascularization with vessels stable for at least 80 days after withdrawal of the growth factor [16]. Vessels induced by higher concentrations of VEGF resorbed within 20 days of growth factor withdrawal while lower concentrations of VEGF failed to induce a high degree of vascularization. Optimal dosing in human patients may be difficult to determine because physiologically relevant dosages can differ from animal models, and patients in need of angiogenic therapy may have an impaired angiogenic response due to various disease states and metabolic disorders whereas most animal models use healthy test subjects.

Besides dose response, scientists are also discerning the role of directionality and gradient in angiogenic signaling. A microcarrier-based angiogenic sprouting assay, an effective *in vitro* screening technique [35, 36], was recently used to examine the effects of VEGF gradient and concentration on endothelial sprouting [37]. Endothelial cells seeded on microcarriers sprouted tubules aligned with VEGF presented in a gradient, with maximal alignment occurring in a 0 to 100 ng/mL gradient. It was also seen that cells at the tip of the sprout bound significantly more VEGF then cells in the body of the sprout. At very high VEGF concentrations, binding was saturated and sprouting directionality was lost. This finding supports previous data that the tip cells of vascular sprouts aid in directionality and propagation of new microvessels down a growth factor gradient [38]. When translated *in vivo* to a hind limb ischemia model, scaffolds containing gradients of VEGF were better at restoring perfusion and avoiding necrosis than non-gradient controls. It is thought that forces such as interstitial flow contribute to the formation of natural growth factor gradients *in vivo* and have been investigated for directing vascular morphogenesis [39-41]. When considered in the context of vascular architecture, gradient formation makes sense to drive directionality of vessel growth. Naturally derived vascular beds have an organized hierarchical structure while tumor vasculature is randomly organized. Gradient delivery of growth factors may be a means of promoting better architecture in induced vascular beds.

While VEGF and FGF have received much attention in the literature, PlGF may prove worthwhile to study in greater detail. PlGF has been shown to be equally as potent as VEGF at promoting angiogenesis while also promoting arteriogenesis [42]. PlGF actually promotes increased expression of VEGF in ischemic tissue and its effects are increased when administered in synergy with VEGF [43]. Notably, PlGF may be a better candidate for arteriogenic therapy than FGF or PDGF which preferentially recruit either endothelial and mural cells or inflammatory cells, respectively, while PlGF can recruit all

three cells types on its own. All three cells types are cited as required for arteriogenesis [44].

In contrast to bolus growth factor deliver, it has shown that controlled growth factor release, given correct dosage and exposure time, is highly beneficial to inducing the growth of functional vasculature in animal models of ischemia [45, 46]. Stabilization and molecular regulation of nascent blood vessels is also critical to achieving a correct angiogenic response [47]. Uncontrolled delivery of FGF or VEGF usually results in unstable vessel growth that resembles immature tumor vasculature [48]. Tumor vessels are chaotic and do not follow the hierarchical branching pattern of normal vascular networks [14, 47]. Several novel approaches are under investigation to more precisely regulate the spatial temporal presentation of the right combination of factors to induce more appropriate vessel architecture and stability [49]. One such approach is the design of polymeric scaffolds that stagger exposure to two or more growth factors such as VEGF and PDGF [49, 50], FGF and HGF [51], or VEGF and angiopoietin-1 [52] to create more stable vessels with regular architecture by more closely mimicking the biological mechanism of vessel induction followed by stabilization. Many other stabilization and growth "on" and "off" signals exist, including activators and inhibitors of the Wnt and Notch pathways [53] and neural guidance cues (netrin, ephrin, etc). More research is needed in the area of branching morphogenesis [54] to solve the intricate programming structure of vascularization.

A different approach to single or multiple staggered growth factor delivery is to induce the expression of upstream activators of a large number of angiogenic regulators such as HIF-1α. Because HIF-1α is naturally degraded, a number of techniques have been employed to ensure its stabilization *in vivo*. Delivery of the gene for a physiologically stable HIF-1α/VP16 fusion protein has been shown to promote recovery of peripheral limb ischemia in animals [55, 56] and was recently tested in a phase I trial with a percentage of patients with peripheral limb ischemia showing pain resolution and

ulcer healing [57]. Another method for HIF-1α stabilization is expression of a mutant HIF-1α that lacks an oxygen degradation domain [58].

There are certain disadvantages to delivering recombinant proteins, included a short half-life *in vivo* and expense and difficulty in manufacturing. Scientists have investigated using gene therapy to deliver a more prolonged and targeted delivery of angiogenic growth factors. Both viral and nonviral vectors have been tested clinically for delivery of angiogenic factors, with results similar to those seen by delivering growth factors. Because of safety concerns with viral vectors, nonviral vectors are initially more attractive for human use. However nonviral vectors are generally less efficient at inducing expression. Novel gene therapy delivery mechanisms are focused on improving nonviral vector delivery. Electroporation has recently been used to deliver cDNA for HIF-1α to improve wound healing in elderly diabetic mice [59]. Other delivery mechanisms such as liposome complexes [60] are under investigation to improve delivery of nonviral vectors and have been tested preclinically for delivery of angiogenesis related genes. Delivery of VEGF activating transcription factors is also under investigation [61, 62]. The concept of engineered cell therapy has been proposed as a solution to problems with direct gene therapy and is briefly discussed further on in the next section.

Cell Therapy

Another approach to treating ischemic disease and promoting angiogenesis is the transplantation of autologous cells which has been studied in large animals [27, 63] and in clinical trials [28, 29]. Some of the cell sources under investigation include bone-marrow stromal cells, mesenchymal stem cells, and endothelial progenitor cells. A number of trials under development and currently ongoing will test the safety and efficacy of autologous cell transplantation in a variety of ischemic diseases. Some of the early cell transplantation trials used skeletal myoblasts and had mixed results at treating

ischemic heart disease [28, 64-66], this may be due to a reduced ability of myoblasts to promote neovascularization and re-perfusion. Transplantation of less-differentiated cell types such as marrow-derived stromal cells, vascular/endothelial progenitor cells, and mesenchymal stem cells, may lead to a stronger healing response. Transplantation of endothelial progenitor cells has shown success in treating peripheral limb ischemia by promoting collateral vessel formation in both humans and animals [67, 68], as well as treating myocardial ischemia [69, 70]. Transplanted mesenchymal stem cells and bone marrow stromal cells promote wound healing through differentiation and release of pro-angiogenic factors [71]. Endothelial progenitor cells have also been studied for improving bone regeneration and healing [72]. Current myocardial delivery mechanisms for cell-based therapy that have proven somewhat effective include intracoronary and intramyocardial delivery [8]. The population of endothelial progenitor cells found in the bone marrow, circulation, or other tissues, first isolated primarily by Asahara and colleagues in 1997 [73], is one of the most promising cell sources due to their regenerative capacity and ability to home to sites of ischemia and shown promising functional recovery in animal models [74] and human trials [75, 76]. One comparative study between mesenchymal progenitors and endothelial progenitors for myocardial infarct regeneration showed better neovascularization and contractility for treatment with endothelial progenitors over mesenchymal [77]. Endothelial progenitor cells (EPC) can be mobilized to circulation from the bone marrow by administration of granulocyte colony stimulating factor (G-CSF) and home to sites of ischemia, inflammation, and biomaterials with artificial EPC capturing motifs [78]. EPC are an intriguing cell type for treating ischemic conditions that are described in greater detail in [30, 79]. Stem cell homing has also been investigated for gene delivery [80].

An alternative to delivering cells directly is administration of cytokines that attract progenitor cells to sites of ischemia. After myocardial infarction there is a mobilization of bone marrow-derived stem/progenitor cells to the circulation [81, 82].

16

Clinical trials investigating the use of granulocyte-colony stimulating factor, a cytokine shown to promote the mobilization of bone marrow stem/progenitor cells and subsequent accumulation in ischemic tissue, have so-far failed to demonstrate significant beneficial effects in the ischemic heart [83-85]. However, other techniques are underway to capture or home endothelial progenitors to sites of ischemia. Systemic administration of anti-α4 integrin antibody was recently shown to promote the mobilization and functional incorporation of bone-marrow endothelial progenitor cells [86], in a method that mimics observed downregulation of α4 integrin in natural progenitor cell mobilization [87, 88]. Asahara and colleagues recently discovered a key piece of the endothelial progenitor homing puzzle, showing that specific Jag-1-derived Notch signaling is required for endothelial progenitor-mediated vasculogenesis [89], although much work remains to be done in this area. According to a recent review article, endothelial progenitors hold much promise for treatment of ischemic disorders, and better techniques for cell isolation, expansion, mobilization, recruitment, and transplantation are under development [90].

Engineered cell therapy is one prospective method to resolve problems related to direct gene delivery in humans. Engineered cell therapy to promote vascularization is growing in popularity and has been used to deliver non-naturally secreted proteins to the heart [91-93] and for delivery of VEGF in tissue-engineered bone repair scaffolds [94].

Cell transplantation is also being investigated as a means of vascularizing tissue engineered constructs. Several examples have been published of microvascular tubules forming in implanted constructs containing endothelial cells. The most successful constructs, in terms of linkage to host vasculature, vessel architecture, and vessel longevity, include at least two cell types in an appropriate matrix that allows for cell migration and promotes the endothelial cell phenotype. A particularly successful model constructed by Jain et al. [95] incorporated a co-culture of human umbilical vein endothelial cells (HUVEC) and 10T1/2 mesenchymal precursor cells in a fibronectin-type I / collagen gel implanted in a mouse. Patent vasculature connected to the host

circulatory system was formed that was stable for at least a year and was responsive to the vasoconstrictor endothelin. In other studies, human dermal microvascular endothelial cell spheriods and preadipocytes were transplanted into a fibrin matrix on a chick chorioallentoic membrane [14] and fibroblast sheets co-cultured with endothelial progenitors were shown to improve cardiac function in infracted hearts [96]. In these examples the transplant formed a patent microvasculature connected to the host system without exogenous angiogenic growth factors or transient transfection. Incorporating appropriate autologous cell types in well-designed matrices may prove a safe and effective means of vascularizing tissue engineered implants, and has been used for developing engineered vascularized skeletal muscle [97].

Matrix Interaction

Much progress has been made towards the development of vascular-inductive tissue engineering matrices. Early work in this area involved passive adsorption or bulk incorporation of growth factors in porous or degradable scaffolds. While somewhat effective at producing initial vascular growth, quick release profiles and rapid diffusion of growth factors do not result in the desired response of functional, stable vasculature. Researchers are investigating covalently tethering growth factors to matrices and incorporating growth factor release mechanisms tied to angiogenic activity such as matrix metalloproteinase (MMP)-degradable sites [98, 99]. In addition to growth factors, extracellular matrix proteins that regulate factors such as cell adhesion and migration have an impact on cell function and gene regulation. Different extracellular matrix proteins and ligands have been shown to modulate the angiogenic response [100], often through integrin activation [101, 102]. Recent research has taken an integrative approach to combine angiogenic growth factors with the appropriate matrix signals to create controlled biomimetic analogs to natural extracellular matrices.

A new generation of bioactive materials is under development, designed to more closely mimic the natural extracellular matrix while providing greater control over the cellular response [103]. Fibrin matrices loaded with a modified version of VEGF that directly binds fibrin and is subsequently locally released in a proteolytic-dependent manner have been shown to induce local and controlled blood vessel growth in animal models [104, 105]. Recent advances have been made in the design of bio-artificial matrices, or artificial scaffold materials that incorporate bioactive motifs, illustrated in Figure 2.3. Conjugation of bio-adhesive signals such as the integrin-binding peptide RGD to surfaces of artificial materials has long been established. Hubbell and West have succeeded in developing 3D artificial matrices that incorporate adhesive signals as well as growth factors such as VEGF [105, 106] and epidermal growth factor [107]. The concept of a bio-artificial matrix is attractive because it allows the presentation of a controlled and tailored environment. In the case of a polyethylene glycol (PEG) –based matrix, intrinsically resistant to non-specific protein adsorption and cell adhesion, biofunctionality can be built onto a "clean-slate" background material. This system can be used to test the functionality of diverse proteins in a controlled environment such as ephrin which was shown to promote the formation of endothelial tubules without additional adhesive signals [108]. Another attractive element of bioartificial matrices is the ability to spatially control presentation of bioactive ligands with fine precision. Photo patterning techniques have been utilized to construct 3D patterned matrices [109-111]. Geometric constraints such as line width have been shown to effect formation of endothelial tubules [112]. In theory, photopattening techniques could be used to control the architecture of a vascular network and has been investigated on 2D surfaces by our laboratory.

The concept of photopatterning guidance channels mimics the natural phenomenon of vascular memory. Figure 2.2 illustates the concept of photopatterning adhesive ligands against a non-adhesive polyethylene glycol background. Vascular

memory, important to the study of tumor angiogenesis, occurs when regressed microvasculature leaves behind empty sleeves of basement membrane and associated pericytes [113]. When conditions permit revascularization, such as reversal of anti-VEGF therapy, a rapid repopulation of vessels along basement membrane sleeves is observed [113, 114], similar to the way nerves regenerate along pre-existing pathways [115]. Vascular memory has also been noted to occur in normal human vasculature [116, 117]. Future study of vascular and neural pathfinding in development and healing will undoubtedly produce future medical benefits. Promising results from combination therapies co-delivering [118] or time-release staggering multiple growth factors [49] support the idea that a robust vascular healing response requires coordination of the correct signaling factors, dosing, and exposure time points. Incorporation of biomaterial delivery vehicles aims to solve some of the complex pharmacokinetics, but this approach is ultimately hindered by a lack of knowledge of optimal dosage and timing and the inability of delivered signals to override the "background noise" of a pro-inflammatory environment. Research into "master switch" upstream activators such as HIF-1α [56, 119] that activate an entire pro-vascular signaling cascade are an exciting direction to the growth factor delivery field. But even if regenerative medicine can one day fully recapitulate the pharmacokinetics of an endogenous healing or developmental vascularization response, ultimately the question arises as to why the natural healing mechanisms failed to begin with or in the case of myocardial infarction, why no native regenerative repair process occurs at all. Various disease states, aging, and scar-tissue formation are obvious blockades to natural endothelial repair mechanisms, and growth factor signaling alone may be an intrinsically limited strategy when delivered in the context of diseased or non-healing tissue [120].

New approaches to treating ischemia are focusing on delivery of regenerative cells alone (**Fig. 2.3B**) and in combination with growth factors and biomaterial scaffolds (**Fig. 2.3E**). For cell therapy, we are beginning to understand the importance of

delivering multiple progenitor cell-types in creating functional tissues. Advances in gene and cell delivery techniques have yielded astonishing results in animal models such as polymeric nanoparticle gene delivery vehicles combined with human embryonic (hEST) and mesenchymal stem cells (MSC) that showed significant vascularization and engraftment [121].
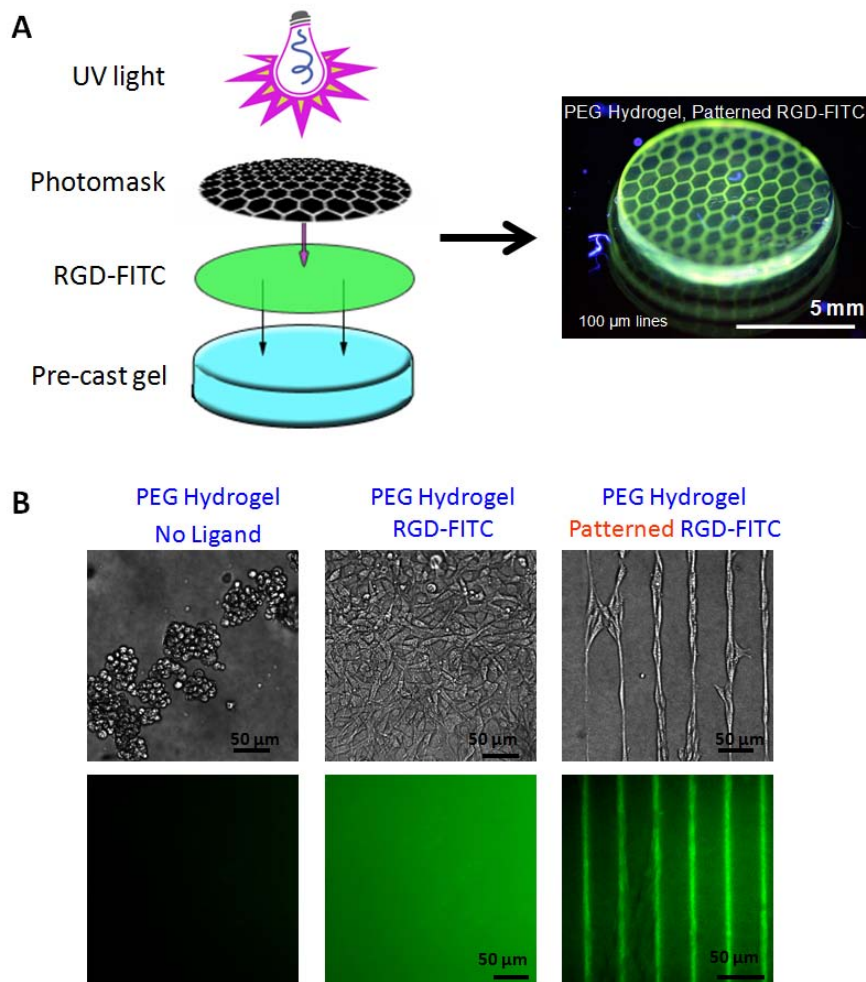
Figure 2.2 UV photopatterning of PEG-DA hydrogel. (A) RGD-FITC is covalently tethered to a PEG hydrogel matrix in a honeycomb pattern by UV activation of photoinitiator through a mask onto a pre-cast gel disc. After a wash step lines are visible. (B) Using gels patterned in this technique, fibroblasts seeded on the gel surface form a spread monolayer, remain rounded, or align to the adhesive ligand.

While current tissue engineering approaches aim to overcome the native tissue dysfunction by delivering effective regenerative cells in conjunction with the appropriate matrix and signaling molecules, the monumental challenge of integrating engineered tissues with the host vasculature remains significant. The challenge of clinically delivering functional and vascularized large-scale tissue substitutes creates a 'chicken-or-the-egg' paradox. Is a functional vasculature required before regenerative cells can be transplanted, or are the regenerative cells needed to give rise to the new vasculature simultaneously as functional tissue develops? Researchers must attempt to either: connect and perfuse a pre-fabricated functional critical-sized tissue, form a pre-vascularized site and subsequently add in functional tissue, or simultaneously form vasculature alongside functional tissue.

From the standpoint of *in situ* tissue formation, tissue engineering research has progressed to the point of predictably and repeatedly producing patent, stable vasculature in a variety of animal models through transplantation of a combination of endothelial and mesenchymal cells or progenitors encapsulated in biological extracellular matrix (ECM) [95] and Matrigel™ implants [122]. The driving force behind this advancement is a mimicry of embryonic vasculogenesis where angioblasts and mesenchymal stem cells organize into a network to form a pericyte-stabilized capillary bed [123]. The ability to recapitulate this capillary network formation using adult cells obtained in routine sampling procedures of the blood and bone marrow represents a useful and feasible pool from which to further develop clinically relevant vascularized tissue constructs.

Matrigel™, a decellularized matrix derived from mouse sarcoma cells, has been a common component for both *in vitro* endothelial tube formation and *in vivo* 3D network vascularization. However, Matrigel™ is a poorly controlled and highly uncharacterized environment from an engineering perspective, containing a mélange of growth factors and matrix-associated bioactive signals. Unfortunately, because of its tumoral and xenogenic origin, Matrigel™ is ultimately not an optimal choice for development of

clinically-relevant therapies. Major effort is being concentrated on development of fully synthetic or well-defined biological matrices with potent pro-angiogenic properties manifested either through encapsulated co-culture systems of endothelial and mesenchymal cells or cell-free smart materials (**Fig. 2.3C**) directly recruiting vascular ingrowth from the surrounding host tissue.

Novel vascular-inductive biomaterial systems include schemes for directly conjugating growth factors to a degradable matrix and releasing them in a cell-demanded manner. One such system that has shown promising results incorporates bioactive ligands into a synthetic polyethylene glycol (PEG) hydrogel. PEG hydrogels for vascularization have been developed with different crosslinking reaction schemes. Popular renditions include 4-arm PEG-vinyl sulfone (PEG-4VS) crosslinked by Michael-type addition [124] and PEG-diacrylate (PEG-DA) crosslinked by photoinitiated free-radical polymerization [125]. Both systems are functionalized with protease (MMP)-cleavable peptide sequences, domains for cell adhesion (RGD peptide), and tethered growth factors. These PEG-based matrices have been used to promote both *in vitro* [126] and *in vivo* [125, 127] vascular network formation from encapsulated cells or vessel ingrowth from the surrounding tissue. These engineered matrices that directly bind growth factor and release it in a proteolytically-dependent or "on-demand" manner induce more stabilized and longer-lasting vasculature compared to diffusive growth factor release. However, even these induced stabilized vessels are reported to regress in time in the absence of true physiological demand [124]. Yet another promising artificial matrix idea utilizes self assembled peptide amphiphile nanofibril matrices with heparin sulfate binding sites to present bioactive ligands and growth factors to promote *de novo* subcutaneous vascularization [128]. Research in engineered matrices has progressed for tissue engineering models including cardiac progenitor differentiation [129], pancreatic islet encapsulation [130], and epithelial morphogenesis [131]. We can expect future

research to combine engineered vascular-inductive matrices with repair or replacement of metabolically active tissues *in vivo*.

An alternative strategy to inducing vascular organization into a scaffold is to fabricate vascular conduits directly prior to implantation (**Fig. 2.3D**). Several clever engineering techniques to generate endothelial-lined channels in tissue engineered constructs have emerged. One simple yet effective technique involves close-packed modular cylindrical collagen matrices coated in endothelial cells to generate endothelial lined channels in a random packed array. These channels remodel *in vivo* to generate a vascularized graft [132]. Another self-assembly technique uses microtissue building blocks made from human artery-derived fibroblasts coated with human umbilical vein endothelial cells (HUVEC) to mold a small diameter vascular graft with high levels of ECM deposition [133]. In theory, such a system could also be used for inducing vascularization of a tissue-engineered construct. Cell sheet technology is another vascular design technique that employs a process of alternatively stacked monolayers of HUVEC and myoblasts to create highly vascularized implants of myoblasts *in vivo* with robust endothelial networks [134].

Developing along-side the effort to create clinically-useful and well-characterized pro-vascular matrices are approaches to merge this technology with relevant tissue-specific replacement models. For example, pancreatic islets are highly vascularized spherical clusters of endocrine cells in the pancreas which include the insulin producing β-cells. Islet transplantation is a promising therapeutic option with freedom from exogenous insulin injection for type-1 diabetes, yet current transplantation techniques are severely limited due to high islet morbidity associated with poor engraftment and reperfusion. Current efforts to improve islet transplantation therapy include gene therapy to overexpress angiogenic growth factors [135, 136] in transplanted islets and seeding of islets into pre-vascularized Matrigel™ [137] and collagen [138] implants.

Engineering mechanically sound and functional cardiac tissue for the repair of myocardial infarction and associated ischemic heart disease, the leading cause of death in developed countries, is one of the most promising and grand targets for tissue engineering. Progress in development of engineered cardiac tissue has not always addressed the need for vascularization and engineered tissues suffer from necrotic cores and little or no integration with the host tissue [139]. Incorporation of HUVEC and mouse embryonic fibroblasts (MEF) in cardiac patches leads to a strong vascular network formation *in vitro* and which, if formed preceding implantation in rat heart tissue, shows vastly improved integration and perfusion than patches without HUVEC and MEF [139, 140]. Taking the process one step further, neonatal cardiac cell patches containing angiogenic factors pre-vascularized for 1 week in the omentum and subsequently transplanted into infracted heart tissue showed improved structural, electrical, and cardiac output over non-vascularized controls [141]. Alternatively, microvascular segments stabilized in collagen and transplanted into ischemic myocardium formed vascularized cardiac patches with improved left ventricular function [142].

Finally, the most direct approach to providing the necessary cues and allowing cells and tissues to control the ultimate shape of the engineered tissue and associated vasculature is direct fabrication of functioning tissue. Technologies to exert spatial control over the placement and organization of individual cells and tissue microstructures include 3D tissue printing [143, 144] and lithographic fabrication [145, 146] of vascular-inductive matrices have emerged as viable options. Microfluidic devices are also becoming employed to create controlled *in vitro* systems for studying underlying mechanisms and testing new ideas [147].

Common Strategies for Vascularization in Tissue Engineering
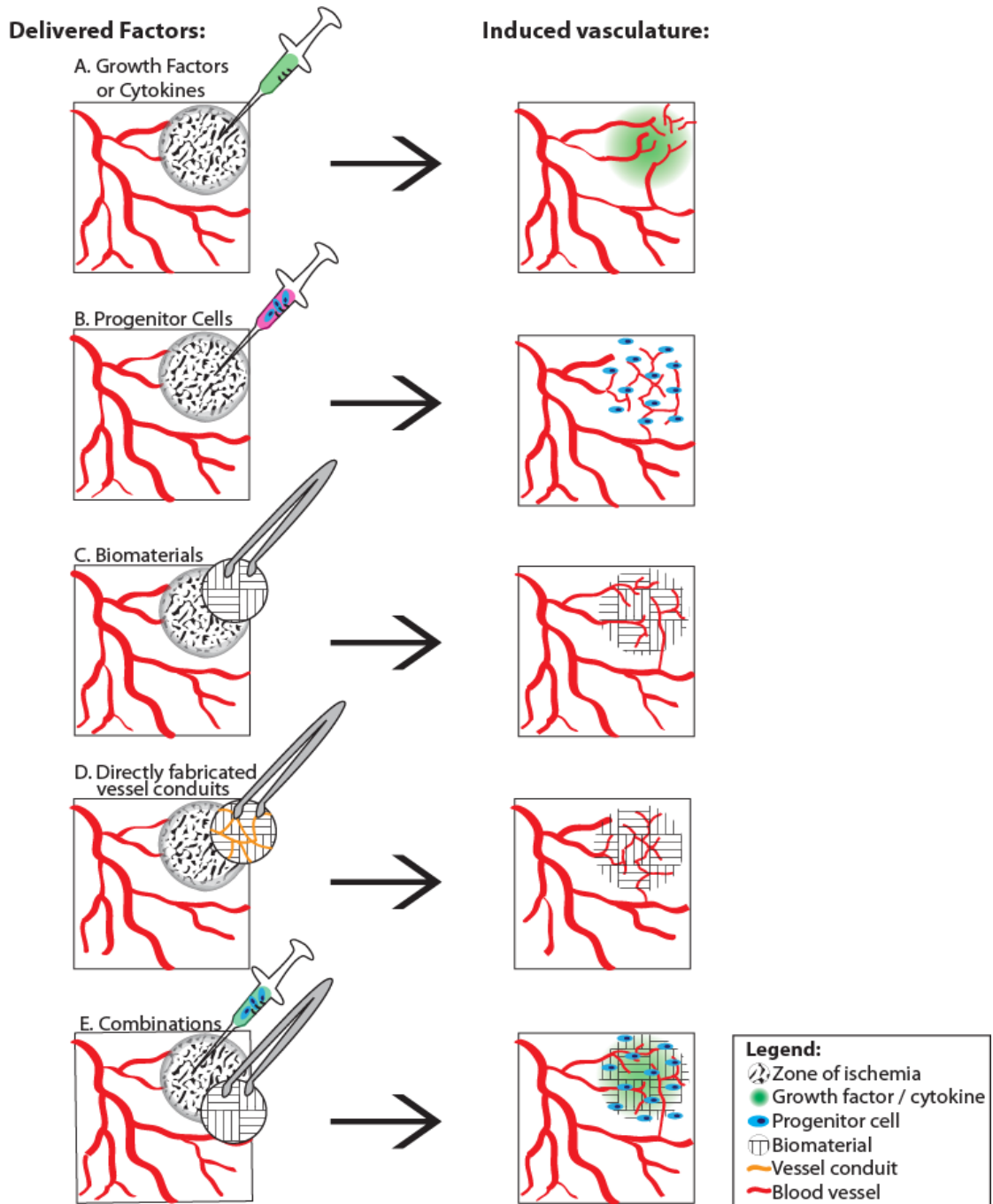
Figure 2.3 Strategies for inducing vascularization in engineered tissues. (A) Growth factors such as VEGF and bFGF as recombinant proteins or gene vectors. EPC-mobilizing cytokines such as G-CSF (B) Progenitor cells such as EPC and MSC
(C) Biomaterials such as bioactive PEG hydrogels (D) Vessel conduits or endothelium-lined channels directly fabricated into an implant (E) Combination therapies such as growth factor binding scaffolds with cells

Metabolic Controls

Some novel unconventional approaches have been proposed to increase vascular perfusion in ischemic tissue. Scientists looking for new approaches have been driven mainly by technical difficulties in delivering pro-angiogenic factors locally to ischemic tissue for sufficiently long periods of time, the often confounding requirements for multiple factors delivered in the right spatial and temporal dosage, and the risk of undesirable side effects from systemic administration of angiogenic factors. One novel approach capitalizes on a large body of research which implicates nitric oxide (NO) as a stimulator of angiogenesis [148-150]. NO increases the expression of VEGF and other angiogenic factors, recruits pericytes, and improves blood perfusion by inducing vessel dilation. NO can also protect tissue against ischemic damage by reprogramming the cell's metabolism to tolerate a lower oxygen environment through nitrosylation of oxygen sensor PHD1 proteins and complex I proteins in the electron-transfer chain to reduce the generation of pro-inflammatory reactive oxygen species. It is important to note that in higher concentrations, or in certain physiological conditions NO can have the opposite effect. Kumar et al. demonstrated the use of nitrite (NO_2^-) as a pro-angiogenic molecule, considering the fact that nitrite is reduced to NO in ischemic conditions but is oxidized into harmless nitrate (NO_3^-) in oxygenated tissue [151]. They showed that administration of sodium nitrite by I.P. injection significantly restored ischemic hind limb blood flow, vascular density, and endothelial cell proliferation. Administration of carboxy PTIO, a NO scavenger, abolished the positive effects, bolstering their argument that NO is responsible for the changes. These results are exciting because they open the possibility of an effective, yet inexpensive treatment option with few side effects and simple administration options allowing for long-term treatment.

Traditional angiogenic factors such as VEGF and FGF stimulate vascularization but do not promote additional metabolic changes [152]. Recent studies are solidifying the link between metabolic demand for oxygen and angiogenesis. Expression of the

transcriptional coactivator peroxisome proliferator-activated receptor-γ coactivator 1α (PGC-1α), a potent metabolic sensor and regulator, is induced by a low-nutrient and low-oxygen environment such as during aerobic exercise training. PGC-1α was recently shown to be a potent stimulator of VEGF expression angiogenesis in ischemic tissues but does not involve the traditional HIF-1 pathway [153]. Activating the PGC-1α pathway may be a novel method of inducing angiogenic response. Another interesting idea is to induce tolerance of a hypoxic environment to stave off tissue damage and necrosis after an infarction [154], allowing time for a subsequent pro-angiogenic therapy to take effect. Aragonés et al. show that prolyl hydroxylase 1 (Phd-1), an oxygen-sensitive enzyme that controls the stability of HIFs, plays a key role in regulating metabolism and reducing oxygen requirements in muscle tissue [154]. While it might seem counter-intuitive to induce hypoxia tolerance, as Phd1-null mice showed reduced exercise performance, the benefit lies in reducing damage. Oxidative consumption under hypoxic conditions has been linked to generation of reactive oxygen species, and limiting oxygen consumption when oxygen levels are low leads to less cell death [155]. Another potential metabolic control involves the experimental concept of ischemia preconditioning where tissues are rendered resistant to ischemia/reperfusion injury, and was first shown to result in reduction of myocardial infarct sizes in 1986 [156]. Ischemia precondition is traditionally induced by brief repeated episodes of coronary artery occlusion prior to a major prolonged occlusion. New research has shown that ischemic preconditioning results in a robust activation of HIF-1α and that pretreatment with the HIF activator dimethyloxalylglycine or selective siRNA repression of prolylhydroxylase-2 resulted in cardioprotection similar to that of traditional ischemic preconditioning [157]. One could imagine a treatment scenario where hypoxia tolerance is initially induced, followed by switching on angiogenesis mechanisms and gradually restoring oxygen consumption back to normal levels as the tissue is revascularized. These new studies show that

targeting oxidative metabolism and capitalizing on its natural link to angiogenesis is a valid and novel therapeutic tool for treating ischemic disease.

Methods for validation and analysis of vascularization techniques

It is important to measure and validate the architecture and function of induced vasculature. Induced vasculature often has little resemblance to native tissue architecture, and has the potential to look and behave like tumor vasculature [47]. Furthermore, induced vasculature may suffer from poor perfusion and functionality. Several robust analysis strategies have been developed for both *in vivo* and *in vitro* models [158].

In vitro analysis techniques: Three dimensional culture of endothelial cell types or co-culture of endothelial and mesenchymal progenitors (MSC or 10T1/2 embryonic fibroblasts [95]) will self-organized to form tubule networks in pro-vascular environments [158]. The addition of a mesenchymal cell type serves to stabilize the endothelial tubes. Furthermore, if these cell types are cultured on the surface of microcarrier beads that are encapsulated in the matrix, endothelial tubes sprout from the beads [35, 158]. These bead-initiated sprouts can be easily quantified for number, length, and branching and used as a screening and analysis tool. Three dimensional tissue culture of small sections of aorta from rat or mouse also sprout endothelial tubes from the aortic tissue in pro-vascular environments and are an alternative to single cell culture [159]. Lastly, the chorioallantoic membrane (CAM) is a vascularized membrane on developing chicken embryos that is widely used as a pseudo-*in vivo* system for testing vascularization effects [158].

In vivo analysis techniques: Traditionally, histological techniques including lectin- and immuno-staining have been used to quantify induced vascularization *in vivo*. Three-dimensional architecture and function (vessel perfusion) are key measures that are difficult to determine from histological sections. One highly effective technique for quantitative analysis of three-dimensional vascular architecture is perfusion with the

silicone rubber radio-opaque injection compound Microfil ® (Flow Tech, Inc.) to create a cast of the vasculature. The vascular cast can then be scanned in three dimensions at high resolution (sub 10 μm) with microCT and analyzed with a number of algorithms for density, branching, and connectivity [159, 160]. One drawback to the microCT method is that it is a terminal procedure. Development of vasculature over time in live animals can be observed by intravital microscopy with window-models and dorsal skin-fold chambers [158]. Blood flow to ischemic limbs can be observed in live animals over time by laser Doppler perfusion imaging [127] (Moor Instruments) or with GFP-cells [158] and infrared dye tracer studies and in vivo fluorescence imaging (IVIS, Caliper Life Sciences).

Conclusions:

The therapeutic vascularization field experienced initial setbacks in the failure of several clinical trials with growth factor therapy going quickly from benchtop to bedside before precise delivery methods and controls were elucidated. A growing body of evidence is beginning to suggest that single growth factor therapy may be insufficient for restoring a large volume of blood flow to an ischemic tissue, especially in a diseased state where vessels may be less responsive. A great deal of effort has gone into identifying upstream activators that induce expression of multiple angiogenic factors as well as alternative pathways to the traditional angiogenic signaling paradigm. Cell-based therapy looks very promising, but continues to suffer from optimal sourcing and delivery strategies. A new generation of therapies is needed to better address the problems with current angiogenesis strategies.

Future Perspective:

Future approaches to therapeutic vascularization will have a better chance of success if a more targeted and careful approach than that of earlier trials is utilized. A clinically successful vascularization therapy is likely to be a combination therapy. Examples of combination therapies such as engineered cell therapy, multiple growth factor release, or growth-factor/cell/matrix combinations [161] are beginning to emerge. We must also consider the importance of inducing arteriogenesis, angiogenesis, neovascularization, or some combination. Future therapies need to consider the end-goal in terms of re-perfusion and what type of therapy or combination strategy is best-suited to obtain both the necessary increase in blood-flow volume as well as ability to deliver oxygen. Ongoing research is helping us to understand the complex signaling and pathfinding mechanisms that lead to branching morphogenesis. Knowledge divulged from studies on development of vascular architecture and pathfinding, such as growth factor gradients, vascular memory, and morphogenesis signaling, needs to be applied to create more physiologically accurate and better functioning induced vasculature. More work is needed to sort out the extremely complex angiogenic molecular program. Metabolic control over angiogenesis is an interesting new approach and further research in this area may provide alternative therapies to patients who do not respond to traditional growth factor therapy or that have metabolic disease-related ischemic disorders. Additionally, advances in engineered bio-artificial and bio-active matrices are illustrating higher levels of control in tissue engineering and regenerative medicine, paving the way towards large-scale engineered tissue substitutes. As work progresses in all of these areas, we can expect more functional therapies to become available to patients. Based on the impressive progress thus far, we can predict that the future of therapeutic vascularization is quite bright.

Type 1 diabetes mellitus and islet transplantation therapy

One in every 400 to 600 children and adolescents suffer from type 1 diabetes mellitus T1DM [162], a condition that results from the autoimmune destruction of the insulin-producing beta cells in the pancreas. Left untreated, T1DM is a fatal disease. The discovery of insulin was a major medical breakthrough, for which Frederick Banting and John Macleod were awarded the 1923 Nobel Prize in medicine [163]. Subsequent developments in exogenous insulin therapy, blood sugar testing, and lifestyle adjustments allow type 1 diabetics to lead long and generally healthy lives. However, treatment is often burdensome, and complications associated with poor blood sugar regulation may lead to seizures or episodes of unconsciousness and long term organ damage.

"This disease controls our lives with all the pricking of the fingers, shots, high and low blood sugars; it's like being on a seesaw. Without a cure, we will be stuck on this seesaw 'til the day we die." - Tre Kawkins, age 12 [164]

For years the holy grail of T1DM research has been a self-regulating insulin source that can maintain blood sugar levels without regular patient monitoring, allowing the patient to live a more normal life. A large focus of research has been on implantable insulin pumps with glucose sensor feedback loops. While insulin pump improvements have been steady, the glucose sensors and pump leads suffer from attack by the innate immune response and must be repositioned regularly [165].

Alternatively, whole pancreas or islet cells can be transplanted and serve as a biological source of insulin. Grafted islets or whole pancreas are often introduced at the same time as a kidney transplant. The need for immunosuppressive therapy for the kidney allows little additional risk to the patient to also transplant an insulin source. Islet cell transplantation is expected to be less invasive than a whole pancreas transplant and does not put the working digestive functions of the existing pancreas at risk. While still highly

experimental, islet cell transplant surgery has progressed to the point that 58% of patients in one study [166] were insulin independent at one year after islet cell transplantation. The current method of islet transplantation involves infusing donor islets into the recipient's hepatic portal vein where they become lodged in the vascular system of the liver. While short term outcomes are promising, patients with islets grafted in this manner have a relatively poor long-term outcome: only about 10% of islet cell transplant recipients maintain exogenous insulin independence at 5 years [167-170]. Islet transplantation therapy in its current form is significantly limited by inadequate islet supply and mass, instant blood-mediated inflammatory reaction (IBMIR) [163], toxic responses to immunosuppressive drugs, and loss of islet viability/function during isolation and following implantation, particularly due to inadequate vascularization of the transplanted islets [171, 172]. It has been proposed that by delivering pancreatic islets in biologically active materials engineered to elicit a vascular-inductive response, significant improvements in the vascular connectivity of transplanted islets and subsequently the overall viability and graft success can be achieved[173, 174].

Blood flow to pancreatic islets is central to islet function [175]. Pancreatic islets have higher densities of blood vessels compared to the surrounding exocrine tissue and receive 15-20% of pancreatic blood supply despite comprising only 1-2% of pancreas mass [176]. A dense network of capillaries maintains blood perfusion through the islet cell mass itself. In fact, it has been shown that nearly every insulin-producing beta cell neighbors an endothelial cell [177]. Our preliminary work has been successful in imaging the intra-islet capillary bed. Following islet isolation and transplantation, the re-establishment of blood flow to islets requires several days and involves angiogenesis and possibly vasculogenesis. New blood vessel growth is often chimeric with endothelial cells arising from both the host tissue and the islets themselves [178]. In addition to ischemic conditions during this revascularization period, the resulting vasculature exhibits lower vessel density and lower oxygen tension than the native pancreas [179,

180]. Studies have shown that transplanted islets have reduced blood flow overall compared with native islets [135, 136, 176, 177, 181-184]. This inadequate revascularization of transplanted islets is a major cause for reduced islet viability, function, and engraftment [185-187]. Delivery of pro-vascularization factors, mostly via genetic manipulation of islets, has been shown to improve vascularization and islet function[135, 182-184, 188-190], but these strategies are hindered by insufficient and/or complex release pharmacokinetics and inadequate delivery matrices as well as technical and safety considerations associated with gene transfer. It has been proposed that optimal formation of a fully functional islet vasculature will require precise control of the timing, dose, and duration of angiogenic factor action [176]. VEGF-A, a potent angiogenic factor, has been shown to be a primary driver for islet vascularization in development, maintenance of the intra-islet capillary bed, and islet graft revascularization [177, 184, 191]. Islets in VEGFloxP mice lacking expression of VEGF-A in the pancreas have severely limited islet capillary perfusion and reduced insulin output and glucose responsiveness [177].

Bio-functionalized PEG hydrogel

Over the past 10 years, much progress has been made towards the development of vascular-inductive tissue engineering matrices. Early work in this area involved passive adsorption or bulk incorporation of growth factors in porous or degradable scaffolds. While somewhat effective at producing initial vascular growth, quick release profiles and rapid diffusion of bolus delivered growth factors do not result in the desired response of functional, stable vasculature [127]. Current research is more focused on sustained delivery of growth factors tethered to matrices, sometimes incorporating growth factor release mechanisms tied to angiogenic activity such as matrix metalloproteinase (MMP)-degradable sites [98, 99]. In addition to growth factors, extracellular matrix proteins that regulate factors such as cell adhesion and migration have an impact on cell function and

34

gene regulation. Different extracellular matrix proteins and ligands have been shown to modulate the angiogenic response [100], often through integrin activation [101, 102]. Recent research has taken an integrative approach to combine angiogenic growth factors with the appropriate matrix signals to create controlled biomimetic analogs to natural extracellular matrices.

The concept of a PEG-based bio-artificial matrix is attractive for cell transplantation therapy because it allows for the presentation of biologically active cues in a highly controlled and tailored environment. Because PEG is intrinsically resistant to non-specific protein adsorption and cell adhesion, biofunctionality can be built onto a "clean-slate" background material with tunable material properties such as pore size and mechanical stiffness [192]. Artificial biomimetic matrices usually contain mechanisms to allow for tissue or cell invasion, usually achieved through adhesive protein attachment / incorporation and either porous structure or degradable cross-links in the case of hydrogel systems . The PEG hydrogel lends itself well to examining the biofunctionality of diverse proteins and peptides in a controlled environment. Another attractive element of PEG-based bioartificial matrices is the ability to spatially control presentation of bioactive ligands with fine precision. Photo-patterning techniques have been utilized to construct 3D patterned matrices [109-111] and geometric constraints such as line width have been shown to effect formation of endothelial tubules [112, 193].

The usefulness of RGD as a cell-adhesion ligand in biomaterials for *in vivo* use is often questioned as it is known to have lower adhesion performance than several other proteins and protein fragments [194]. However, RGD is a ligand for αvβ3 integrin, known to be highly expressed in endothelial cells undergoing angiogenesis [195], and our preliminary results have demonstrated that RGD supports vessel invasion into degradable bio-artificial matrices. Therefore we argue that RGD is an acceptable ligand for vascularization studies while the PEG platform is amenable to experimentation with other types of adhesive molecules. Other adhesive ligands such as the collagen-mimetic peptide

GFOGER [196], the fibronectin fragment FNIII7-10 [194], and sequences from the ECM protein laminin can be used with the bio-artificial system for studying other types of regenerative applications such as neurite outgrowth, epithelial morphogenesis [131], and osteogenesis.

While RGD seems an acceptable ligand to support vascular growth, the optimal adhesion molecule to support islet biology is more elusive. Basement membrane proteins are highly expressed in islets and it appears that most all cells types within the islet are capable of recognizing the RGD sequence. However, it remains to be seen whether RGD is a modulator of exocrine function or merely serves as a minimal adhesion molecule. Laminin is prevalent in the islet ECM in isoforms containing the familiar adhesive peptide sequences YIGSR, IKVAV, IKLLI, among others (reviewed in [197]) A majority of the beta-cells that produce insulin are buried within the islet interior and thus may have less contact with an exogenous encapsulating biomaterial than cells on the exterior of the islet. Therefore it is plausible that matrix-based signaling that affects beta cell function is translated through intercellular means to cells on the interior of the islet. Maintenance of islet basement membrane adhesion signals and rapid-reestablishment of a stable pro-vascular environment seem the most likely chance to mitigate the severe effects of isolating the islets from their native tissue environment.

We emphasize that our strategy is not for synthetic bio-mimetic matrices to fully recapitulate the complete biological activities of native ECM. However, from an engineering perspective, bio-artificial matrices provide many advantages that make their use for regenerative therapeutics attractive. Most importantly, bio-artificial systems provide a high level of control to the designer using reproducible and synthetic components in modular "plug and play" architecture. A major conceptual aspect of these bio-artificial matrices is their application as engineered platforms for directed cell invasion: incorporating bioactive adhesion motifs and enzyme-specific cleavage sites rather than serving as simple polymeric growth-factor reservoirs.

CHAPTER 3

BIO-FUNCTIONALIZED PEG-DIACRYLATE HYDROGEL TO PROMOTE VASCULARIZATION IN VIVO *

Summary

Therapeutic vascularization remains a significant challenge in regenerative medicine applications. Whether the goal is to induce vascular growth in ischemic tissue or scale up tissue-engineered constructs, the ability to induce the growth of patent, stable vasculature is a critical obstacle. We engineered polyethylene glycol (PEG)-based bio-artificial hydrogel matrices presenting protease-degradable sites, cell-adhesion motifs, and growth factors to induce the growth of vasculature in vivo. Compared to injection of soluble VEGF, these matrices delivered sustained in vivo levels of VEGF over two weeks as the matrix degraded. When implanted subcutaneously in rats, degradable constructs containing VEGF and RGD induced a significant number of vessels to grow into the implant at two weeks with increasing vessel density at four weeks. The mechanism of enhanced vascularization is likely cell-demanded proteolytic release of VEGF, as the hydrogels may degrade substantially within about two weeks through tissue remodeling. In a mouse model of hind limb ischemia, delivery of these matrices resulted in significantly increased rate of re-perfusion. These results support the application of engineered bio-artificial matrices to promote vascularization for directed regenerative therapies.

Introduction

Reduced vascular perfusion represents a significant cause of death and hospitalization in the United States, including 8 million Americans with peripheral artery disease [198] and 16.8 million Americans with coronary heart disease [199]. Clinically viable therapeutic vascularization therapies will lead to better treatment for peripheral vascular disease, ischemic heart disease, and survival of cell and tissue transplants. Therapeutic vascularization has become a major research focus in regenerative medicine with several strategies being pursued [12, 200-206]. Most clinical trials have focused on delivery of a single angiogenic gene or growth factor, while several groups are developing strategies to deliver or activate different progenitor cell types. At present, a large focus of clinical and preclinical work is centered on identifying the ideal angiogenic agent (or combination therapy), delivery strategy, and dosing regimen [207]. There is a significant need for a suitable delivery vehicle to study novel vascular therapies in a controlled microenvironment.

Hydrogel matrices enable a high level of control for delivering regenerative therapeutic treatments. While a large number of synthetic polymers have been shown to be useful implantable hydrogel materials [208, 209], polyethylene glycol diacrylate (PEG-DA) provides several advantages for regenerative therapeutics. PEG has a well-established chemistry and long history of safety in vivo. Addition of acrylate groups flanking the PEG chain allows for photo- or chemical cross-linking of a PEG-DA macromer solution, as well as incorporation of biomolecules such as protease degradable sites, adhesive ligands, and growth factors. A major strength of this strategy is the modular "plug-and-play" design of the base hydrogel system that allows the tailoring of the biochemical and mechanical properties of the delivery vehicle. Due to its high water affinity, PEG is intrinsically resistant to protein adsorption and cell adhesion, providing extremely low background interference with incorporated biofunctionalities. Due to its

modular nature and excellent in vivo properties, PEG-DA is an appealing platform for delivering regenerative medicine therapies.

PEG-DA-based bio-artificial matrices have been shown to promote cell survival and endothelial tube formation in vitro [108]. PEG vinyl-sulfone (PEG-4VS) matrices containing matrix metalloproteinase (MMP)-degradable, sites, adhesive ligands, and bone morphogenetic protein (BMP-2) promote bone formation in a cranial defect to similar extents as BMP-2-loaded collagen [210]. These bio-artificial matrices serve simultaneously as engineered delivery vehicles and temporary matrices to support tissue ingrowth and remodeling. The goal of this study was to further the use of modular PEG-based matrices toward developing pro-vascularization therapies. We hypothesized that PEG-DA matrices containing a combination of protease degradable sites, adhesive ligands, and vascular endothelial growth factor (VEGF) would induce the growth of new vasculature into the implant in vivo and establish the therapeutic potential of this delivery vehicle in a model of hind limb ischemia.

Results

Regenerative biomaterials designed to integrate with the host tissue must provide mechanisms for cell invasion. We engineered bio-artificial hydrogel matrices to contain MMP-sensitive cross-links, adhesive ligands, and the growth factor VEGF (**Fig. 3.2**). MMP-degradable PEG-DA macromer (A-PEG-GPQ-PEG-A) was synthesized by reacting the proteolytically cleavable peptide GPQGIWGQK [210] with acrylate-PEG_{3400}-NHS, a primary amine reactive cross-linker. PEG-acrylate functionalized RGD adhesive ligand (A-PEG-RGD) was synthesized by reacting acrylate-PEG_{3400}-NHS with the cell-adhesive peptide GRGDSPC. PEG-acrylate functionalized VEGF (A-PEG-VEGF) was synthesized by reacting acrylate-PEG_{3400}-maleimide, a sulfohydryl-reacting cross-linker, with $VEGF_{121}$-cys, a growth factor containing an additional C-terminal cysteine [211]. A-PEG-VEGF activity was assessed by endothelial cell proliferation

39

assay and found to be equivalent to commercially available VEGF$_{165}$. Hydrogel matrices consisting of A-PEG-GPQ-PEG-A, A-PEG-RGD, and A-PEG-VEGF, were generated by polymerizing the acrylate end-functional groups with low intensity UV light in the presence of the photoinitiator Ciba Irgacure 2959 (**Fig. 3.2**). Non-degradable matrices consisted of photopolymerized PEG-DA.

Successful functionalization of bioactive ligands with acrylate-PEG-NHS was confirmed by demonstrating increased molecular weight distributions (**Fig. 3.1**). Cells express MMPs as they invade tissue and biological matrices such as collagen. The degradation profile of the bio-artificial matrix is an important aspect as it is designed to maintain structural integrity in vivo and only degrade subsequent to tissue invasion. Susceptibility of A-PEG-GPQ-PEG-A hydrogels to MMP-mediated degradation was confirmed by progressive dissolution during incubation with active MMP-2 enzyme or collagenase-I over 20 hours (**Fig. 3.3**). Gel degradation was slowed by addition of the MMP-2 inhibitor oleoyl-N-hydroxylamide. Untreated gels with MMP-degradable sequences swelled slightly over 20 hours with no weight loss and remained intact for 4 weeks in PBS. These results demonstrate that controlled degradation of synthetic hydrogels can be achieved by incorporating MMP-sensitive cross-links.
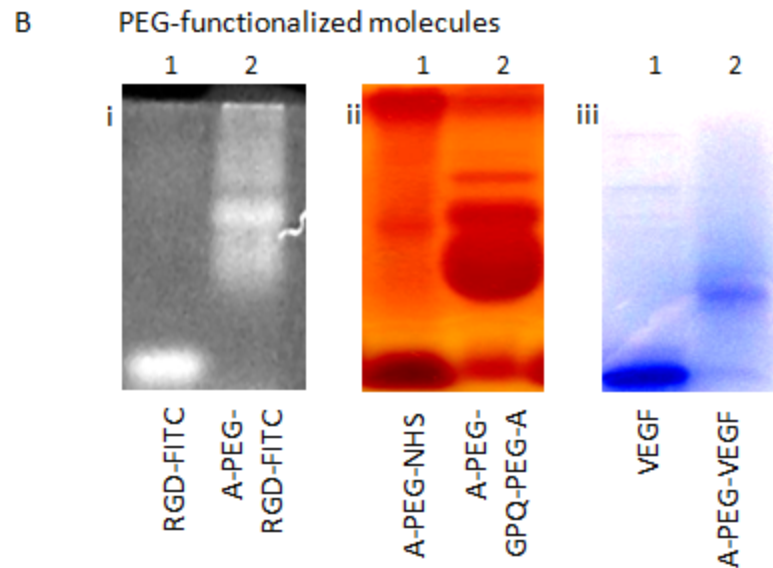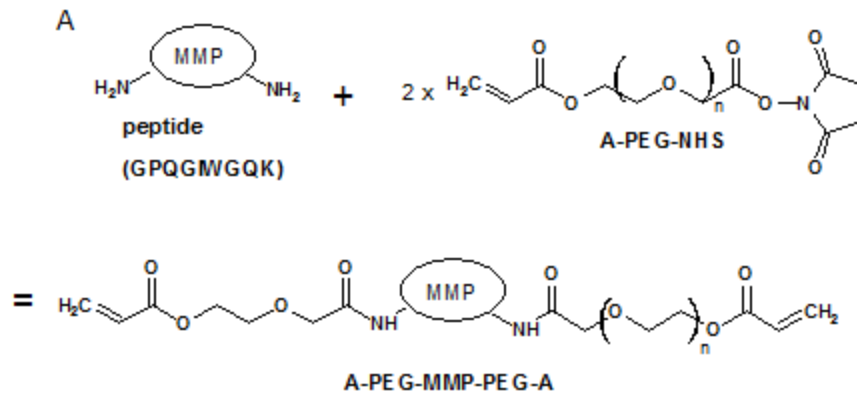
Figure 3.1 PEG-acrylate modification of bioactive ligands prior to gel formation. (A) MMP-degradable peptide cross-linker is functionalized with two molecules of A-PEG-NHS to make a bi-PEG-acrylated flanked degradable sequence. Adhesive ligands and growth factors are mono-PEG-acrylated. (B) Biomolecules functionalized with PEG-acrylate have increased molecular weight when run on an SDS-PAGE gel. (i) Fluorescent imaging - Lane 1: RGD-FITC, Lane 2: A-PEG-RGD-FITC. (ii) BaCl$_2$ / Iodine stain: Lane 1: A-PEG-NHS, Lane 2 A-PEG-GPQ-PEG-A. (iii) Lane 1: VEGF-121-cys, Lane 2: A-PEG-VEGF-121-cys
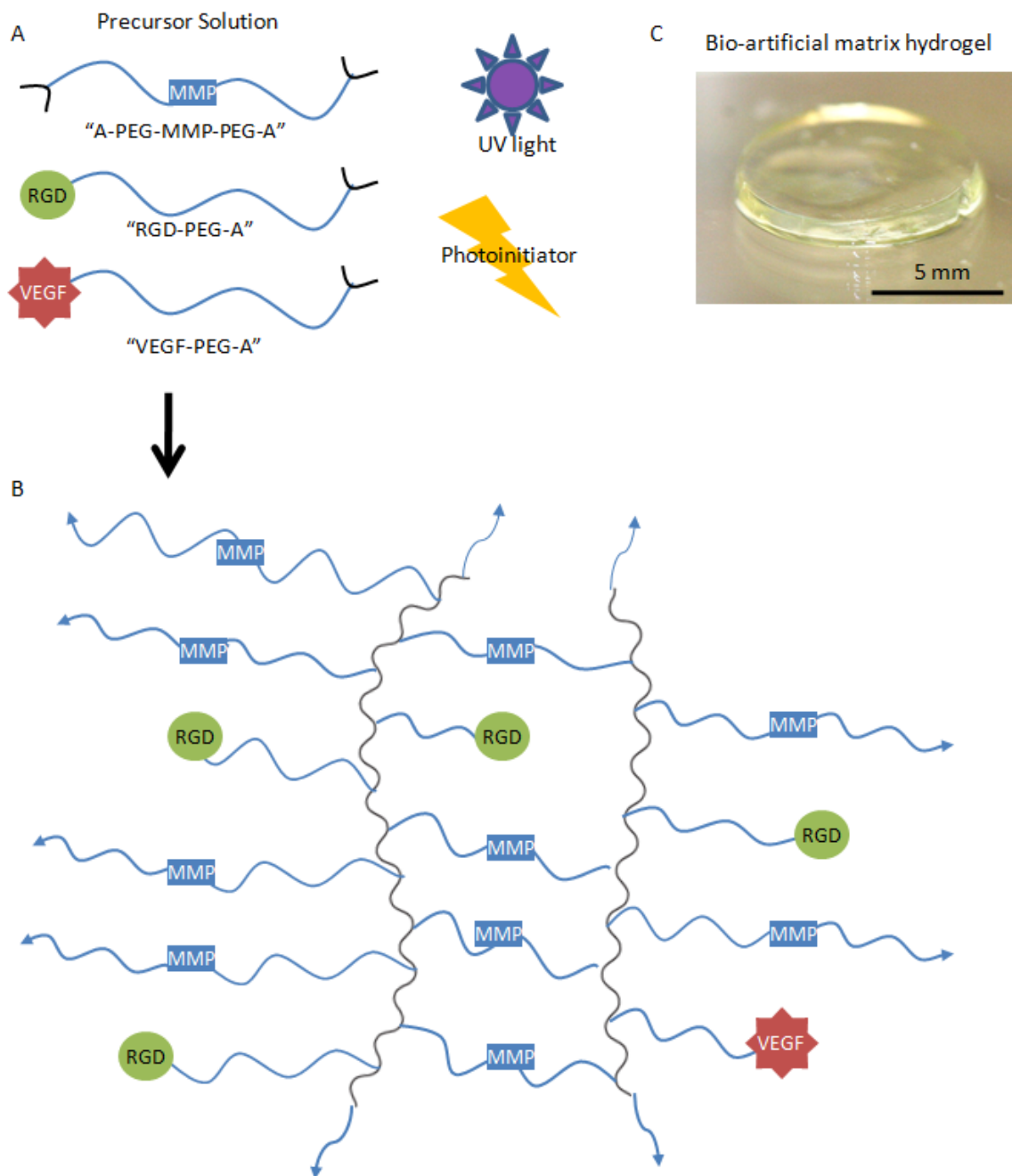
Figure 3.2 PEG-DA hydrogel formation schematic. (A) An aqueous solution of PEGylated precursors is exposure to UV light in the presence of photoinitiator compounds. (B) Polymerization of acrylate end groups into polyacrylic acid results in a cross-linked hydrogel (C) Macroscopic view of a PEG-DA hydrogel cast in an 8 mm x 2 mm silicone mold.
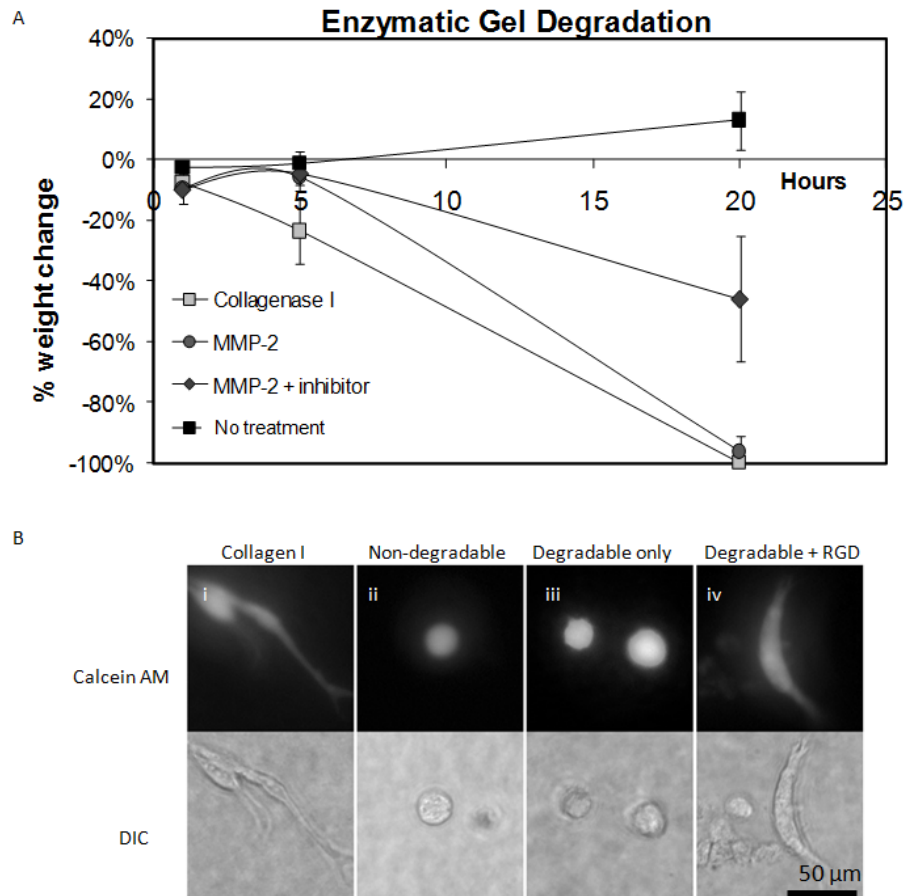
Figure 3.3 In vitro results for PEG-DA hydrogel degradation and encapsulated cell spreading. (A) Degradation of bio-artificial hydrogels incubated in collagenase-1 or MMP-2. Gels are seen to degrade after several hours of incubation, while degradation is decreased by addition of inhibitor and gels in PBS do not degrade. (B) Calcein viability stain of NIH-3T3 fibroblasts seeded in hydrogel formulations spread and migrate in bio-artificial matrices with degradable sequences and adhesive sites (i) similar to type I collagen (iv) but remain rounded in non-degradable (ii) or non-adhesive (iii) matrices.

In order to assess the functionality of the adhesive and degradation components of 3D hydrogels prior to implantation, NIH3T3 fibroblasts were encapsulated in gel formulations containing MMP-degradable sites, RGD, neither, or both. Cells remained rounded in gels containing only RGD or MMP-degradable sites but exhibited a spread morphology in gels containing both RGD and MMP-degradable sites, similar to cells in type I collagen (**Fig. 3.3**). These results indicate that both adhesive ligands and MMP-degradable sites are necessary for cells to spread within the bio-artificial 3D environment and are in agreement with published in vitro studies [212]. The intrinsically low background signal of PEG permits detection of sensitive engineered biofunctional effects, and subsequent focused manipulation of these effects.

VEGF release from the hydrogel was measured in vivo by labeling A-PEG-VEGF with the amine-reactive infrared dye ICG-sulfo-OSu. ICG was observed to have significantly higher fluorescence after exposure to UV-photocross-linking compared to other dyes tested. Pre-formed constructs consisting of 10% PEG-DA or A-PEG-GPQ-PEG-A and 2.8 µmol/mL A-PEG-RGD + 80 µg/mL A-PEG-VEGF-ICG were implanted subcutaneously in male Lewis rats. Control rats received subcutaneous injections of A-PEG-VEGF-ICG in PBS or matrices with no VEGF. The fluorescent signal in the rats was measured on a Caliper Xenogen IVIS Lumina bioluminescent imaging system at 0, 1, 3, 7, and 14 days post implantation. The fluorescent signal in the implant was quantified by gating a region of interest (ROI) around the periphery of the implant and subtracting the average background counts in the surrounding tissue from the average total counts in the implant, as background intensity varied between animals. A steady decline in signal intensity for the soluble VEGF injection was observed, with 90% of the signal lost by two weeks of implantation (**Fig 3.4**). In contrast, the degradable hydrogel matrix exhibited constant VEGF levels during the first two days followed by a gradual decrease over the next 12 days. The non-degradable matrix with VEGF showed nearly constant levels of VEGF over the two week implantation period. The soluble VEGF

group had much higher initial fluorescence because this group was not exposed to UV light. We found that ICG exposure to UV light without the addition of PEG chains to absorb photoinitiator-generated radicals resulted in elimination of any detectable ICG signal. Samples containing un-labeled VEGF were undistinguishable from background fluorescence. Upon retrieval of the implants at day 14, the degradable samples were seen to have partially degenerated, and in some animals the gel was entirely dissociated. The non-degradable samples remained completely intact. New vessels were seen to grow in the tissue surrounding the implants with a general trend of a higher density of small blood vessels in tissue immediately adjacent to the implant. Larger and more regular vessels were seen growing into and around degradable implants, while non-degradable implants induced a large number of small vessels in the surrounding tissue.
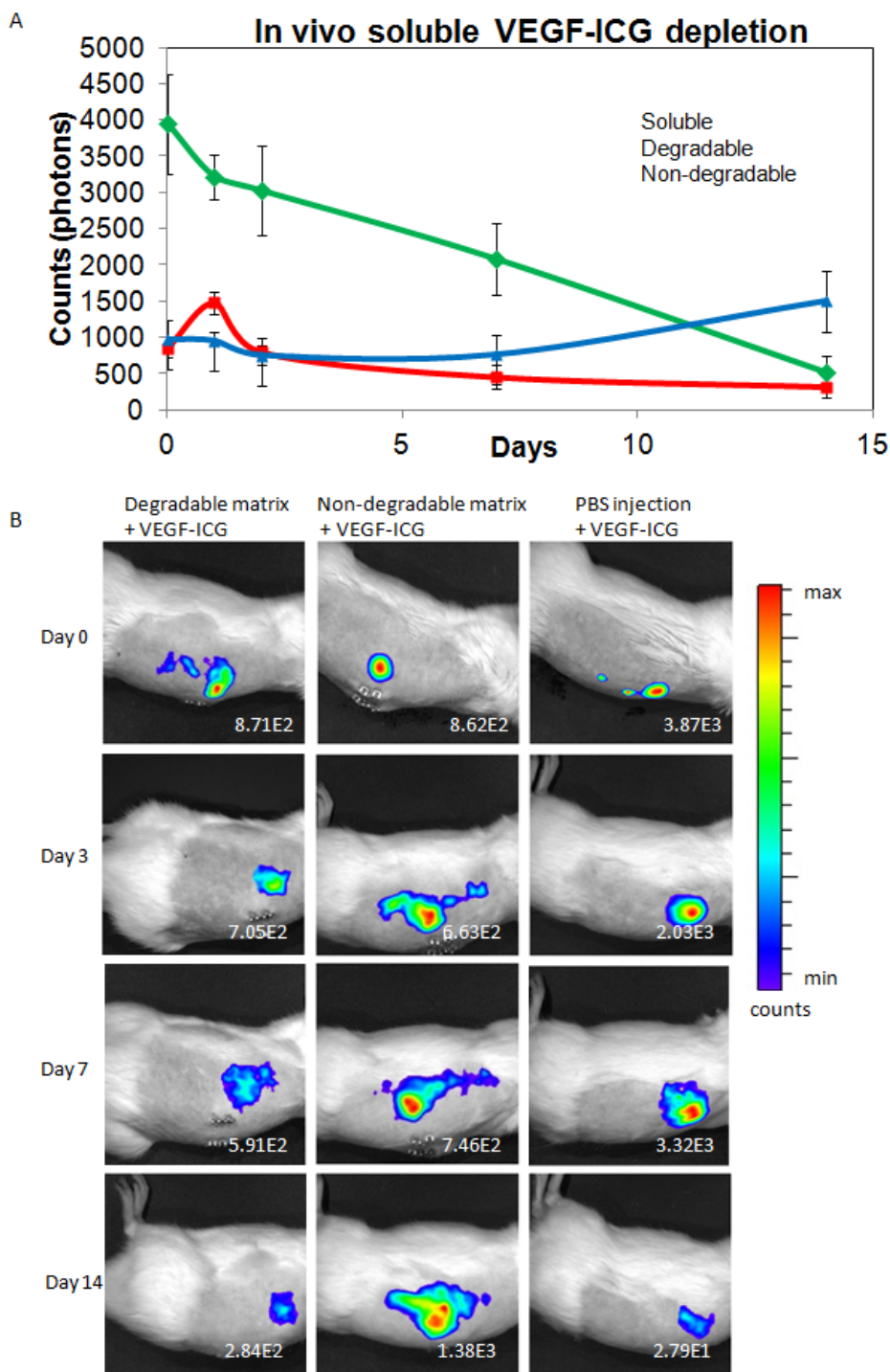
Figure 3.4 Degradation of subcutaneous implants containing ICG-labeled VEGF. (A) Quantification of VEGF fluorescent signal in implants shows early release for degradable matrix and late release for non-degradable matrix. Soluble injection shows continuous decline in signal strength. N=10 (B) Representative images from IVIS scanning of fluorescently labeled VEGF in degradable implants, non-degradable implants, and PBS injection. Number indicates average counts per unit area within ROI.

We next evaluated the ability of these bio-artificial matrices to promote vascularization in a subcutaneous implantation site. Hydrogels were photopolymerized in cylindrical silicone molds (9mm dia, 2mm thick) around poly-caprolactone (PCL) mesh disks to allow for visualization and retrieval of implants. Gel formulations included unfunctionalized PEG-DA, MMP-degradable, MMP-degradable + RGD, or MMP-degradable + RGD + VEGF. The gel concentrations of 10% (w/v) PEG-DA or A-PEG-GPQ-PEG-A [213], 2.8 µmol/mL A-PEG-RGD [214], and 80 µg/mL A-PEG-VEGF [211] were used. Hydrogel constructs were implanted dorsally in male Lewis rats. At 2 or 4 weeks, subjects were perfused with a radio-opaque silicon-based vascular contrast agent to gather quantitative and 3D structural data on patent blood vessel ingrowth [215]. Examination of explanted constructs revealed that hydrogels remained intact except for degradation by invading blood vessels, even after 4 weeks in vivo. Micro-CT analysis of the scanned constructs was gated within the periphery of the PCL ring to ensure only vessels inside the hydrogel were measured (**Fig. 3.5**). Evaluation of the scanned explants revealed approximately 6-fold increased vascular density at 2 weeks and 12-fold increased vascular density at 4 weeks for degradable gels containing adhesive ligands, degradable sites, and VEGF compared to all other groups. The patency of the neo-vasculature was shown to be connected to the host circulatory system because contrast agent perfused through the aorta reached the vessels in the implant. These results validate the in vivo vascularization potential of the engineered hydrogel constructs.

Bio-artificial matrices with VEGF increase rate of perfusion in a mouse model of hind limb ischemia
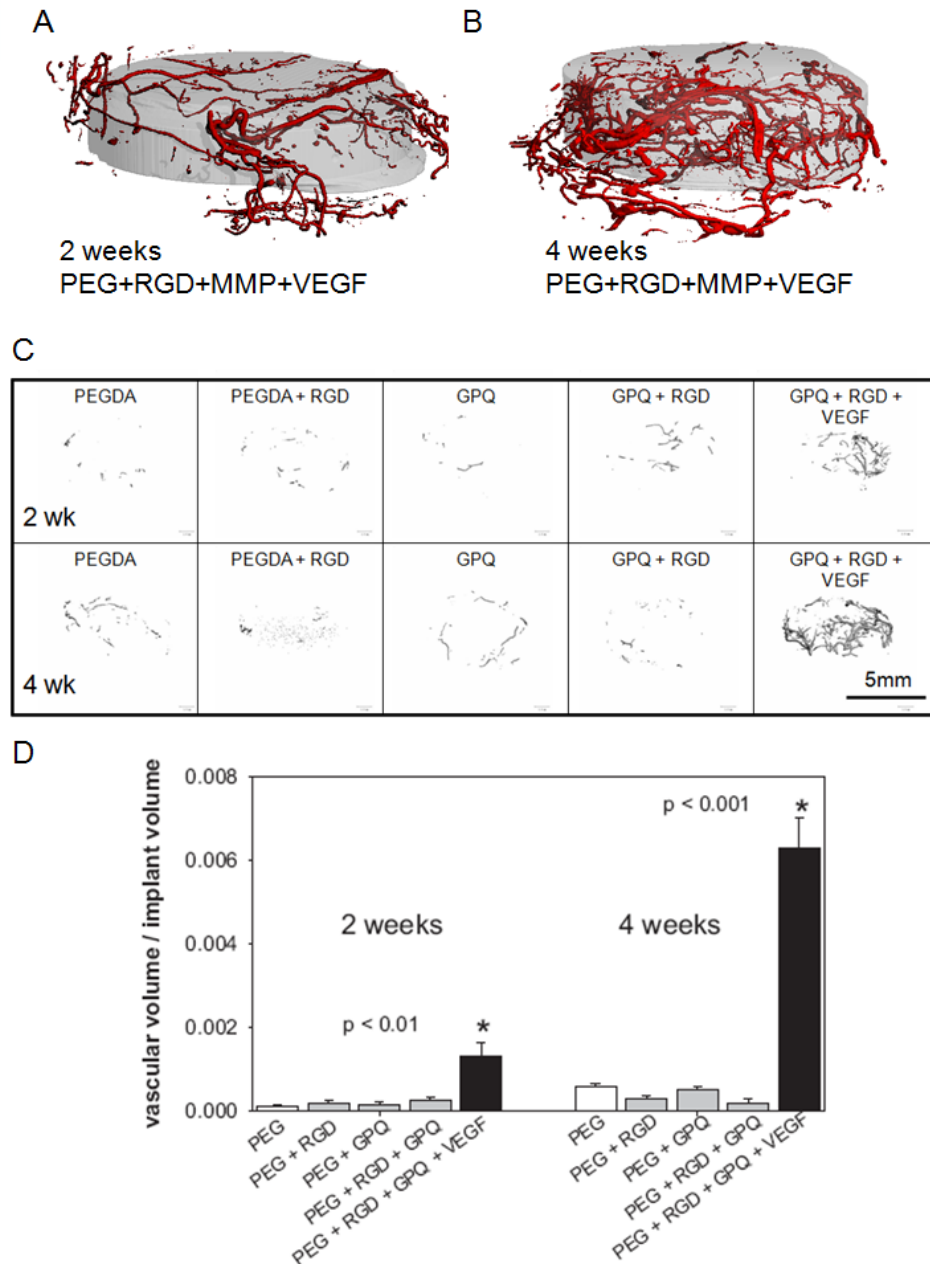
Figure 3.5 MicroCT tomograms of bio-artificial matrices implanted subcutaneously in rats perfused with Microfil radio-opaque contrast agent. (A,B) At 2 and 4 weeks, GPQ + RGD + VEGF implants showing vasculature in surrounding tissue growing into implant, grey area defines extent of implant. (C) Representative scans from non-degradable implants with no adhesive ligands (PEG-DA), non-degradable with adhesive ligands (PEG-DA + RGD), degradable with no adhesive ligands (GPQ), degradable with adhesive ligands (GPQ + RGD), and degradable with adhesive ligands and bound VEGF (GPQ + RGD + VEGF). (D) Quantification of vascular volume / total implant volume. ± s.e.m. N=5

Depending on the therapeutic application, bio-artificial matrices can be delivered as pre-formed constructs containing cells and other regenerative agents such as growth factors, or can be delivered as macromer solutions and polymerized in situ. To test the ability of PEG-based bioartificial matrices to improve reperfusion rates in a model of peripheral limb ischemia, we chose to deliver the matrix as a macromer solution and polymerize it in situ. By delivering the matrix as a macromer solution followed by in situ polymerization, we integrated the matrix more deeply within the target tissue than application of a pre-formed construct would have allowed. Macromer solutions of the PEG-DA-based bio-artificial matrix components were formulated to include RGD and MMP-degradable sites, with or without the addition of VEGF. Our preliminary studies indicated that better cell invasion and tissue integration occurs at lower concentrations of PEG hydrogel. We therefore reduced the concentration of A-PEG-GPQ-PEG-A to 5% (w/v) for this study, but kept the concentrations of A-PEG-RGD and A-PEG-VEGF at 2.8 µmol/mL and 80 µg/mL, respectively. The left leg femoral artery of 8-9 week old 129 mice was ligated and excised in compliance with a well-established model of peripheral limb ischemia [159, 160, 216, 217]. The right leg was left undisturbed to serve as a control reference. During femoral artery excision surgery, mice received (i) no treatment, or injections of (ii) PBS (vehicle control), (iii) soluble A-PEG-VEGF, (iv) soluble hydrogel precursors, or (v) soluble hydrogel precursors with A-PEG-VEGF at 3 sites (50 µL each) in the muscle groups surrounding the femoral artery region. Injected precursor solutions were immediately polymerized with low-intensity UV light exposure. The precursor solution injected into the muscle was seen to fully polymerize in situ during necropsy of test mice, indicating that the UV light penetrated the tissue deeply enough to cross-link the precursor solution. Preliminary studies established that exposure to the same UV wavelength, intensity, and duration on skin, muscle, or small bowel mesentery resulted in no detectable inflammation, tissue damage, or increased angiogenesis. At 4 and 7 days post-surgery, mice were imaged on a Laser Doppler Perfusion Imaging

(LDPI) system to quantitatively analyze perfusion to the peripheral limb. The perfusion ratio of the ischemic limb compared to the non-ischemic limb in each animal was taken as the measurement for comparison in both the foot and the leg (ankle to proximal ligation) (**Fig. 3.6**). At day 4, the mice receiving matrix with VEGF showed a trend of increased perfusion in the leg although the differences were not statistically significant (p=0.056), and no trend was seen in the feet, although the PBS control group is slightly elevated. By day 7, animals receiving hydrogels with VEGF exhibited a 50% increase in perfusion to the legs and a 100% increase in perfusion to the feet compared to untreated subjects.
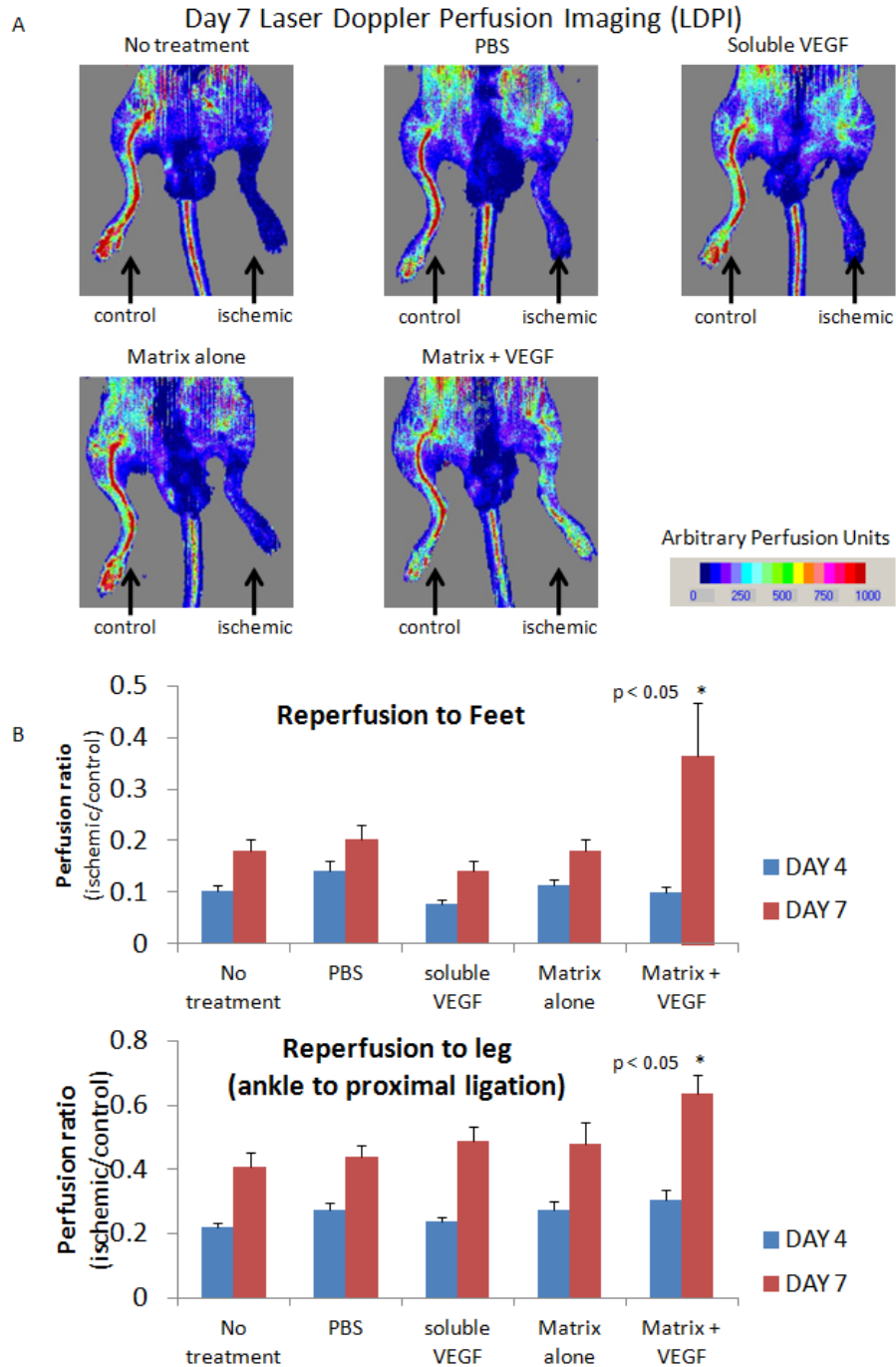
Figure 3.6 Hind limb perfusion in mice with ligated femoral artery. (A) LDPI imaging of limb perfusion at day 7 responding to treatment conditions: no treatment, PBS injection, soluble A-PEG-VEGF121-cys injection, degradable matrix with adhesive ligands (GPQ + RGD), and degradable with adhesive ligands and bound VEGF (GPQ + RGD + VEGF). (B) Quantification of perfusion ratio (normal leg : ischemic leg) at days 4 and 7 post-surgery. ± s.e.m. N=10. Data and figure produced by Natalia Landazuri

Discussion

Pro-vascularization therapy remains a significant challenge in regenerative medicine. We adapted the PEG-DA platform for in vivo vascularization applications and demonstrated efficacy with both construct implantation and in situ polymerization in subcutaneous and ischemia models. We first demonstrated ability to generate the PEGylated matrix components and form a hydrogel construct by UV photopolymerization. We showed that the hydrogels degrade in the presence of enzymes typically expressed by invading cells but not in buffer solution. We also showed that cells in the matrix require both adhesive sequences and degradable sites in order to spread within the bio-artificial gel. This result indicates that the bio-artificial material is a suitable matrix to promote tissue ingrowth and remodeling.

We showed that incorporation of VEGF in engineered hydrogel matrices modulated in vivo release kinetics. In gels containing proteolytically degradable cross-links, the matrix is designed to only release VEGF as the matrix is digested by invading cells. Degradable hydrogel matrices exhibited constant VEGF levels during the first two days followed by a gradual decrease over the next 12 days, whereas non-degradable matrices with VEGF showed nearly constant levels of VEGF over the two week implantation period. These results indicate that incorporation of degradable cross-links in the hydrogel controlled the release of VEGF from the matrix. In contrast, injected soluble VEGF levels steady declined with 90% of the signal lost by two weeks of implantation as expected for diffusion and turnover.

We next tested the ability of pre-cast constructs to vascularize in a rat subcutaneous implant model. Engineered hydrogels containing MMP cleavage sites, RGD, and bound VEGF significantly enhanced vessel ingrowth by 2 weeks with increasing vasculature at 4 weeks. Importantly, the patency of this observed vascular ingrowth at 4 weeks was preserved, as shown by the ability of contrast agent perfused through the aorta to reach vessels within the implant. Matrices lacking either VEGF or

52

RGD showed minimal tissue invasion. Non-degradable matrices failed to integrate with the host tissue on any level. We attribute the presence of long-term patent vessels at 2 and 4 weeks to controlled VEGF release and bioavailability from the degradable hydrogel. The subcutaneous implantation experiment used 10% (w/v) hydrogels, consistent with the polymer density used in published reports [210, 212, 213]. While conducting preliminary research for another in vivo study, we discovered that lower density hydrogels are potentially more useful for vascularization purposes as vessel invasion is faster and of higher density in more-easily degradable gels. Many researchers are interested in vascular-inductive matrices for cell-transplant applications, in which case vessel ingrowth will need to occur within a matter of days and not weeks to avoid ischemic-related die-off of transplanted cells. Future studies with bio-artificial matrices for construct implantation should examine ways to improve vessel density and ingrowth-rate, one method being through reducing the amount of material that needs to be degraded for cell invasion.

Lastly, we implemented in situ polymerization of the bio-artificial matrix in a mouse hind-limb ischemia functional model. Macromer solutions of matrix and matrix + VEGF injected into the muscle in areas made ischemic by femoral artery ligation were polymerized in situ with UV light. Blood perfusion to the ischemic limb was measured by LDPI and found to be greatest in animals that received matrices with bound VEGF at day 7 post-surgery. The result that the engineered matrix containing VEGF performs better than injection of soluble VEGF is noteworthy because it indicates that the delivery vehicle is acting synergistically to amplify the effect of the growth factor. It is presumed that the increased perfusion is due to growth factor sequestration in the matrix, resulting in prolonged exposure that persists as the matrix is degraded and remodeled, as shown with sustained release in the in vivo degradation experiment. Furthermore, the adhesive ligands and degradable sequences in the matrix are designed to interact with endothelial cells undergoing angiogenesis. In reperfusion to the leg, the matrix alone (no VEGF)

53

performed as well as soluble VEGF injection, indicating that the engineered adhesive and degradable hydrogel matrix itself has a beneficial healing or supportive effect. These results demonstrate the effective use a bio-artificial hydrogel to act synergistically as a directive scaffold and a growth factor delivery vehicle.

Several noteworthy studies indicate that delivery of VEGF has limited therapeutic success at achieving long-term, stable, vascular growth in humans [200]. While a strong stimulator of vascular growth, VEGF administration alone has limited ability to induce the growth of larger vessels. Long-duration exposure is necessary to produce stable microvasculature that does not regress after withdrawal of the VEGF stimulus [218, 219]. In this study, we achieved steady vascular ingrowth continuing to a mid-range time point of 4-weeks when the study was terminated. Based on the VEGF release results, we attribute the persistent vascularization to the conjugation of VEGF to the matrix, where it is only released in a proteolytically-dependent manner as opposed to diffuse or bolus injection delivery methods. This result is consistent with other reports that have used sustained-release strategies [99, 211, 220]. By binding the growth factor to the matrix, a persistent pro-vascularization signal is generated that does not quickly ramp up and fade away as in a soluble delivery method. The modular nature of bio-artificial matrices makes studying the effects of other pro-vascularization factors in the same controlled environment extremely straightforward. Future studies incorporating more or different factors may be able to achieve even more robust healing effects.

The use of RGD as an adhesive ligand is often disputed as it is known to have lower adhesion performance than several other proteins and protein fragments [194]. However, RGD is a ligand for αvβ3 integrin, known to be highly expressed in endothelial cells undergoing angiogenesis [195], and our results have demonstrated that RGD supports vessel invasion into degradable bio-artificial matrices. The PEGDA platform is amenable to experimentation with other types of adhesive molecules. For example, ephrin was demonstrated to support endothelial cell adhesion and tubulogenesis [213].

Other adhesive ligands such as the collagen-mimetic peptide GFOGER [196], the fibronectin fragment FNIII7-10 [194], and sequences from the ECM protein laminin can be used with the bio-artificial system for studying other types of regenerative applications such as neurite outgrowth, epithelial morphogenesis [131], and osteogenesis.

Conclusion

We emphasize that our strategy is not for synthetic bio-mimetic matrices to fully recapitulate the complete biological activities of native ECM. However, from an engineering perspective, bio-artificial matrices provide many advantages that make their use for regenerative therapeutics attractive. Most importantly, bio-artificial systems provide a high level of control to the designer using reproducible and synthetic components in modular "plug and play" architecture. A major conceptual aspect of these bio-artificial matrices is their application as engineered platforms for directed cell invasion: incorporating bioactive adhesion motifs and enzyme-specific cleavage sites rather than serving as simple polymeric growth-factor reservoirs. In the implantation studies it appears that the matrix does not remain long term and is fully degraded over a period of weeks as new tissue forms. Based on this observation, the dominant mechanism of vascularization is likely cell-demanded / proteolysis-dependent release of VEGF. Further studies into the growth factor release kinetics in vivo and cellular activity at the tissue-hydrogel interface are warranted to better characterize the specific nature of the observed therapeutic effects.

Materials and Methods

Matrix synthesis and degradation profile

Peptides were custom prepared by a commercial manufacturer (AAPPTEC) and supplied at 95% purity. Two molar equivalents of A-PEG-SCM (Creative PEGworks) per mole of GPQGIWGQK were dissolved in toluene and evaporated to a thick oil; the molar ratio of A-PEG-SCM to GRGDSPC and GGRGDSPGGK-carboxyfluorescein (RGD-FITC) was 1:3. The evaporated oil was dissolved in DMF to bring the concentration of A-PEG-SCM to 50 mg/mL. The peptides to be PEGylated were added along with one molar equivalent of TEA per mole of A-PEG-SCM and reacted for 4 hours. The product was precipitated in ether and dried, then dissolved in diH_2O, sterile filtered, and purified by dialysis. Products were lyophilized and stored at -20°C. PEGylated products were run on a 20% SDS-PAGE gel to check for molecular weight increase. A-PEG-RGD-FITC was visualized directly by fluorescence to confirm small peptide PEGylation. A-PEG-GPQ-PEG-A was visualized by barium chloride / iodine stain described in [221]. Gels were degraded in vitro with 20 mU/mL collagenase-I (Sigma), 200 pM MMP-2 (Calbiochem), or 200 pM MMP-2 + 40 µM oleoyl-N-hydroxylamide (Calbiochem). Weight loss was determined by wet weight percent change.

VEGF synthesis

BL21 Star(DE3) *E. coli* (Invitrogen) were transformed with $VEGF_{121}$-cys plasmid prepped from DH5α *E. coli* (Invitrogen) following manufacturer's instructions. Transformed BL21 Star(DE3) cells were induced with 1mM IPTG at OD_{600}=0.8. After 4 hours, cells were pelleted and frozen at -20°C. Pelleted cells were thawed and lysed in B-PER protein extraction reagent (Pierce). Inclusion bodies containing $VEGF_{121}$-cys were separated from soluble protein by centrifugation at 15,000xg and were solubilized for 1

hour on ice in 10 mL B-PER reagent + 6M urea. $VEGF_{121}$-cys was purified by 6X His-Bind column (Pierce) following manufacturer's instructions with addition of 6M urea to wash and elution buffers. 2mM DTT was added to the elution fraction which was sequentially dialyzed for 24 hours against 4M urea, 1mM EDTA, 150mM NaCl, 25mM Tris-HCl, pH 7.5, followed by dialysis against 2M urea, 1mM EDTA, 150mM NaCl, 25mM Tris-HCl, pH 7.5, and dialysis against 1X PBS. Endotoxin was removed from protein solution by a Detoxi-Gel Endotoxin Removing Column (Pierce) and endotoxin levels were verified to be below 0.1 EU/mL by Limulus Amebocyte Lysate colorimetric assay (Lonza). Protein was concentrated to 1 mg/mL and stored at -80°C in 50% glycerol. $VEGF_{121}$-cys purity was verified by SDS-PAGE with Coomassie staining / Western blot and specificity by ELISA detection. $VEGF_{121}$-cys was functionalized by incubation overnight at 4°C with 50 molar excess acrylate-PEG-maleimide (Laysan Bio, custom order) in PBS. Functionalization was verified by molecular weight increase seen by SDS-PAGE and Coomassie staining. A-PEG-$VEGF_{121}$-cys activity was verified by addition to endothelial basal media (MCDB-121, 5% FBS, + ascorbate, L-glutamine) at concentration intervals and observing the effect on endothelial cell proliferation as compared to $VEGF_{165}$ (Invitrogen).

3D construct cell seeding

A-PEG-GPQ-PEG-A was dissolved in PBS at 10% (w/v) with 0.05% Irgacure 2959 (Ciba) photoinitiator. NIH3T3 cells were added at 300,000 cells/mL. 9 mm x 1 mm silicone isolator wells (Grace Bio Labs) were adhered to glass slides and filled with 70 µL PEGDA solution per well. Macromer solutions were cross-linked by exposure to 365 nm UV light at 10 mW/cm^2 for 12 min and placed in 1 mL of DMEM + 10% FBS and incubated for 24 hours. Cells in 3D culture were stained with calcein AM for imaging and to ensure viabilility.

In vivo degradation study

A-PEG-VEGF$_{121}$-cys was labeled by overnight incubation at 4°C with 200 molar excess of the dye ICG-sulfo-OSu (Dojindo). Excess dye was removed by two rounds of gel filtration through Zeba Spin desalting columns (Pierce). 150 µL constructs consisting of 10% (w/v) A-PEG-GPQ-PEG-A, 2.8 µmol/mL A-PEG-RGD, 80 µg/mL ICG-VEGF with 0.05% Irgacure 2959 in PBS were cast in 9 mm x 2 mm molds and polymerized with a 10 min exposure to UV light. Constructs consisting of 10% PEG-DA + RGD + ICG-VEGF were used as non-degradable controls, while constructs with unlabeled A-PEG-VEGF$_{121}$ were used as imaging controls. Implants were equilibrated in PBS for 24 hours to leach out any unbound ligand. Five rats per condition each received 2 dorsal subcutaneous implants or 150 µL subcutaneous injections of soluble ICG-VEGF. Rats were imaged at 745 nm excitation, 840 nm emission, and 60 s exposure time in a 700 series Xenogen IVIS machine. Images were analyzed for background-subtracted average photon counts within an ROI gated over the implant site.

Subcutaneous vascularization, microfil perfusion, and microCT imaging

Rings of 2 mm thickness PCL mesh (66% porosity, 300-500 um pore size) were made with concentric 8 mm and 5 mm sterile biopsy punches. The macroporous nature of these meshes readily allows tissue and vascular ingrowth. 100 µL constructs consisting of 10% (w/v) A-PEG-GPQ-PEG-A, 2.8 µmol/mL A-PEG-RGD, 80 µg/mL A-PEG-VEGF with 0.05% Irgacure 2959 in PBS were cast in 9 mm x 2 mm molds containing the PCL rings. Implants were equilibrated in PBS for 24 hours. 16 male Lewis rats each received 4 randomized dorsal subcutaneous implants. After sacrifice by CO_2 inhalation, rats were perfused with 0.9% saline + 4 mg/mL papaverine hydrocholoride (Sigma), followed by 0.9% saline, and 10% neutral buffered formalin. After fixation, 30 mL of 80% (v/v)

diluted MV-122 Microfil (Flowtec) was injected into the aorta with a syringe and allowed to polymerize overnight before implant retrieval. Explants were scanned at 16 µm resolution with a Scanco µCT-40 microCT machine. ROI's were gated inside the edge of the PCL rings.

Hind limb ischemia and LDPI imaging

At eight to nine weeks of age, male 129 mice (Charles River) were anesthetized with intraperitoneal injections of xylazine (10 mg/kg) and ketamine (80 mg/kg). A unilateral incision was made over the left medial thigh of the mouse. The superficial femoral artery and vein were ligated proximal to the caudally branching deep femoral artery and proximal to the branching of the tibial arteries. The portion of the artery and vein between the ligation points was excised. One hundred and fifty microliters of PBS, A-PEG-VEGF suspended in PBS, or non-polymerized A-PEG-GPQ-PEG-A (5% w/v) + A-PEG-RGD (2.8 µmol/mL) (with or without 80 µg/mL A-PEG-VEGF) + 0.05% Irgacure 2959 were injected into 3 sites in the ischemic muscle. The muscle was then exposed to 15 minutes of UV light (365 nm, 10 mW/cm^2), which induced polymerization of the matrix. As an additional control, no solution was injected to the muscle and the mice were not exposed to UV light. The skin was closed with interrupted silk sutures. LDPI (Moor Instruments) was used to evaluate the perfusion in the ischemic and non-ischemic legs at 4ms/pixel scan speed, 256 x 256 resolution in arbitrary perfusion units. Perfusion was estimated (1) in the feet and (2) in the ischemic portion of the legs not including the feet. The non-ischemic legs and feet were used as controls. The results were reported as ratios of surgery to non-surgery leg/foot for each animal to account for natural variation in vasodilation between animals.

Statistics

Statistical analyses were performed using one-way ANOVA with Tukey's test for post-hoc comparisons. For LDPI analysis, the perfusion values for the contra-lateral non-operated leg were used as covariants. A p-value of 0.05 was considered significant.

Acknowledgements

CHAPTER 4

ENGINEERING OF BIO-FUNCTIONALIZED PEG-MALEIMIDE HYDROGEL TO SUPPORT CELL ENCAPSULATION *

Summary

We developed an improved polyethylene glycol bioartificial matrix for regenerative medicine by utilizing maleimide cross-linking chemistry. This hydrogel chemistry is advantageous for cell delivery due to the mild cross-linking reaction that occurs rapidly enough for in situ delivery, while easily lending itself to "plug-and-play" design variations such as incorporation of enzyme-cleavable cross-links and cell-adhesion peptides. We have shown improved reaction efficiency, wider range of Young's moduli and polyer weight percentage gels, faster gelation, and applicability for *in situ* delivery. These numerous advantages place the maleimide crosslinked gels ahead of other Michael-addition crosslinker and polyethylene glycol diacrylate for our application of *in vivo* delivery of angiogenic therapeutics and islet cell transplantation.

Introduction

Hydrogels, highly hydrated cross-linked polymer networks, have emerged as powerful synthetic analogs of extracellular matrices for basic cell studies as well as promising biomaterials for regenerative medicine applications.[209] A critical advantage of these artificial matrices over natural networks is that bioactive functionalities, such as cell adhesive sequences and growth factors, can be incorporated in precise densities while

_____

the substrate mechanical properties are independently controlled.[222-227] Polyethylene glycol (PEG) hydrogels represent the 'gold standard' in this field due to their intrinsic low-protein adsorption properties, minimal inflammatory profile and history of safe *in vivo* use, ease in incorporating various functionalities, and commercial availability of reagents. In the present study, we explored the use of an alternative reactive cross-linking moiety for PEG hydrogels, the maleimide functional group. We demonstrate several advantages over other cross-linking chemistries, namely stoichiometric hydrogels with improved cross-linking efficiency, bioligand incorporation and reaction time scales appropriate for clinical use for *in situ* gelation. The maleimide reactive group is extensively used in peptide bioconjugate chemistry because of its fast reaction kinetics and high specificity for thiols at physiological pH.[228] For these experiments, we used a 4-arm PEG-maleimide (PEG-4MAL) macromer and compared it to 4-arm PEG-acrylate (PEG-4A), 4-arm PEG-vinylsulfone (PEG-4VS), and UV photo-cross-linked PEG-DA.

Various cross-linking chemistries have been described to create bioactive hydrogel networks of PEG macromers, with Michael-type addition reactions and acrylate polymerization being the most widely utilized.[224] Cross-linking chemistry, gelation time, polymer network structure, and buffer conditions are important considerations when selecting a hydrogel cross-linking format for basic cell biology studies or regenerative medicine applications. In PEG-diacrylate (PEG-DA) hydrogels, PEG-DA macromers are cross-linked via free-radical initiated polymerization of acrylate end groups. Free radicals are created either by chemical activation or UV cleavage of a photoinitiator with the added ability to spatially control the presentation of incorporated ligands or mechanical properties through additive [229, 230] or subtractive [231] photo-patterning. A major drawback of free-radical cross-linking is that it can significantly reduce encapsulated cell viability and is unwieldy for *in vivo* delivery of hydrogels cross-linked *in situ*. In contrast, for hydrogels cross-linked by Michael-type addition, functionalized end groups on branched PEG macromers are reacted with bi-functional or branched cross-linking

molecules. Michael-addition PEG hydrogels based on 4- or 8-arm PEG macromers with acrylate [98, 232, 233], vinyl-sulfone [234-238], and thiol [239-243] end-groups have been extensively investigated. Michael-type addition cross-linking avoids the use of cytotoxic free-radicals and UV light, but instead require a nucleophilic buffering reagent [244], such as triethanolamine (TEA) or HEPES [245], to facilitate the addition reaction. However, hydrogels formed in the presence of high concentrations of TEA have cytotoxic effects on sensitive cell types such as endothelial cells, and cells in ovarian follicles [246] and pancreatic islets.
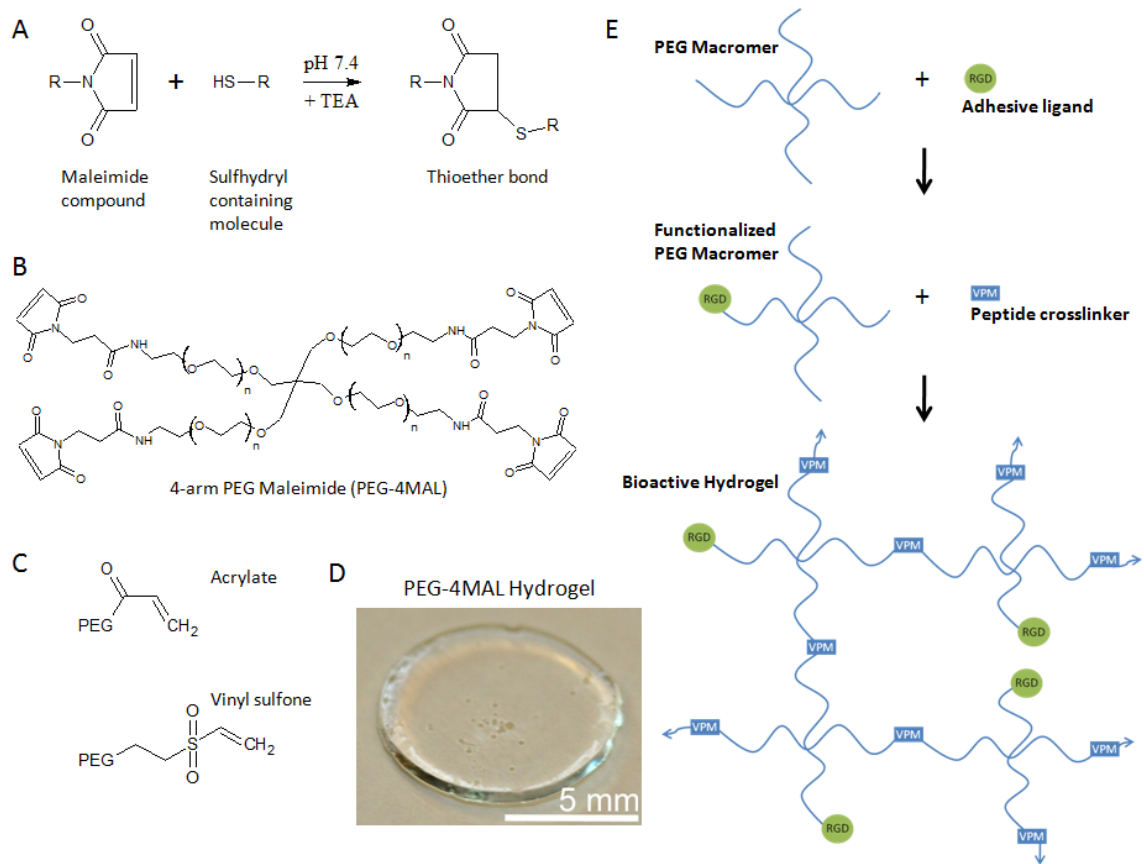
Figure 4.1 PEG-maleimide hydrogel chemistry (A) Maleimide Michael-type addition reaction. (B) 4-arm PEG Maleimide macromer. (C) Acrylate and vinyl sulfone reactive groups. (D) Sample cross-linked PEG-4MAL hydrogel. E) Michael-type addition hydrogel reaction scheme: PEG-macromers are first functionalized with RGD adhesive ligand followed by crosslinking with a thiol-flanked enzyme-degradable peptide.
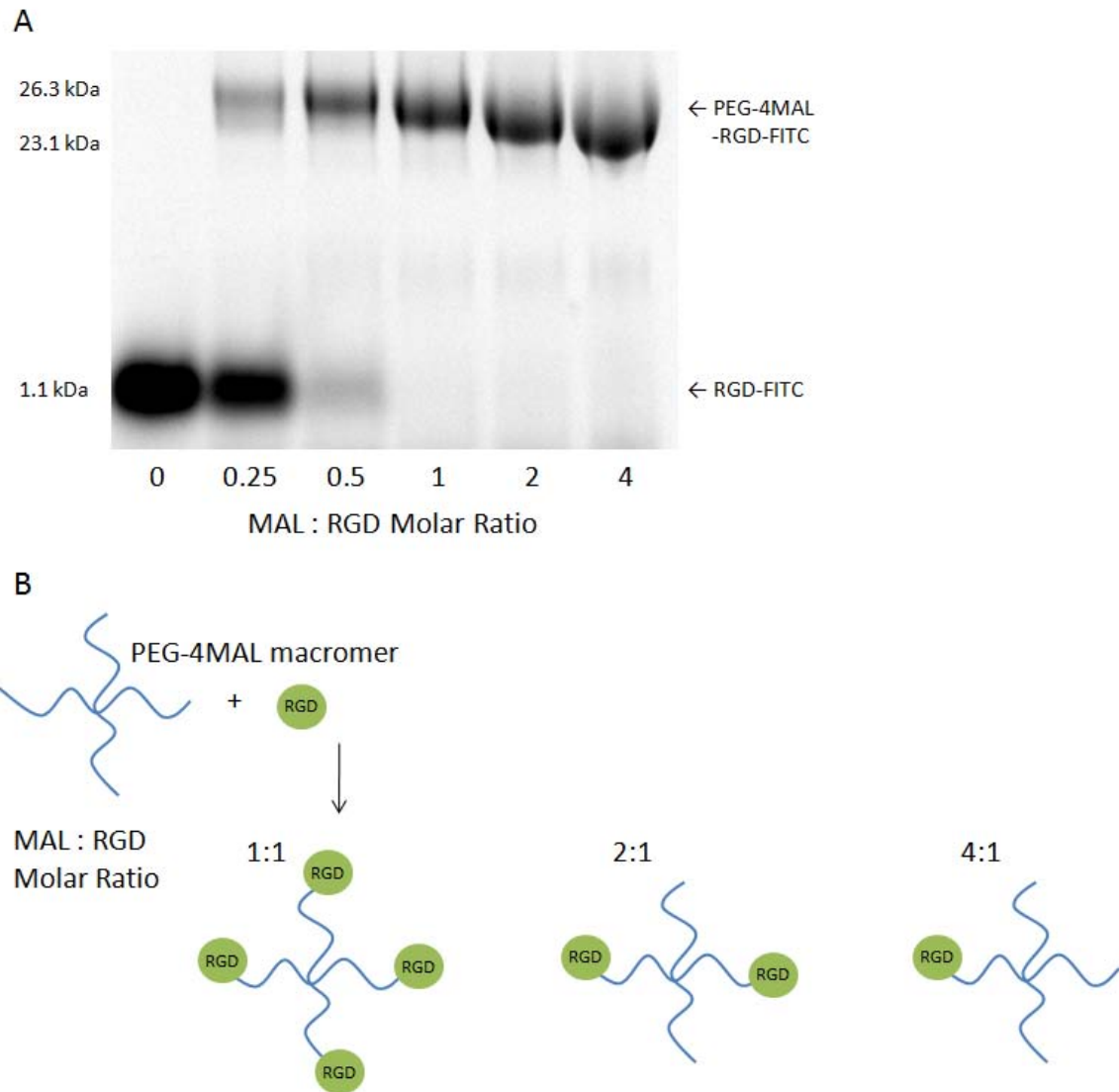
Figure 4.2 PEG-4MAL reacted with GRGSPC-Fluorescein at increasing PEG-4MAL to RGD molar ratios. (A) Increased molecular weight seen by SDS-PAGE indicates RGD conjugated to 4-arm PEG. (B) Lower MAL:RGD molar ratios with excess RGD (ex: 1:1) result in multiple RGD conjugations per 4-arm PEG compared to reactions with excess MAL (ex 4:1) have only 1 RGD conjugated per PEG.

Results

PEG-DA, PEG-4MAL, and PEG-4A macromers (20 kDa, >95% end-group substitution) were obtained from Laysan Bio. PEG-4VS (20 kDa) was synthesized as previously reported.[131] Michael-type addition hydrogels incorporating cell adhesive ligands were formed in two steps. First, end-functionalized 20 kDa four-arm PEG macromers (PEG-4A, PEG-4MAL, PEG-4VS) were reacted with a thiol-containing adhesive peptide GRGDSPC in PBS with 4 mM or 400 mM TEA at pH 7.4 for 1 hour (**Fig. 4.1**). Physical conjugation of the peptide to PEG-macromer was confirmed by increased molecular weight of fluorescein-labeled RGD visualized by SDS-PAGE (**Fig. 4.2**). RGD-functionalized PEG macromers were subsequently cross-linked into a hydrogel by addition of the dithiol protease-cleavable peptide cross-linker GCRDVPMSMRGGDRCG[247, 248] at a 1:1 molar ratio of remaining PEG reactive end groups to peptide thiols. The protease-cleavable peptide cross-linker is necessary for cell encapsulation studies (see below).[131, 249] It has been reported that RGD concentrations ranging between 25 µM and 3.5 mM support 3D cell adhesion and spreading in PEG hydrogels.[125, 212, 213, 247, 250-252] We used an RGD concentration of 2.0 mM to maximize adhesion sites while retaining cross-linking ability in tetra-functionalized PEG macromers. To determine the incorporation efficiency of RGD peptide and the conjugation efficiency of the different Michael-addition reagents, we measured unreacted/free thiols in the reaction buffer over time with the Measure-iT thiol quantification kit (Invitrogen). We observed rapid reaction of RGD with PEG-4MAL and nearly 100% incorporation at MAL:RGD molar ratios 1:1 and higher in both 4 mM and 400 mM TEA as early as 10 min (**Fig. 4.3A**). Both PEG-4VS and PEG-4A exhibited poor RGD incorporation in 4 mM TEA. At 400 mM TEA, PEG-4VS showed complete RGD incorporation only at VS:peptide molar ratios 4:1 and higher and after 60 min incubation, whereas PEG-4A required a A:peptide molar ratio of 8:1 for complete RGD incorporation at 60 min. For all 4-arm PEG hydrogels incorporating 2.0 mM RGD,

the reactive group to RGD molar ratio was 2.73:1 or greater. PEG-DA functionalization with RGD required a separate 1 hour reaction with acrylate-PEG-NHS with excess RGD peptide followed by purification and concentration of the product.

The lower reaction efficiency of PEG-4VS and PEG-4A macromers is also reflected in the inability to form low weight percentage gels. Whereas PEG-4MAL forms gels as low as 3%, we observed lower polymer weight percentage limits of 7.5% for PEG-4A, 4% for PEG-4VS, and 7.5% for PEG-DA. Additionally, the time to gelation was significantly shorter in PEG-4MAL (~1-5 min) in 4 mM TEA compared to PEG-4VS (~ 30-60 min) or PEG-4A (> 60 min) in 400 mM TEA and 10 minutes for PEG-DA under 10 mW/cm^2 365 nm UV light. Fast gelation times are critically important for uniform distribution of encapsulated cells in 3D cultures and allow for *in situ* gelation of conformal gels in regenerative medicine applications. For the remaining studies, PEG-4MAL gels were formed in 4 mM TEA while PEG-4VS and PEG-4A were formed in 400 mM TEA.

Hydrogel swelling ratio is related to the average distance between cross-links by the modified Flory-Rehner equations as described by Peppas [253, 254] and is an indication of overall hydrogel network structure [192, 226, 235, 236, 255]. A higher mass swelling ratio indicates a more loosely cross-linked network. We measured the equilibrium mass swelling ratio for PEG-4MAL, PEG-4VS, PEG-4A, and PEG-DA gels containing 2.0 mM RGD at multiple polymer weight percentages (wt/v) (**Fig. 4.3B**). For PEG-4MAL hydrogels, the equilibrium mass swelling ratio (Q_m) was greater than 500 for 3.0% gels indicating a very loose network. Q_m was dramatically lower in 4.0% PEG-4MAL gels (~150) with swelling decreasing only moderately in higher percent gels. For both PEG-4A and PEG-4VS gels, the swelling ratio was higher compared to PEG-4MAL and decreased as polymer weight percentage increased from 7.5% to 10.0%. PEG-4A swelling remained 2 -3 fold higher than PEG-4MAL swelling between 7.5% and 10%. PEG-4VS swelling was 2-fold higher than PEG-4MAL swelling at 7.5% but the swelling

ratio was identical at 10.0%. The PEG-4MAL swelling curve features an inflection that suggests a transition from a non-ideal, high-swelling network at 3.0% to a more robust, moderate-swelling network (Q_m <200) at polymer weight percentage greater than or equal to 4.0%. In contrast, PEG-4VS network swelling ratio remains above this threshold until the polymer weight percentage exceeds 7.5%. PEG-4A gels remain in a high-swelling regime even at 10%. PEG-DA had a low mass swelling ratio for all polymer weight percentages. This low-swelling ratio results from the acrylate polymerization cross-linking reaction which generates in a highly entangled and cross-linked network structure. These mass swelling ratio measurements suggest that PEG-4MAL gels offer superior network-forming characteristics compared to PEG-4VS and PEG-4A. The very low mass swelling ratio of the PEG-DA gel suggests that degradation by host-tissue or encapsulated cells would be more difficult due to denser bulk properties.

We next measured hydrogel Young's modulus using atomic force microscopy indentation testing. PEG hydrogel samples with 2 mM RGD were prepared and allowed to swell overnight in H_2O prior to mechanical testing. Measurements for hydrogels below 10% (wt/v) for PEG-DA, PEG-4A, and PEG-4VS or below 4% (wt/v) PEG-4MAL were not obtained as the material was too viscous for the AFM probe to accurately measure. Comparison among the Michael-type addition hydrogels of the same polymer weight percentage indicated the highest modulus for PEG-4MAL (**Fig. 4.3C**), consistent with a more fully cross-linked network. Young's modulus measurement for a variety of polymer weight percentages of PEG-4MAL (**Fig. 4.3D**) varied linearly with polymer weight percentage (R^2 = 0.96). Importantly, because PEG-4MAL was able to form robust networks at low polymer weight percentages, mechanical properties in the range of natural collagen gels used for 3D cell culture and *in vivo* delivery was possible with 4% and 5% PEG-4MAL gels while other higher percentage gels were much stiffer.
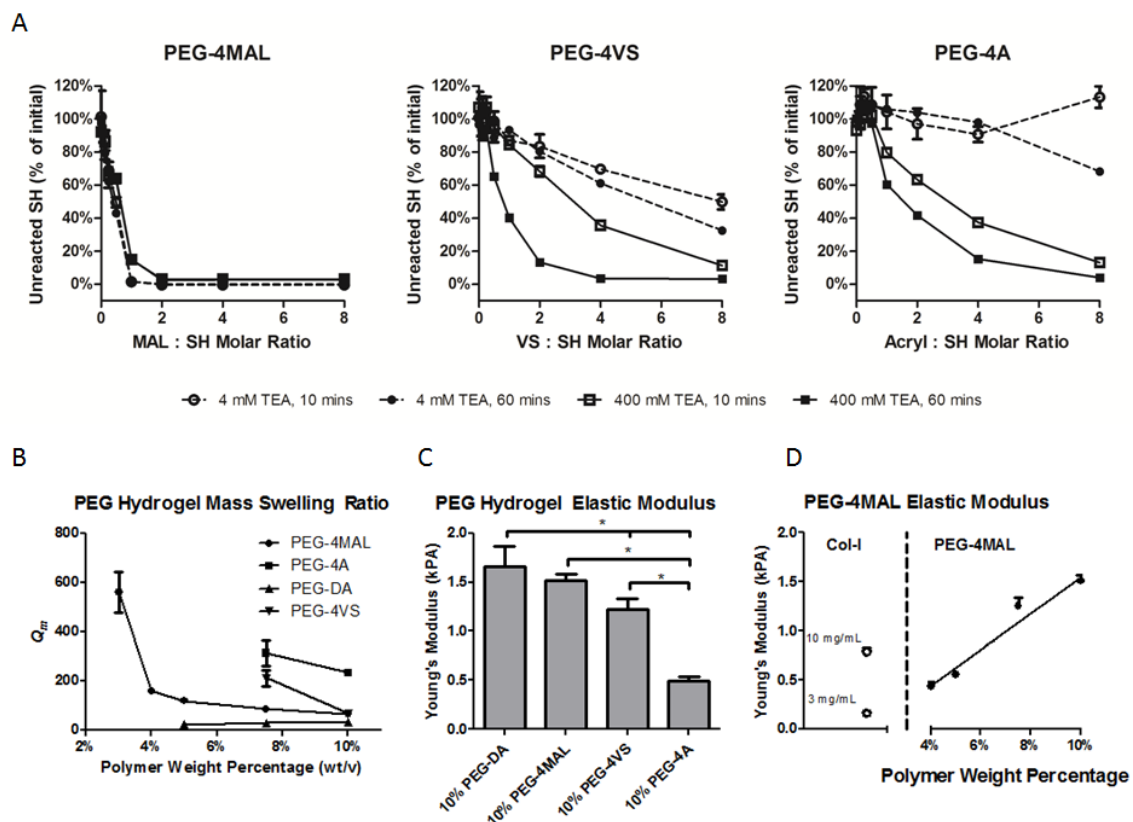
Figure 4.3 Michael-addition hydrogel reaction and material properties characterization (A) 4-arm PEG macromer functionalization with RGD peptide at 10 and 60 mins, 4 and 400 mM TEA in PBS with varying end-group to thiol molar ratio. (B) Influence of polymer weight percentage on equilibrium swelling ratio (Q_m) for networks made from PEG-4MAL, PEG-4A, PEG-4VS, or linear PEG-DA. (C) Young's modulus measured by AFM for 10% (wt/v) PEG gels. (D) Young's modulus measured by AFM for PEG-4MAL gels with varying polymer weight percentage and for 3 mg/mL collagen-I gel.
Data for (B) produced by Nduka Enemchukwu. Data for (D) produced by Vince Fiore.

To examine the ability of these hydrogels to support cellular activities, murine C2C12 myoblast cells were encapsulated in 3 mg/mL collagen-I and 10%, 7.5%, 5%, 4%, and 3% (wt/v) PEG hydrogels (50 µL) incorporating 2.0 mM RGD peptide at 3 x 10^6 cells/mL and cultured for 3 days followed by Live/Dead staining (Invitrogen) (**Fig. 4.4A**). Due to differential swelling ratios and gelation times (cells settling out of gel to bottom of well), post-encapsulation cell density varied among groups. PEG-4A and PEG-DA with cells did not form gels at polymer weight percentages below 7.5%. Three percent PEG-4MAL gels containing cells dissipated before 3 days due to cell-mediated proteolysis and were not imaged. A large fraction of cells in all conditions stained positive for viability. More dead cells were visible in 4% PEG-4VS gels and in 10% PEG-DA gels than other conditions. Cell spreading was the highest in 4% PEG-4MAL and was the most comparable to the natural collagen matrix. Encapsulated cells were also assayed for metabolic activity at 3 days by MTS assay. C2C12 cells encapsulated in PEG-4MAL and PEG-4VS had metabolic activities similar to controls consisting of samples with same number of cells seeded at day 0. Collagen gels had metabolic activity significantly higher than the initial seeding density indicating signs of cell proliferation. 4% PEG-4VS, PEG-DA, PEG-4A, gels had significantly lower metabolic activities compared to controls, indicating cell loss attributed to cyto-toxicity. Notably metabolic activity was only 60% of the control in PEG-DA and PEG-4A gels. Exposure to high TEA concentrations, free radicals, and UV light could be responsible for the lower metabolic activity/viability. We observed that high TEA concentrations (400 mM) alone had negative effects on sensitive cells types such as endothelial cells (HUVEC) assayed by MTS assay (**Fig. 4.5**).

Lastly, we examined the potential for *in situ* application of PEG-4MAL as a myocardial surface patch. A 5% PEG-4MAL precursor solution with addition of labeled FITC-PEG-MAL for visualization was mixed and pipetted directly onto the pericardium of a rat heart. The hydrogel formed rapidly and was observed to bond with the contacting

tissue. Hematoxylin and eosin staining showed a continuous interfacial surface between the hydrogel and the myocardial wall (**Fig. 4.4B**). Fluorescence microscopy of the hydrogel-tissue interface revealed excellent hydrogel incorporation into the tissue with a penetration depth of approximately 50 µm. The FITC signal penetration was not due to diffuse or unbonded FITC-PEG-MAL which would have washed out during the multiple wash steps of the tissue fixation, processing, and staining procedures.
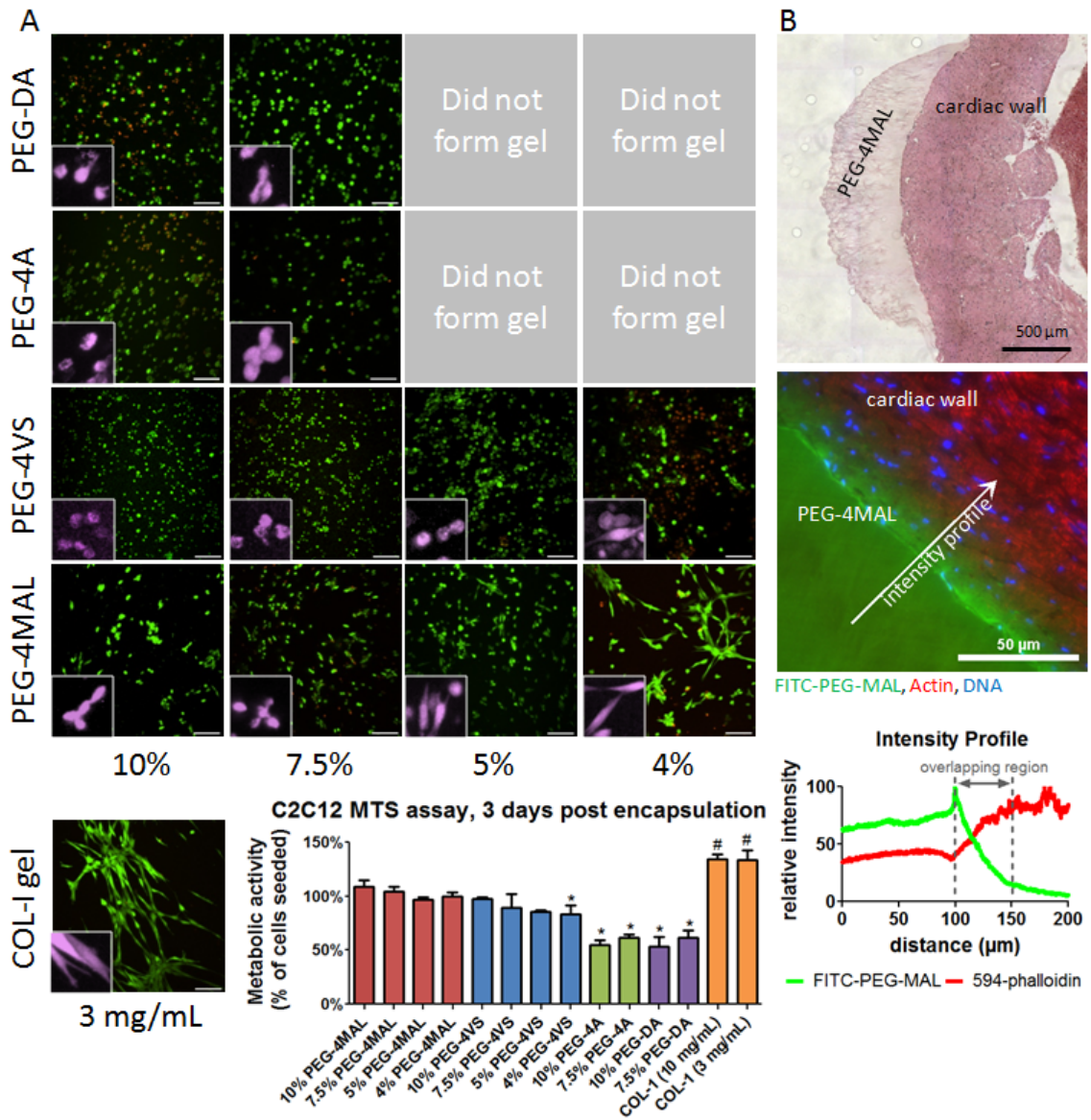
Figure 4.4 Hydrogel cyto-compatibility and tissue integration properties (A) Live/Dead staining of C2C12 murine myoblasts encapsulated in PEG hydrogels of varying polymer weight percentage compared to collagen-I gel (3 mg/mL). Cross-linked hydrogels could not be generated for low percentage PEG-4A and PEG-DA gels. Scale bar = 100 µm. Inset false color higher magnification showing individual cell spreading. MTS metabolic activity assay of encapsulated C2C12 cells indicates viability similar to number of cells seeded for PEG-4MAL and PEG-4VS, with PEG-4A and PEG-DA approximately 60% (B) H&E stain of PEG-4MAL matrix cross-linked directly on mouse myocardial wall. PEG-4MAL matrix incorporating 1% polymer substitution FITC-PEG-MAL cross-linked directly on mouse myocardial wall, counterstained with Alexa-Fluor 594 phalloidin and DAPI. Fluorescence intensity profiles for FITC-PEG-MAL and 594-phalloidin illustrate a physical incorporation depth of hydrogel into tissue of approximately 50 µm.
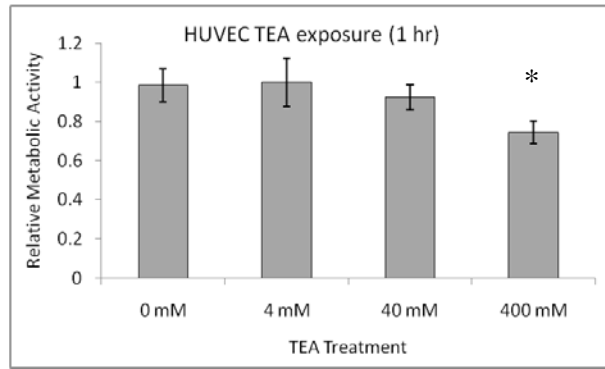
Figure 4.5 MTS assay of HUVEC exposed to high concentrations of TEA

Discussion

The PEG-4MAL, PEG-4VS, and PEG-4A 4-arm macromers are identical in structure aside from the reactive end groups and should form similar networks if all the available reactive groups are able to combine with the dithiol cross-linker at 100% efficiency. However, the considerable differences in RGD incorporation, swelling behavior, gelation time, Young's modulus, and cell viability observed among the different Michael-type addition reactive groups indicates that hydrogel cross-linking efficiency and gelation are markedly different among the reactive macromers. Taken together, our results indicate that PEG-4MAL exhibits faster reaction kinetics and tighter network structure than PEG-4A or PEG-4VS. Additionally, we found that the PEG-4MAL cross-linking reaction requires two orders of magnitude less TEA than either PEG-4A or PEG-4VS. Furthermore, we were able to create hydrogels of lower polymer weight-percentage and with a wider range of Young's moduli than gels based on PEG-DA, PEG-4A, or PEG-4VS. Importantly, low polymer weight percentage PEG-4MAL gels could be formed with mechanical properties that ranged in the low modulus environment of naturally-derived extracellular matrices such as type I collagen. These lower polymer weight percentage PEG-4MAL networks promoted increased spreading of encapsulated cells which could not be recapitulated in the other macromers. Many published articles report gelation times on the order of 15-60 minutes for Michael-addition crosslinking [98, 245, 256, 257] which is unwieldy for *in situ* clinical application where the gel must set up quickly and not flow from the administration site or be diluted with fluid. We found that PEG-4MAL hydrogels had significantly faster cross-linking

times of 1-5 minutes depending on the weight percentage and hold strong potential for clinical use with *in situ* gelation.

Conclusion

These results establish PEG-4MAL hydrogels with improved cross-linking efficiency, bioligand incorporation, encapsulated cell viability and reaction time scales appropriate for *in situ* gelation as versatile synthetic analogs of extracellular matrices for basic cell studies and regenerative medicine applications.

Methods

Measure-iT Thiol Assay

Serial dilutions of end-group functionalized PEG macromers were added to a standard concentration of 10 mM GRGDSPC in 4 or 400 mM TEA in PBS. At specified time points, the reaction was quenched by 1:100 dilution in water. One hundred microliters of PEG-RGD plus 10 μL of thiol-quantitation reagent was added per well of a black 96-well plate and read using a microplate reader. Dilutions of RGD in 4 or 400 mM TEA in PBS were used as standards. All samples were measured in triplicate.

PEG macromer synthesis

For PEG-4VS, 4-arm PEG (Sunbright PTE-20000, MW=19858; NEKTAR Therapeutics, San Carlos, CA) was functionalized at the OH-termini with divinyl sulfone (Sigma-Aldrich) as described previously [131, 256]. In brief, PEG-4VS was synthesized by reacting a dichloromethane solution of the PEG-OH (previously dried over molecular sieves) with NaH under argon gas and then, after hydrogen evolution, with diVS (molar ratios: OH 1 / NaH 5 / diVS 50), at room temperature for 3 days, under argon with

stirring. The resulting solution was neutralized with 99.8% acetic acid and filtered through filter paper until clear. VS-functionalized PEG was then precipitated in ice-cold diethyl ether, washed, and re-dissolved in dichloromethane; this cycle was repeated twice to remove all excess diVS, and the PEG-4VS was finally dried under vacuum. The success of VS conversion on the OH-termini was confirmed by NMR spectroscopy to be 90-95% as previously described [131].

For PEG-DA hydrogels, the protease degradable peptide cross-linker GCRDVPMSMRGGDRCG (VPM) was incorporated into the backbone of the PEG-DA macromer as previously reported [249]. PEG-diacrylate (3400 MW, Laysan Bio) was reacted with the VPM peptide at a 2:1 PEG to peptide molar ratio in PBS + 400 mM TEA for 6 hours at 1 mg/mL PEG concentration to create the macromer acrylate-PEG-VPM-PEG-acrylate. The reaction product was dialyzed three times against di-H_2O and lyophilized for storage. The cell adhesion peptide GRGDSP was similarly conjugated to PEG-acrylate with the amine-reactive molecule acrylate-PEG-NHS (Laysan Bio) in 50 mM sodium biocarbonate buffer at 1:2 molar ratio for 6 hours followed by dialysis against di-H2O and lyophilization. PEG-peptide conjugates were confirmed by molecular weight increases of products vs. reactants on SDS-PAGE.

PEG Hydrogel Formation

PEG-DA gels were formed by adding 2 mM acrylate-PEG-RGD with various polymer weight percentage solutions of acrylate-PEG-VPM-PEG-acrylate in PBS + 0.05% Irgacure 2959 (Ciba) photoinitiator and exposure to 10 mW/cm^2 UV light for 10 minutes. Michael-type addition PEG hydrogels (PEG-4A, PEG-4VS, PEG-4MAL) were formed by reacting 4-arm functionalized PEG-macromer with the cell-adhesion peptide GRGDSPC followed by cross-linking with the protease degradable peptide VPM at stoichiometrically balanced 1:1 cysteine to remaining reactive group molar ratio. For

most experiments, PEG-4A and PEG-4VS were reacted in PBS + 400 mM TEA, pH 7.4, whereas PEG-4MAL was reacted in PBS + 4 mM TEA, pH 7.4.

Mass Swelling Ratio

Six hydrogels per condition were formed in 9 mm diameter x 1 mm deep silicone isolator wells sandwiched between two coverslips coated in Sigmacote® (Sigma-Aldrich). After cross-linking, hydrogels were allowed to freely swell in di-H_2O for 24 hours and the swollen hydrogel mass measured. Hydrogels were then snap-frozen in liquid N_2 and lyophilized followed by dry mass measurement. The mass swelling ratio is reported as the ratio of swollen mass to dry mass.

AFM Modulus Testing

Using an MFP-3D-BIO atomic force microscope (Asylum Research; Santa Barbara, CA), samples were probed under fluid conditions (ultrapure-H_2O) using a pyramidal tipped-silicon nitride cantilever (Bruker, Camarillo, CA). Cantilever spring constants were measured prior to sample analysis using the thermal fluctuation method,[258] with nominal values of 20-30 mN/m. The force-indentation curve was obtained for each measurement and then analyzed with a Hertzian model for a pyramidal tip (Wavemetrics, IgorPro software routines) from which the Young's modulus values were calculated. The sample Poisson's ratio was assumed as 0.33, and a power law of 2.0 for the sample indentation distance was used to model tip geometry. All AFM measurements were made using a cantilever deflection set point of 100 nm, and the rate of indentation was 22.86 µm/s. 100 nm was chosen as the cantilever deflection set point for mechanical testing, as this corresponds to loading forces of approximately 5-10 nN. This scale of probe conditions is within the range of the traction forces applied through single adhesions to the ECM, and is thus a relevant range for mechanical testing [259],

[260]. Furthermore, similar testing forces have been recently published for PEG-containing hydrogels [261]. A minimum of 9 independent measurements was obtained and analyzed for each sample condition.

Cell Encapsulation

Murine C2C12 myoblast cells (ATCC) were encapsulated in 3 mg/mL collagen-I or 10%, 7.5%, 5%, and 4% (wt/v) 50 µL PEG matrices with 2 mM RGD at 3×10^6 cells/mL and cultured in DMEM + 20% fetal bovine serum + 1% penicillin/streptomycin. PEG-4A and PEG-4VS were cross-linked with VPM peptide for 1 hour in 400 mM TEA. PEG-4MAL was cross-linked with VPM peptide for 10 minutes in 4 mM TEA. PEG-DA was cross-linked by addition of 0.05% Irgacure 2959 and 10 min exposure to a UV lamp at 10 mW/cm^2. At 3 days post-encapsulation, culture media was replaced with PBS containing 2 µM calcein AM and 4 µM ethidium homodimer-1 for Live/Dead staining. Hydrogels were incubated in Live/Dead stain for 30 minutes and visualized on a Nikon-C1 laser scanning confocal microscope with a 20X air objective. Z-stack projections through a 100 µm thick section of the swollen hydrogel were rendered. For MTS measurements, gels containing cells were degraded with 1 mg/mL collagenase 1 in PBS to eliminate differences due to diffusivity in the gels followed by incubation for 4 hours with MTS reagent (Promega). For direct effects of TEA on cell viability, human umbilical vein endothelial cells (HUVEC, Lonza) were suspended in PBS containing 0, 4, 40, or 400 mM TEA pH 7.4 for one hour. The cells were subsequently examined for differences in metabolism by MTS assay (Promega).

Myocardial Patch

Fifty microliters of 5% PEG-4MAL with 2 mM RGD hydrogel and 1% dry weight substation of labeled FITC-PEG-MAL for visualization in 4 mM TEA was mixed

and pipetted directly onto the pericardium of a freshly excised rat heart. The tissue was fixed and processed for preservation in Immuno-Bed (Polysciences) plastic resin, sectioned at 2 µm, and counterstained with Alexa-Fluor 594-phalloidin (Invitrogen) and DAPI.

Acknowledgements

CHAPTER 5

IN VIVO ISLET GRAFTING AND VASCULARIZATION
POTENTIAL OF ENGINEERED HYDROGELS IN HEALTHY RATS

Summary

Polyethylene glycol (PEG)-based matrices were designed to support pancreatic islet encapsulation and *in vivo* vascularization. VEGF, a potent stimulator of angiogenesis, was tethered to the matrix by pre-functionalization with 4-arm PEG maleimide. The lifetime of VEGF signal in the matrix was greater than two weeks *in vitro* and one week *in vivo*. Isolated rat islets encapsulated in PEG-maleimide hydrogel matrices remained viable for at least 5 days in culture, secreted insulin, and sprouted endothelial processes when stimulated with VEGF. Islets transplanted in the small bowel mesentery of healthy rats with the PEG-4MAL matrix as a delivery vehicle grafted to the host tissue and intra-islet endothelial beds were re-perfused as visualized by FITC-lectin perfusion staining. Islets encapsulated in photo-cross-linked PEG-diacrylate showed low insulin secretion *in vitro* and poor grafting potential *in vivo*. These results establish the validity of PEG-4MAL engineered matrices as a vascular-inductive cell delivery vehicle and warrant their further investigation as islet transplantation vehicles in diabetic animal models.

Introduction

Type 1 diabetes affects one in every 400-600 children in the US and as many as three million Americans in total. Standard therapy with exogenous insulin is burdensome, associated with significant hypoglycemia risk, and only partially efficacious in preventing long term complications.

Pancreatic islet transplantation has emerged as a promising therapy for type 1 diabetes, a safer alternative to whole organ transplantation and a long-term replacement for exogenous insulin therapy. However, this cell-based biological therapy is significantly limited by acute and long-term rejection of allografted cells due in part to inadequate revascularization of transplanted islets resulting in reduced islet viability, function, and engraftment. Biomaterials have long been investigated as a means to improve or augment islet and beta cell transplants. There are two distinct approaches to islet encapsulation: one strategy is to encapsulate donor cells in a barrier material that isolates them from the host immune system but allows for passive transport of oxygen, glucose, insulin, and other small molecules. The alternative is the administration of immuno-suppressive drugs to prevent rejection by host lymphocytes of islets infused directly into host organs such as the liver or kidney, sometimes augmented by an engineered delivery vehicle.

West and Anseth developed UV-initiated free radical polymerization schemes for crosslinking PEG hydrogels and proved their efficacy for cell encapsulation and tissue engineering studies [262-266]. Hubbell published early work showing islet cell survival in encapsulating PEG hydrogel [267] and later Anseth showed promotion of pancreatic beta cell [268-270] and islet activity [130, 271, 272] in PEG hydrogels.

We engineered PEG-4MAL hydrogel matrices as an islet engraftment and vascularization delivery vehicle. The PEG-4MAL hydrogel chemistry is advantageous for cell delivery due to the mild cross-linking that occurs rapidly enough for *in situ* delivery, while easily lending itself to "plug-and-play" design variations. Combined with a novel transplantation model, we developed a robust strategy incorporating advanced biomaterials for rapid vascularization of islet cell grafts. The innovation in this project lies in the engineering of a bioactive hydrogel delivery vehicle that promotes controlled vascularization of transplanted pancreatic islets via on-demand release of angiogenic factors. Based on previous reports that sustained delivery of VEGF from a PEG hydrogel [105] results in stable vasculature, we hypothesized that controlled/sustained presentation

of angiogenic cues within this bioartificial matrix would enhance the vascularization and function of transplanted islets. This strategy is fundamentally different from other biomaterial approaches (reviewed in [197, 273]) focusing on coatings for immunoprotection [130, 272, 274, 275] and simple matrix carriers that serve as growth factor reservoirs [136, 138, 182, 183, 188, 189] but do not control the delivery profile of bio-therapeutics. By controlling the delivery of angiogenic factors and tissue invasion in an on-demand fashion, we hypothesize that these engineered delivery matrices will promote rapid vascularization of the islets to effectively support islet viability and function. Another innovative feature is the development of a novel implantation site in the small bowel mesentery. In contrast to other commonly used implant sites such as subcutaneous space, epididymal fat pad, and renal subcapsule [276, 277], we explore the small bowel mesentery as a novel islet implantation site with significant vascularization potential, accessibility, and direct supply to the hepatic portal vein. The liver is significant sink of physiologically produced insulin where circulating blood glucose is quickly converted to stored glycogen. By transplanted islets in a vascularized bed located upstream from the liver, small amounts of insulin produced may have a greater effect on reducing blood sugar as the insulin will be more concentrated when it reaches the liver than had it been diluted through the peripheral circulation if the islets were transplanted in more remote sites such as subcutaneously.

VEGF was selected as the angiogenic agent due to multiple reports indicating that VEGF-A augments islet vascular bed formation, insulin production, and islet cell mass [278-280] and has been reported to be essential for islet revascularization and function [177].

Results

We engineered PEG-based hydrogels cross-linked by maleimide Michael-addition chemistry as described in the previous chapter. To form bioactive hydrogels, a 4-arm PEG-maleimide macromer was first reacted with the cell adhesive sequence GRGDSPC followed by crosslinking into a gel with a cysteine-flanked proteolytically degradable peptide sequence GCRDVPMSRMGGDRCG (VPM). VEGF$_{165}$, a homodimer protein with C-terminal unpaired cysteine, was physically incorporated into the gel by pre-incubation with the PEG-4MAL macromer prior to crosslinking. Conjugation of RGD and VEGF to PEG-4MAL was confirmed by increases in molecular weight on SDS-PAGE gels (**Fig. 5.1 A**). We compared the performance of RGD/VEGF functionalized PEG-4MAL gels with previously described PEG-DA gels (Chp. 3).

We examined the release profile of VEGF from PEG-4MAL hydrogel *in vitro* and *in vivo* (**Fig. 5.1 B-D**). VEGF was labeled with VivoTag-S 750 (Perkin Elmer), an amine-reactive near-infra-red fluorochrome coupled via an NHS ester linkage to make VEGF-750. After purification from free dye with Zeba desalting columns, conjugation of VivoTag-S 750 to VEGF was confirmed by SDS-PAGE and infrared imaging of the labeled protein band. Cylindrical PEG-4MAL hydrogels (9mm x 1 mm) containing 10 µg/mL VEGF-750 were cast in silicon molds, floated in media baths of PBS, and imaged on an IVIS Lumina (Caliper Life Science) *in vivo* imaging system due to its near-IR imaging and analysis capabilities. Collagenase-I enzyme was added to half of the samples and gels were imaged daily for VEGF-750 release into the media over two weeks. The collagenase-treated samples degraded completely overnight and released all of their VEGF into the media. Samples in PBS retained a strong IR signal confined to the implant volume with 40% signal remaining at 14 days ($\tau_{1/2} = 2.67$ days). In a separate experiment, PEG-4MAL hydrogels containing VEGF were incubated in PBS or collagenase and samples from the media were analyzed for VEGF content by ELISA. VEGF was released from the hydrogel upon proteolytic degradation but not when incubated in PBS. This

result confirms the measured IR fluorescence was a result of VEGF release and not free dye.

VEGF release from the hydrogel was also measured *in vivo* (**Fig. 5.2**). Gels with VEGF were implanted according to the surgical model developed for transplantation of pancreatic islets into the small bowel mesentery. PEG-4MAL hydrogels (100 µL) with 10 µg/mL VEGF-750 and 2 mM RGD were cast directly onto the small bowel mesentery. Animals were imaged by IR fluorescence through the abdominal wall at day 0, 1, 3, and 7 for VEGF-750 fluorescence with an IVIS Lumina (Caliper Life Science) *in vivo* imaging system. VEGF-750 signal bright enough to be imaged through the abdominal wall of rat persisted *in vivo* for at least 7 days with an approximate *in vivo* half life of 1.4 days. For comparison, VEGF delivered by diffusion release in calcium cross-linked alginate gels had no signal remaining at 3 days. This result indicates that the PEG-4MAL matrix can increase the lifetime of the delivered therapeutic *in vivo* over passive release (alginate).
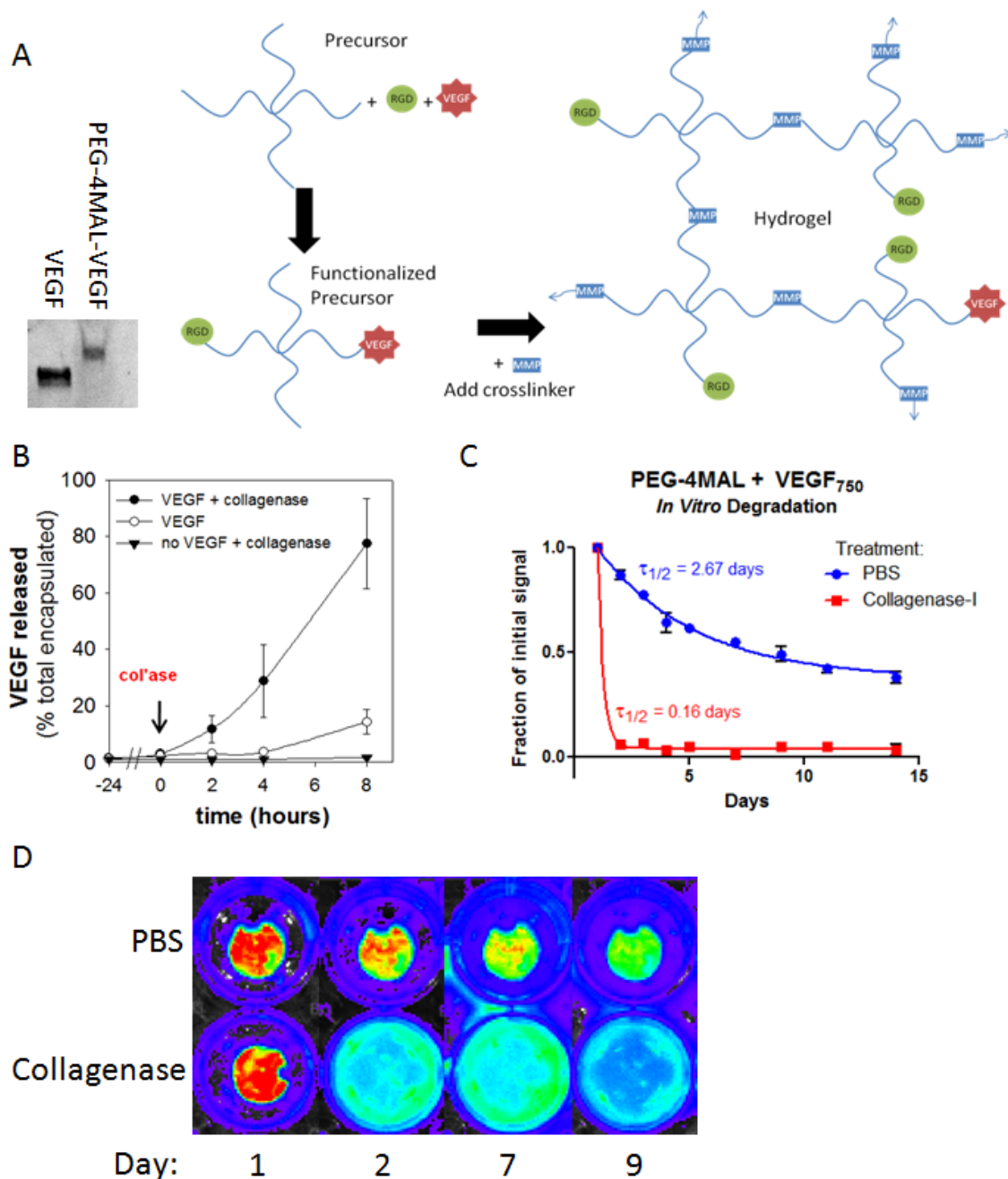
Figure 5.1 VEGF-modified PEG-4MAL hydrogel schematic and growth factor release. (A) VEGF modified by PEG-4MAL displays increased molecular weight on a western blot. RGD and VEGF are first functionalized with PEG-4MAL before crosslinking into a hydrogel with cysteine-flanked MMP-degradable cross-linker. (B) VEGF released from PEG-4MAL gels into the media measured by ELISA from gels treated with PBS (-○-) or Collagenase-I (-●-). (C,D) IVIS fluorescence intensity quantification of VEGF-750 release from PEG-4MAL gels treated with PBS or Collagenase-I
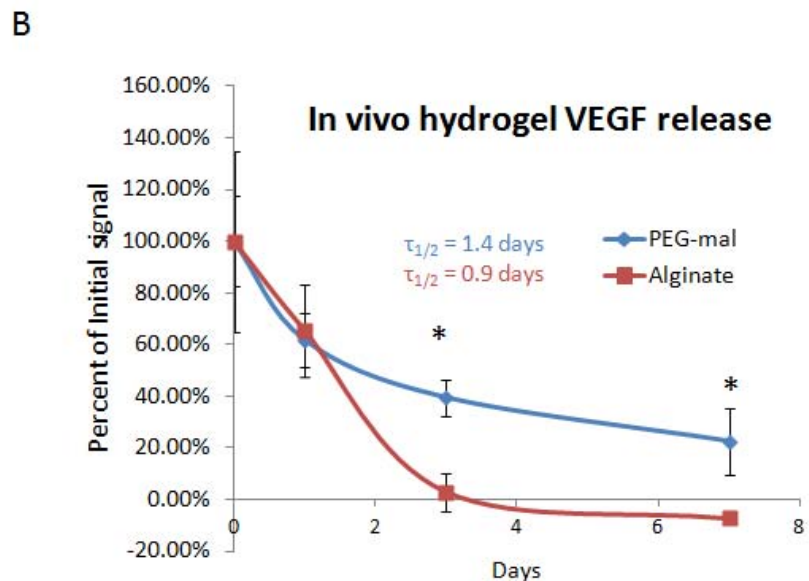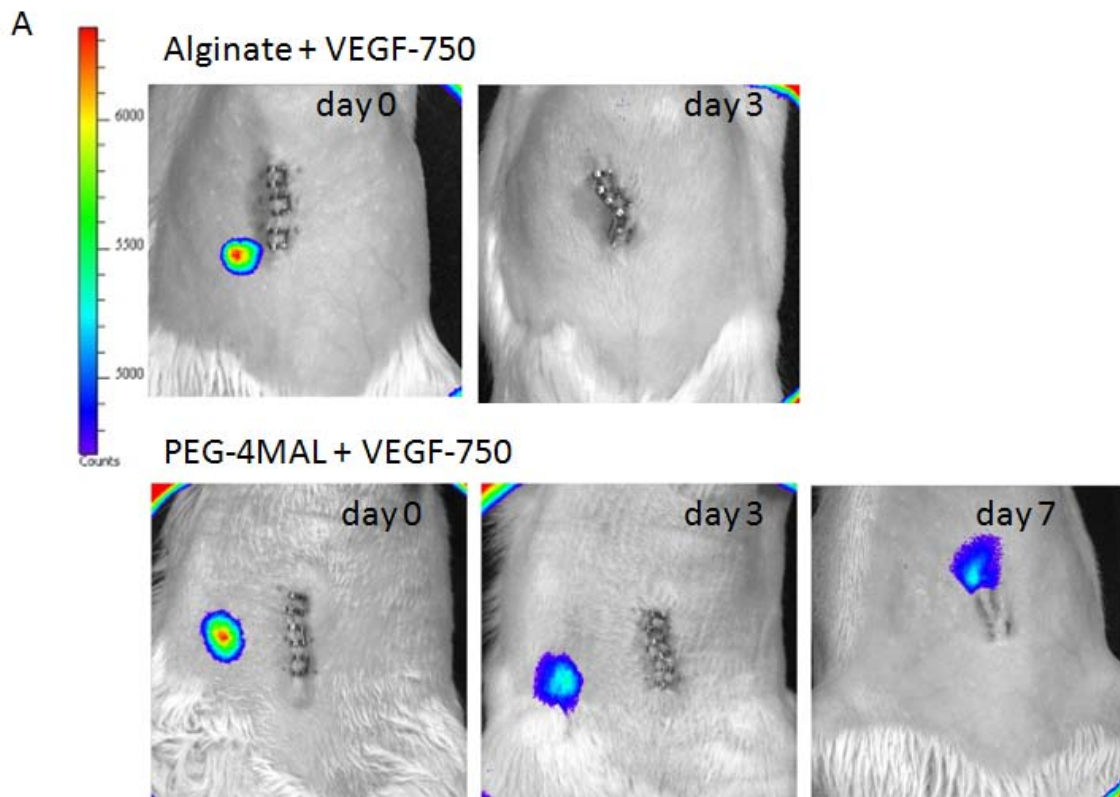
Figure 5.2 *In vivo* release of VEGF from PEG-4MAL vs. alginate. (A) IVIS imagery of hydrogel on small bowel mesentery. (B) Quantification of IVIS data.

Next we examined the effects of encapsulation in bulk PEG-4MAL and PEG-DA hydrogel on isolated islets. Pancreatic islets were isolated from healthy male Lewis rats by collagenase digestion of the pancreas and Ficoll density gradient centrifugation (**Fig. 5.3 A**). Isolated islet structures were examined for purity by dithizone staining for zinc in beta cells (**Fig. 5.3 B**) and immunostaining for insulin (**Fig. 5.3 C**). One set of islets was isolated from rats injected intravenously with FITC-lectin to visualize the intra-islet vascular system (**Fig. 5.3 D**). Islets were evaluated for survival after the encapsulation process in PEG-4MAL + 2 mM RGD gels by Live/Dead staining at 0, 3, and 5 days post-encapsulation (**Fig. 5.4 A**). Viability was high for islets at all three time points. Islets were also evaluated for metabolic activity by MTS assay (**Fig. 5.4 D**).

To evaluate endocrine function, islets were encapsulated in RGD-functionalized hydrogels PEG-4MAL, PEG-4MAL + VEGF, PEG-DA, and PEG-DA + VEGF. Collagen-I gels and free islets were used as positive control groups. Hydrogels containing islets were cultured in RPMI-1640 media supplemented with 10% FBS. At 48 hours post-encapsulation the media was measured for insulin production by ELISA (**Fig. 5.5**). Islets in PEG-DA gels produced little to no insulin, but islets in PEG-MAL produced 70 ng/mL per islet or 120 ng/mL per islet with addition of VEGF which was equivalent to free islets.

We observed islets sprouting cellular processes several hundred microns into the surrounding matrix in PEG-4MAL gels incorporating VEGF (**Fig. 5.4 B**). These sprouting structures stained positive with lectin and some of them developed lumens suggesting that they are endothelial sprouts originating from intra-islet endothelial cells. The sprouting behavior was investigated with respect to choice of adhesive peptide (**Fig. 5.4 C**). Hydrogels containing the laminin-derived peptide IKVAV were compared to fibronectin-derived RGD, collagen-I gels, un-functionalized PEG-4MAL gels, and PEG-4MAL gels with RGD but not VEGF. Samples were scored according to percentage of islets in the gel that were exhibit sprouting behavior at 48 hours. Collagen-I performed

the best with 95% of islets sprouting while RGD at 65% was significantly better than IKVAV at 45%. Islets in un-functionalized gels failed to sprout. Cell migration in RGD functionalized gels without VEGF was observed but it did not resemble the same type of sprouting behavior.
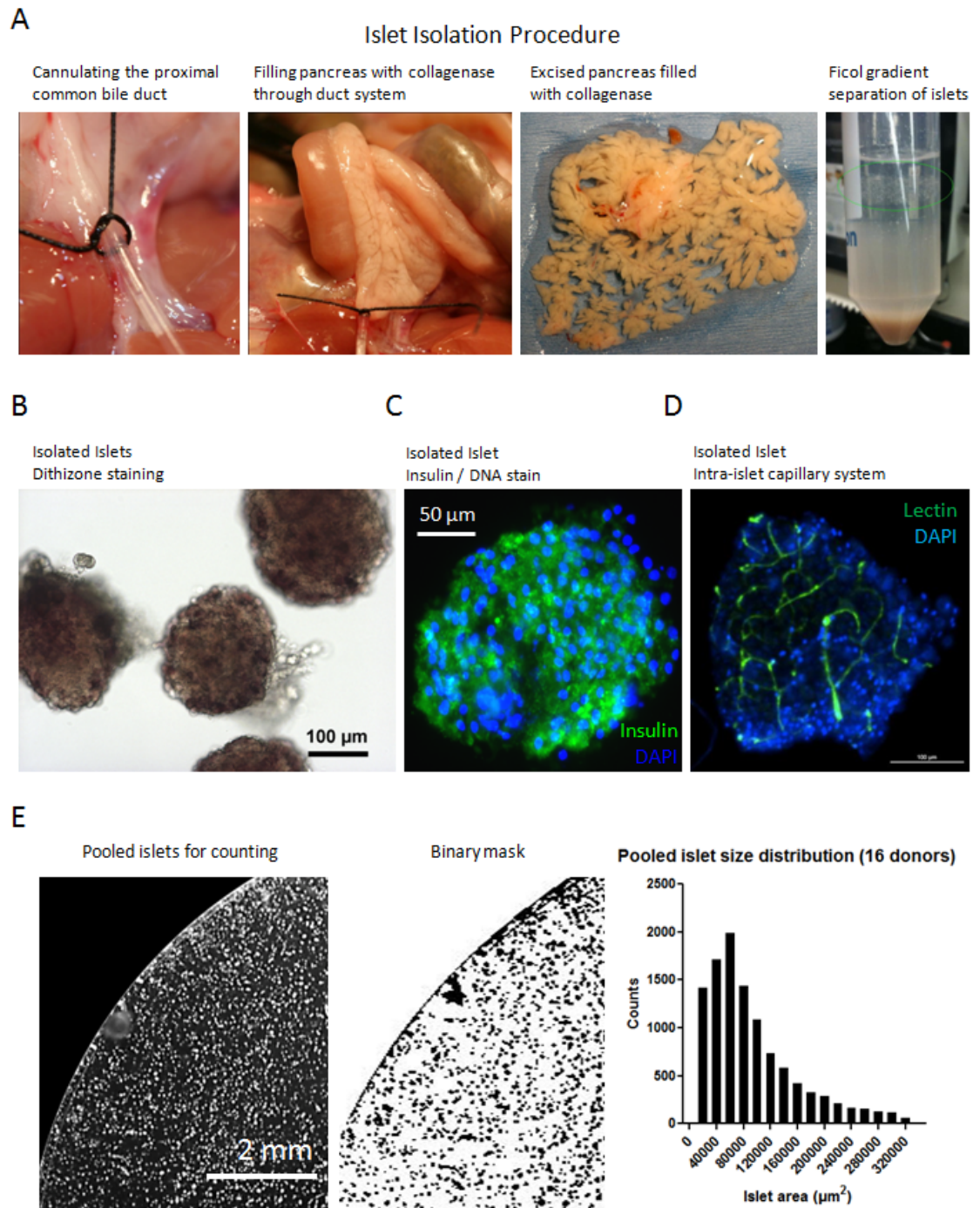
Figure 5.3 Islet isolation procedure. (A) Surgical procedure for filling the pancreas with collagenase enzyme and density gradient separation of islets from other cells. (B) Isolated islets stain positive with dithizone as a quality check. (C) Isolated islets stain positive for insulin (D) The intra-islets vascular bed is visible in islets isolated from animals perfused with FITC-lectin. (E) For quantification, islets were pooled in a 100 mm petri dish, photographed, and counted using a binary mask.
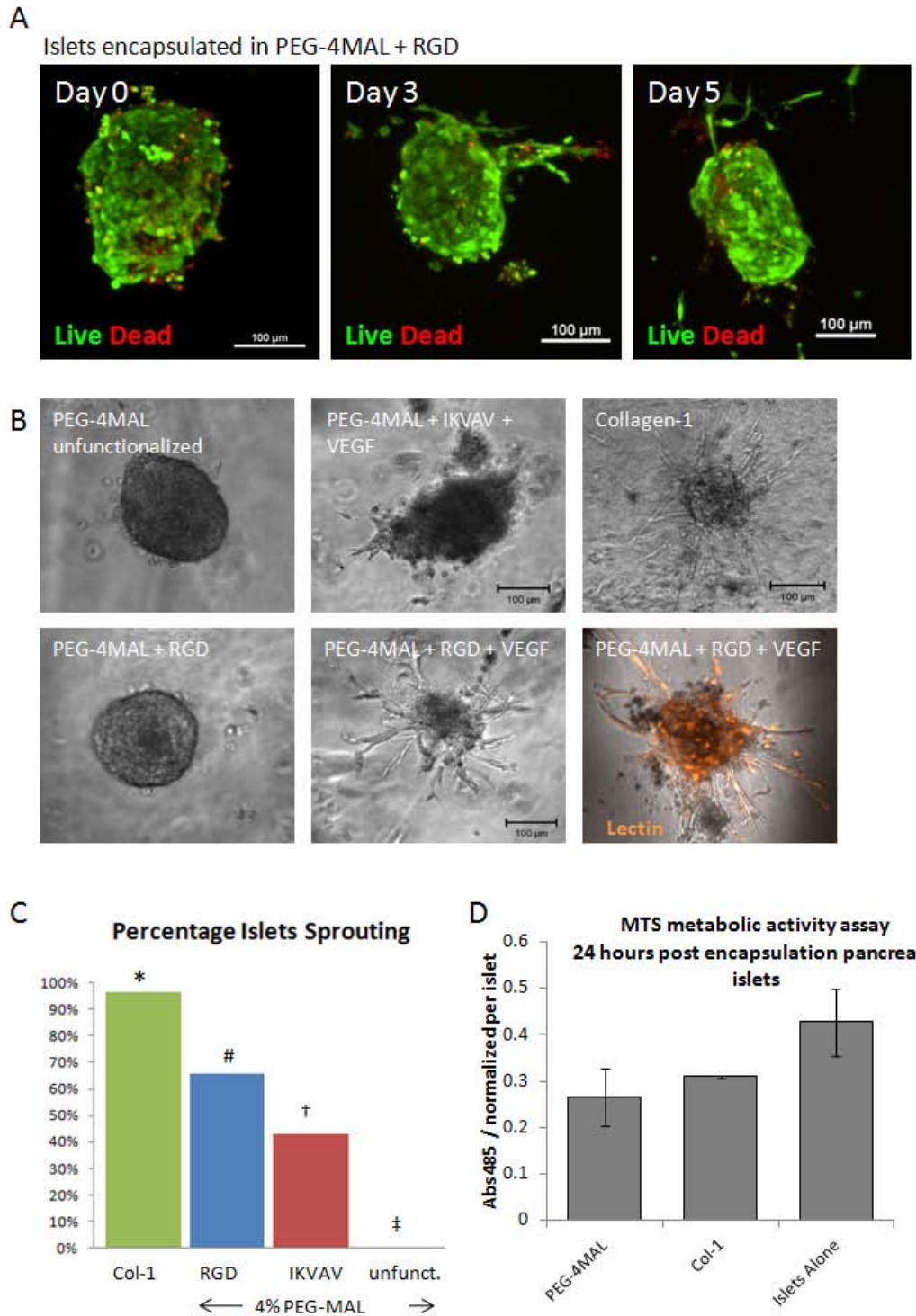
Figure 5.4 Islet encapsulation in PEG-4MAL hydrogel. (A) Islets encapsulated in PEG-4MAL gel maintain high viability over at least 5 days in culture. (B) Islets encapsulated in hydrogel sprout endothelial tubes in the presence of RGD and VEGF. (C) Quantification of islet sprouting as a function of adhesive ligand. (D) Cells encapsulated in PEG-4MAL maintain metabolism comparable to collagen-1 gel.
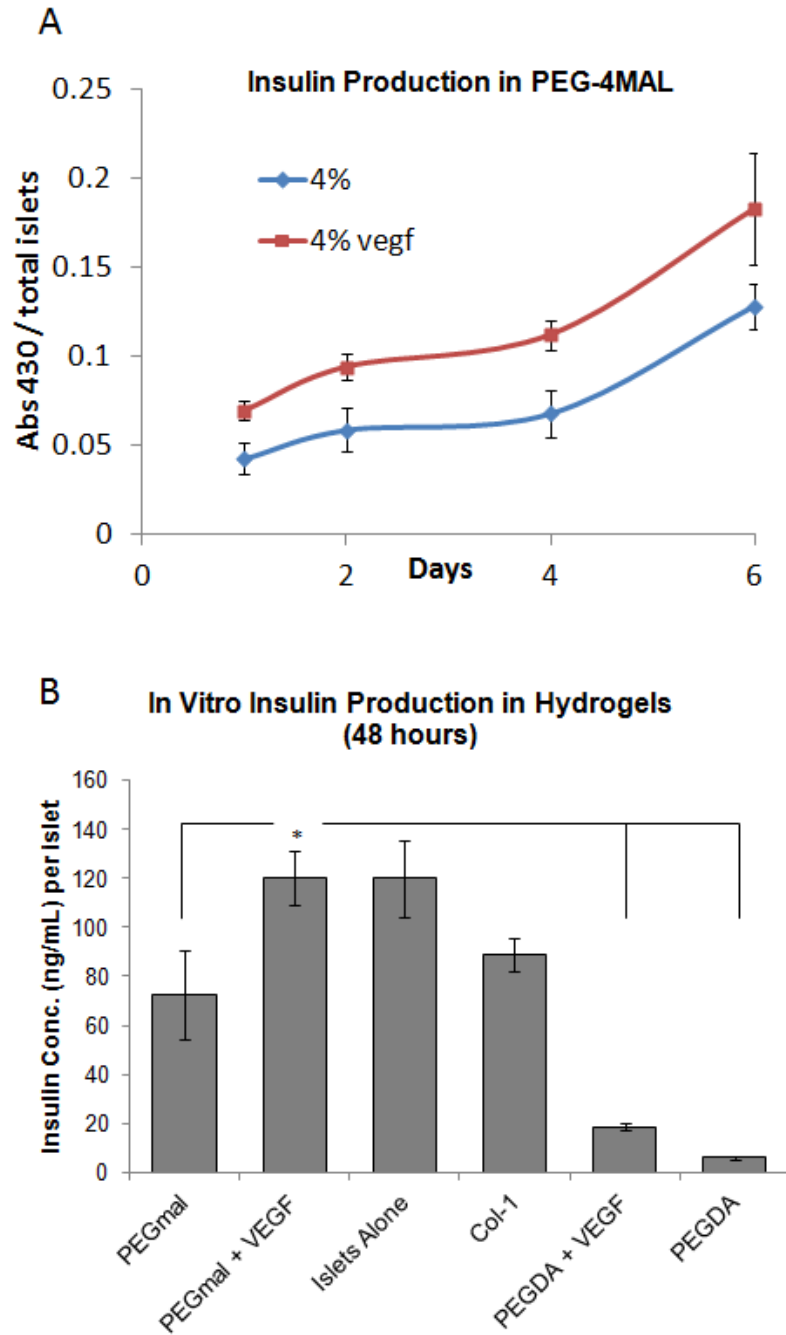
Figure 5.5 Insulin production of islets encapsulated in bulk hydrogels. (A) Insulin production per islet rises over time in culture, addition of VEGF improves insulin output. (B) Insulin production per islet in various hydrogel formulations.

The *in vivo* vascularization and grafting potential of pancreatic islets encapsulated in PEG-4MAL and PEG-DA matrices to the small bowel mesentery was investigated with a surgical model. Islets were isolated from 2 donor pancreases to generate approximately 1500 islets for each recipient. Syngenic inbred Lewis rats were used for both the donor and recipient animals to eliminate risk of a tissue-type mismatch graft rejection. During the surgical procedure a small section of small bowel was gently exteriorized through a midline incision (**Fig. 5.6 A**). Two 100 μL 4% PEG-4MAL hydrogels with 2 mM RGD and +/- 10 μg /mL VEGF containing approximately 750 islets each were pipetted onto the surface of the clear mesenteric tissue and allowed to cross-link for 10 minutes (**Fig. 5.6 B**) before re-insertion of the small bowel into the abdominal cavity and wound closure.

PEG-DA was also evaluated as an islet transplantation matrix. PEG-DA proved to be unwieldy for *in situ* polymerization due to the low viscosity of the precursor solution and inconsistent gelation under UV light at the tissue site. Therefore the PEG-DA matrices with encapsulated islets were pre-cast in silicon molds around a small polycaprolactone (PCL) rings. The preformed constructs were sutured in place to the small bowel mesentery through the PCL ring as an anchor point (**Fig. 5.6 C,D**). The PEG-4MAL and PEG-DA matrices were tested *in vivo* in separate studies.

In both studies, islets were transplanted in gels with and without VEGF as well as compared to calcium cross-linked alginate gels. Animals were sacrificed at 1 and 4 weeks to evaluate grafting and vascularization behavior. By one week new vessels could be clearly seen growing into the surface of the hydrogels from surrounding tissue in both PEG-DA and PEG-4MAL (**Fig. 5.7**). By 4 weeks a strong and dense vascular in-growth response was evident, and especially apparent in the PEG-4MAL + VEGF group. The vascular response to the PEG-DA gels appeared to be limited to the surface of the implant (**Fig. 5.8**) whereas PEG-4MAL had vessels reaching throughout the interior of the implant (**Fig. 5.9**). New vessels were not visible in the alginate groups. For

histological preparation and to prove patency of vascular in-growth, FITC-lectin was injected intravenously in the PEG-4MAL groups and allowed to circulate before the animals were euthanized.

Explanted tissue samples from the PEG-4MAL hydrogels were stained as whole mounts for insulin and imaged on a fluorescent stereoscope to examine overall islet survival (**Fig 5.10**). On average 65 independent insulin-positive structures per field were visible in PEG-4MAL + VEGF gels, 42 for PEG-4MAL without growth factor, and 1-2 for alginate. Explants from both PEG-4MAL and PEG-DA were embedded in Immuno-Bed plastic resin, sectioned at 2 µm and, analyzed histologically by hematoxylin and eosin stain (**Fig. 5.9 A**), Masson's trichrome stain (**Fig. 5.9 B**), and immuno-fluorescence (**Fig. 5.11**). All islets in PEG-DA gels appeared necrotic with few discernable nuclei and stained very weakly or negatively for insulin. The primary host response to the PEG-DA gel was fibrous encapsulation with vascularization limited to the implant periphery and significant CD-68 positive macrophage activity in the fibrous capsule.

Fluorescence microscopy imaging of the PEG-4MAL implants for insulin, FITC-lectin, and nuclei revealed many surviving islets with signs of initial early revascularization at 1 week which improved to robust reperfusion of the intra-islet endothelial bed similar to native islets in the pancreas by 4 weeks. Positive staining for lectin in intra-islet capillaries indicated that the vessels were well perfused in connection with the host circulatory system. A higher density of islets was apparent in the PEG-4MAL + VEGF group than in the PEG-4MAL, but all surviving islets in both groups appeared to be vascularized. H&E and trichrome staining revealed a degree of monocyte / macrophage activity remodeling in the PEG-4MAL matrix. Trichrome staining also revealed new vessels to be associated with connective tissue and erythrocytes were confined to the interior of endothelial tubes.

To quantify differences in vascularization response to PEG-4MAL hydrogels with and without VEGF and with and without islets, animals were perfused with microfil

vascular contrast agent to quantify vascularization by microCT (**Fig. 5.12**). PEG-4MAL hydrogels containing RGD, +/-VEGF and +/- islets were cross-linked directly on the small bowel mesentery of healthy rats. At 4 weeks the vascular system of the animals was perfused with microfil polymerizing contrast agent as previously reported [249]. After 24 hours to cure, the tissue at the implant site was explanted, fixed overnight, and scanned in a SCANCO µCT 40 system at medium resolution. Vasculature was quantified based on vascular volume percentage of total explant volume, vessel thickness, and connectivity.
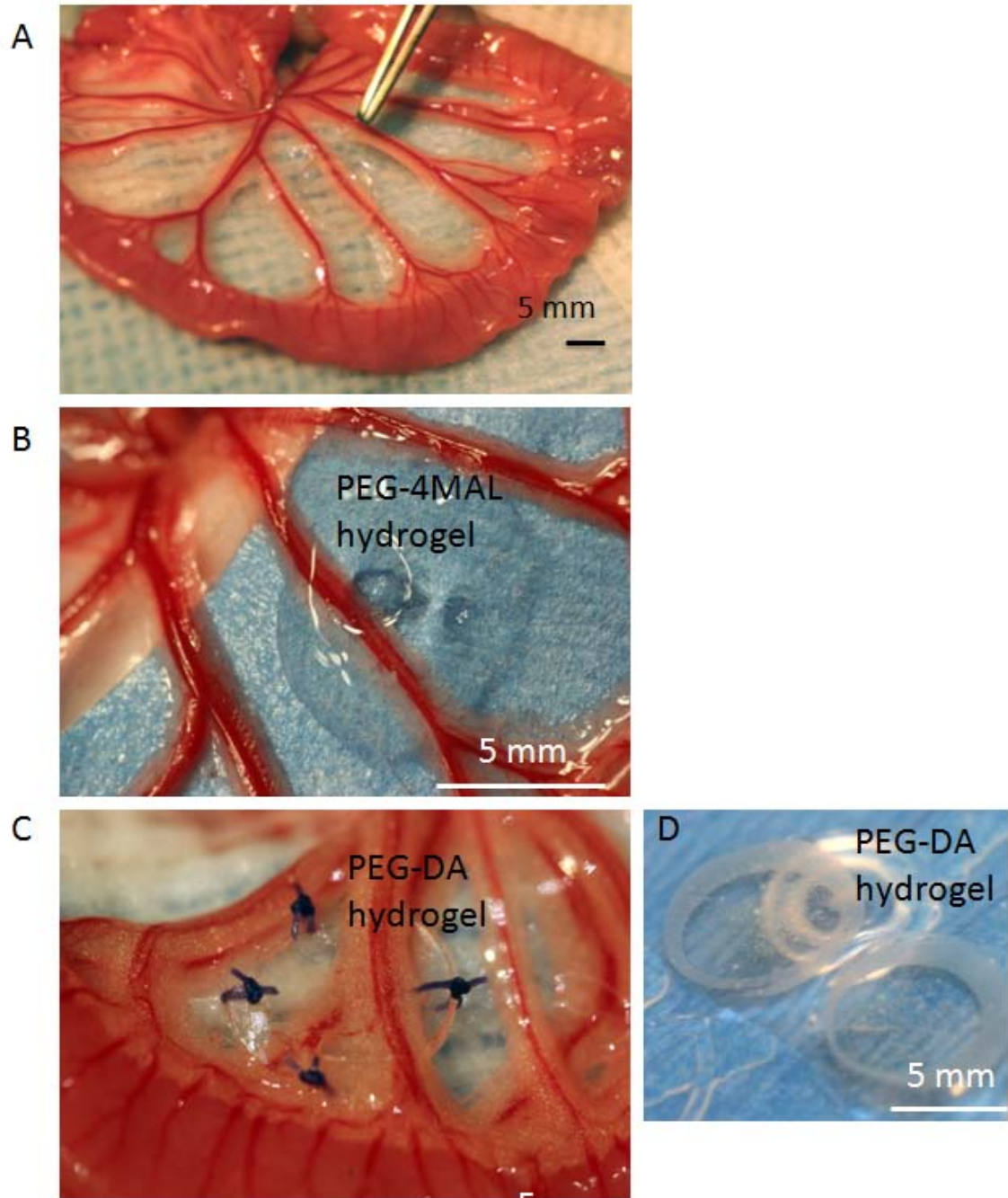
Figure 5.6 Hydrogel implantation procedure. (A) Loop of exteriorized small bowel with mesentery, forceps point to implantation site. (B) PEG-4MAL hydrogel formed directly on the mesentery tissue (C) PEG-DA hydrogel pre-cast construct sutured in place to small bowel mesentery. (D) Pre-cast PEG-DA hydrogels around PCL rings.
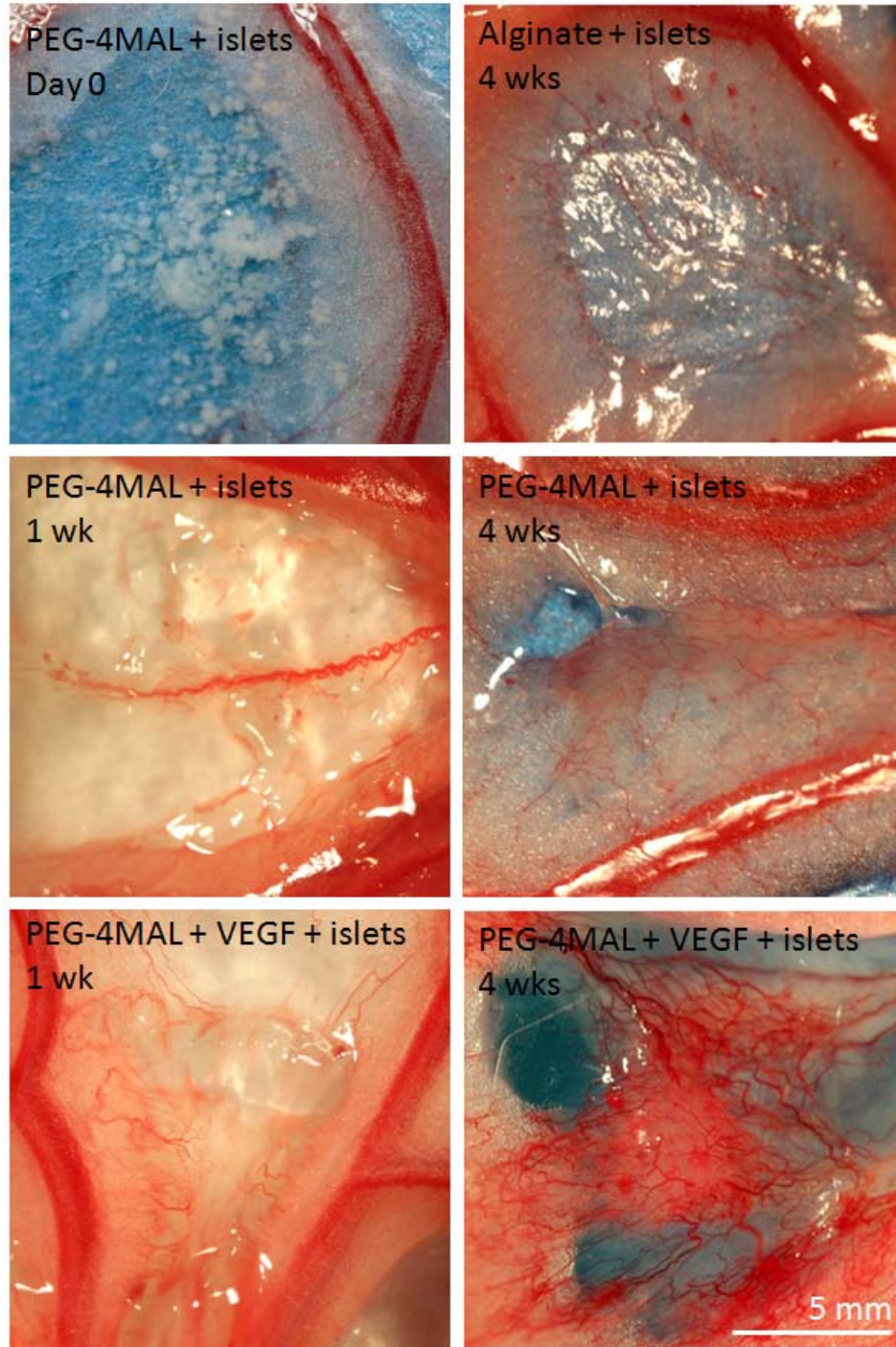
Figure 5.7 Macroscopic vascular response to PEG-4MAL islet transplantation with and without VEGF at 1 and 4 weeks.
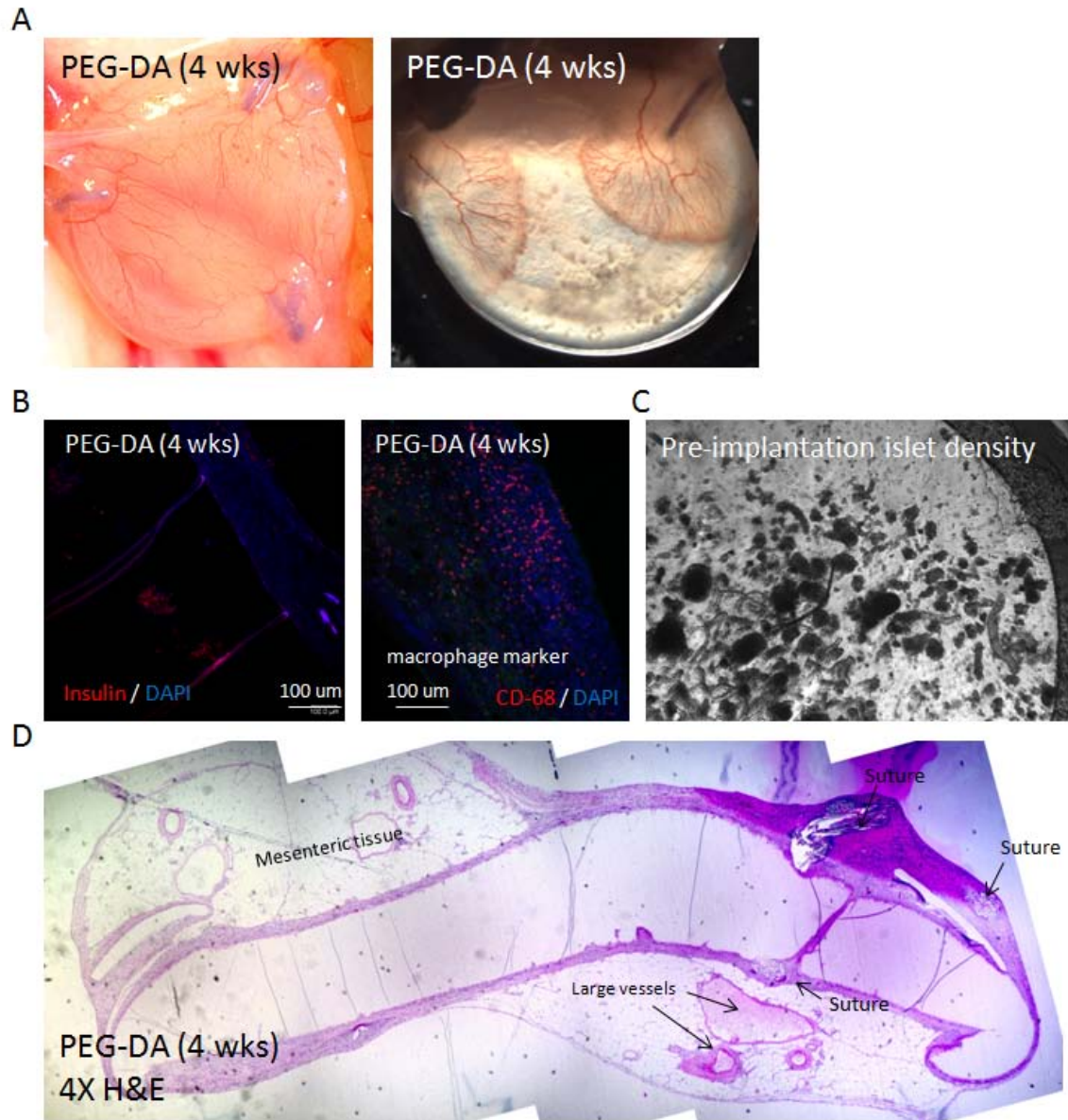
Figure 5.8 Response to islets transplanted in PEG-DA hydrogel. (A) Vascular response visualized with epi-illumination and back illumination. (B) Immuno-fluorescence staining of section of explanted PEG-DA for insulin and CD-68. (C) Pre-implantation density of islets in PEG-DA construct for comparison. (D) Compost H&E stain showing fibrous encapsulation response of PEG-DA hydrogel.
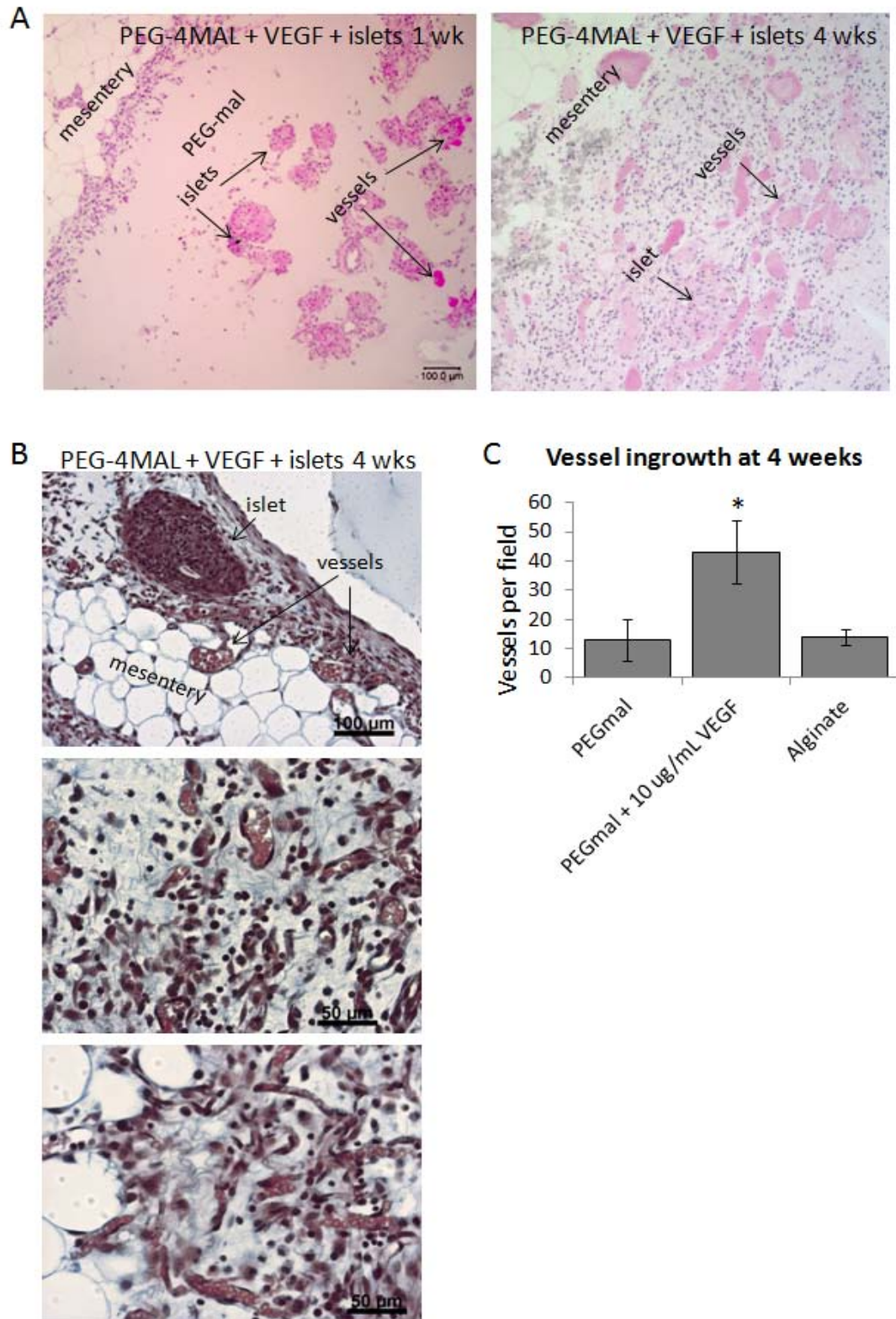
Figure 5.9 Response to islets transplanted in PEG-4MAL hydrogel. (A) H&E of transplant site at 1 and 4 weeks. (B) Trichrome stain of implant site at 4 wks illustrating vascular response. (C) Vessel ingrowth quantified by counting vascular structures
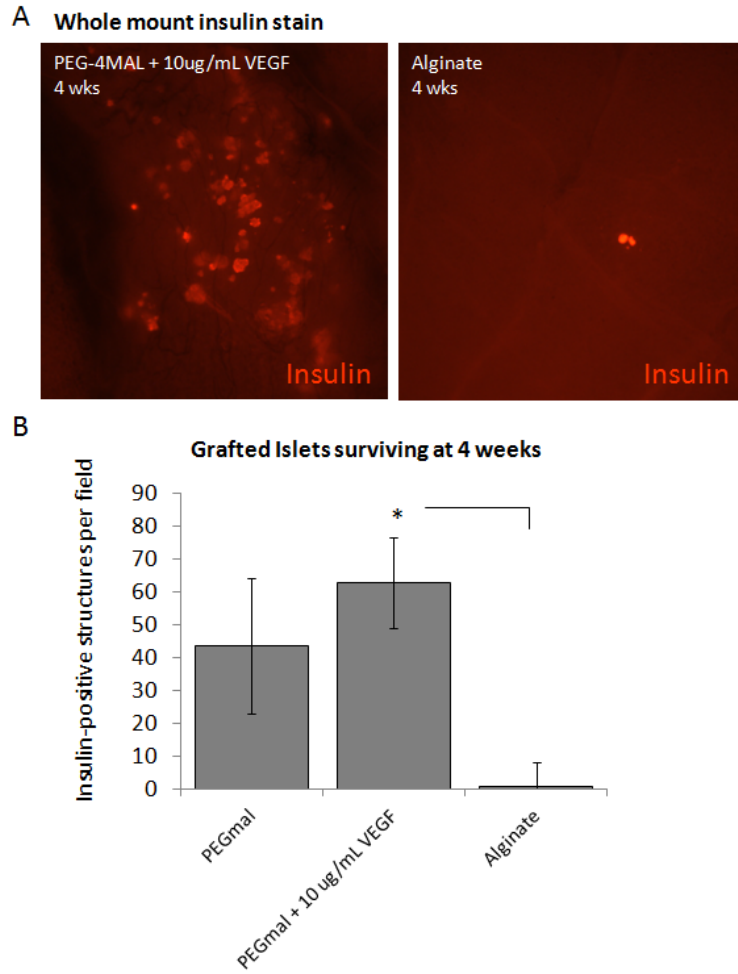
Figure 5.10 Whole mount immuno-fluorescent stain for insulin and quantification islet structures in PEG-4MAL gel explants.
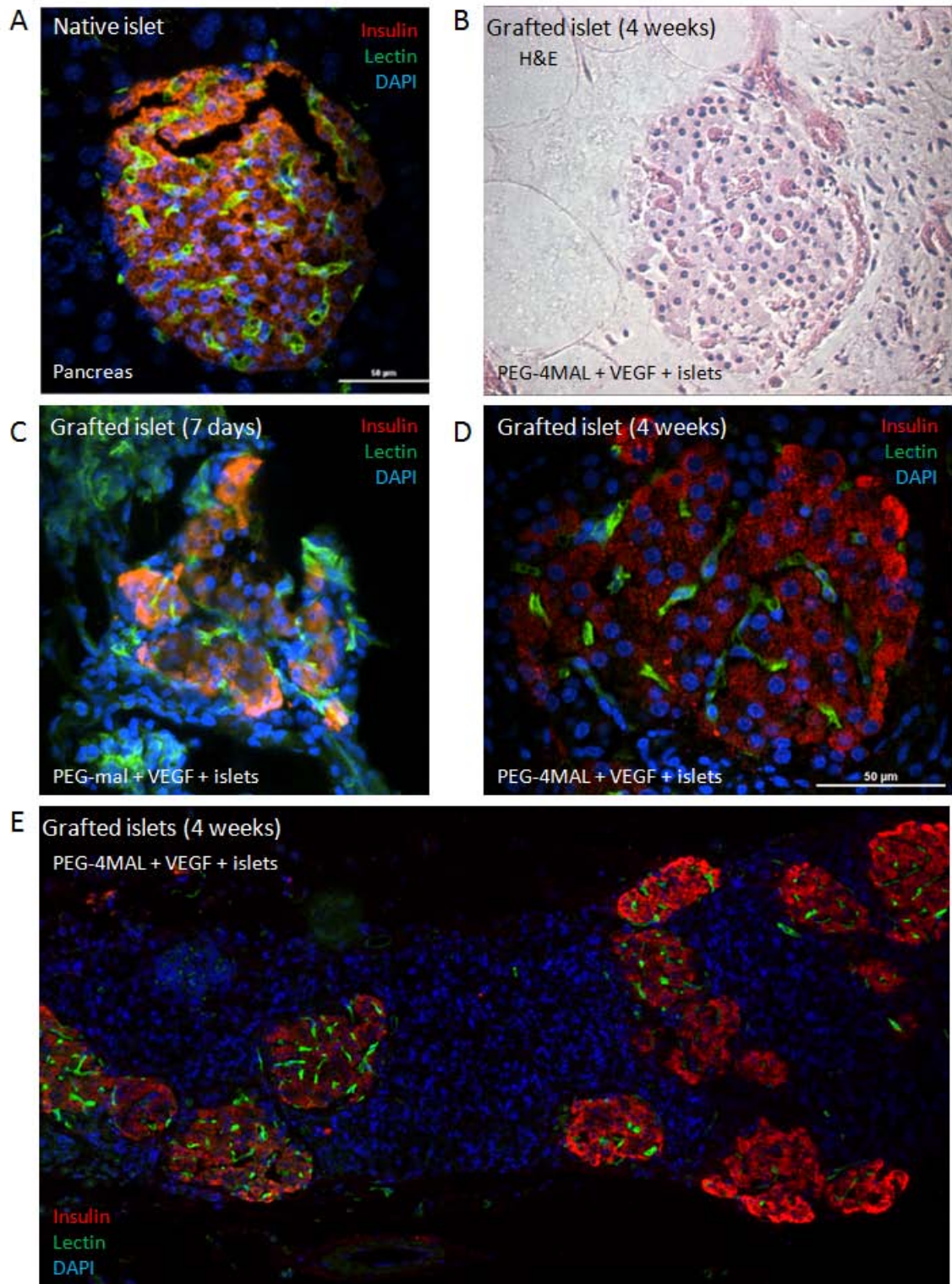
Figure 5.11 Immuno-fluorescent histological sections of grafted islets in PEG-4MAL gel explants. (A) Native islet in the pancreas with lectin staining capillary bed. (B) H&E of grafted islet (C) Grafted islet at 1 week (D) Grafted islet at 4 weeks (E) Grafted islets at 4 weeks.
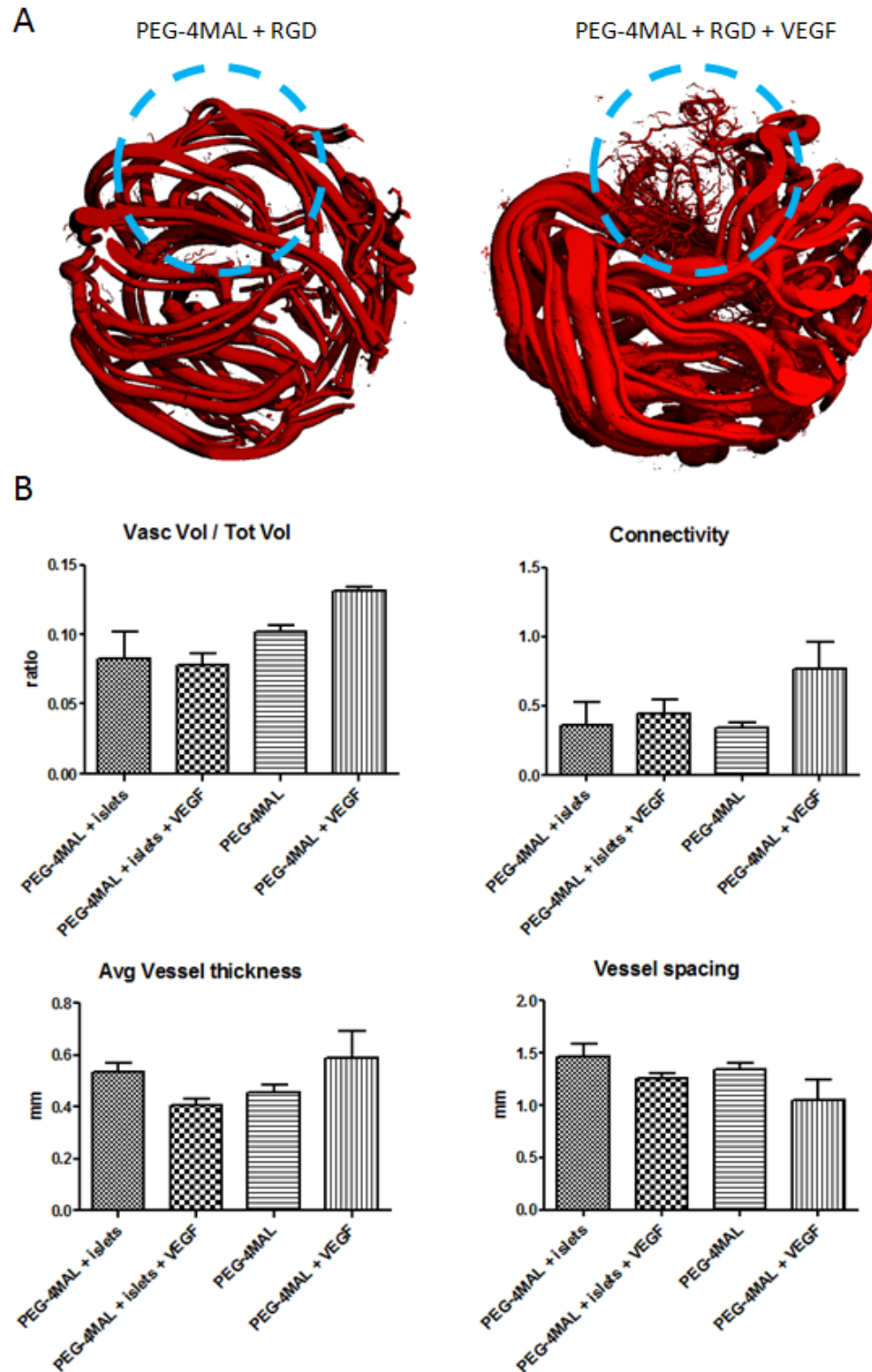
Figure 5.12 MicroCT tomograms and analysis of PEG-4MAL gels implanted in small bowel mesentery. (A) Renderings of small bowel mesentery vasculature with blue line indicating approximate location of transplant. (B) Analysis results of tomograms.

Discussion

The release profile of VEGF from the hydrogel as measured by both ELISA and near-IR fluorescence of labeled VEGF indicates that the growth factor is sequestered within the matrix and the predominant mode of release is through proteolytic degradation of the gel and not by diffuse release. The extremely rapid release and degradation of the collagenase-treated gels is a result of both an artificially high concentration of collagenase and the rapid-degradation profile of the chosen cross-linker peptide sequence. We also have shown that VEGF is conjugated to the PEG-4MAL macromer based on increased molecular weight after the addition reaction. Therefore there is considerable evidence to substantiate the claim the growth factor is covalently bound to the matrix and not just entrapped within the nano-porous polymer network.

Pancreatic islets encapsulated in photo-polymerized RGD functionalized PEG-DA hydrogel failed to produce insulin and showed low viability. While it has been postulated that beta cells encapsulated in photo-polymerized hydrogel have low viability due to a lack of ECM and cell-cell interactions [281], it is also likely that toxicity to both the free-radical cross-linking process and the bulk properties of the PEG-DA hydrogel contribute to poor islet compatibility. In contrast, islets encapsulated in PEG-4MAL hydrogel had higher viability and produced insulin similarly to free islets. This is likely due to milder crosslinking reaction of the PEG-4MAL hydrogel as previously shown in Chapter 4. Addition of VEGF to the matrix improved *in vitro* insulin production in both PEG-4MAL and PEG-DA. It has been reported that VEGF-A co-localizes with cells expressing insulin in islets indicating that beta cells express VEGF [177]. Additionally VEGF receptor 2 (VEGFR2) is more highly expressed in the microvasculature of islets compared to other capillaries in the exocrine pancreas [177]. VEGF-deficient islets result in reduced insulin output [177]. These factors lend support to the idea that VEGF signaling is intrinsically important to the homeostasis and health of the islets.

Islet sprouting behavior of lectin-positive cells similar to that observed in our cultures has been observed by Stupp and colleagues in peptide amphiphile hydrogels on a similar time frame (day 3 post-encapsulation) [173]. Stupp also reports a similar percentage of sprouting islets in matrices augmented by addition of VEGF and FGF2. This repetition of results indicates that isolated islets in synthetic matrix systems can undergo angiogenic sprouting under the right conditions. The RGD adhesive ligand initiated significantly more sprouting behavior than laminin-derived IKVAV. RGD is a preferential ligand for αvβ3 integrin, highly expressed on sprouting endothelial cells while IKVAV does not ligate αvβ3 integrin. Therefore it is plausible that endothelial cell sprouting was improved in the RGD matrix over IKVAV due the presence of endothelial cell-specific adhesion ligands. Islets in the artificial matrix did not sprout as well as in natural collagen matrix which has higher density, variety, and stronger-affinity adhesive ligands. Additionally the sprouting behavior is an indication that the islet endothelial cells are able to degrade the protease-sensitive peptide cross-linker effectively. It has been previously shown that intra-islet endothelial cells play an important role in transplanted islet revascularization [178, 282, 283].

Both PEG-DA and PEG-4MAL matrices were tested *in vivo* for islet delivery and grafting potential. PEG-DA proved unsuitable for *in situ* delivery so pre-cast matrices were sutured to the graft site in the small bowel mesentery instead of cross-linked in place. The host tissue failed to significantly degrade the PEG-DA hydrogel and instead responded with fibrous encapsulation. The islets in the PEG-DA hydrogel which appeared dead or missing in the histology analysis most likely succumbed to oxygen and nutrient deprivation if the encapsulation process itself was not too toxic. The reason for the host fibrous encapsulation response to the PEG-DA is two-fold. One reason is that the host tissue was unable to degrade the higher density PEG-DA matrix in the small bowel mesentery site. Although we previously observed degradation of the PEG-DA matrix in subcutaneous implants this trend does not necessarily carry over to other implant sites.

The other reason for fibrous encapsulation is that without a cohesive interface between the matrix and host tissue, the micro-motion of the implant in addition to local inflammation and tissue damage from the suturing resulted in an inflammatory foreign body response.

In contrast to PEG-DA, PEG-4MAL matrices were far more suitable for *in situ* delivery, readily adhering to the mesenteric tissue during the gelation process without any need for suture or other foreign material. The early vascular ingrowth (7 days) appeared leaky from diffuse lectin staining but not altogether unexpected in VEGF-induced angiogenesis. However the VEGF-induced vessels persisting at 4 weeks had a more stable appearance with lectin staining confined to the interior of vessels coinciding with the IVIS imaging evidence that VEGF *in vivo* release was depleted by 1 week.

Without long-term and continuous VEGF signaling from the matrix it is plausible that intrinsic signaling from the islets themselves is responsible for vessel maintenance after the initial VEGF dosage was depleted. We also found surviving islets in matrices cast without VEGF suggesting that the signaling from islets alone might be enough to induce sufficient vascularization for some islet survival. With microCT scanning we attempted to gather quantitative information regarding the vascularization of the PEG-4MAL implants and the relative signaling contributions of islets vs. VEGF. In scans of the implant connected to a large portion of surrounding mesentery it was possible to clearly see the vascular growth from surrounding vessels into the implant and observe the architecture of the vascular tree. The microCT data indicated that VEGF significantly increased the vascularization response in the matrices without islets. But in matrices with islets there was no significant difference between with and without VEGF. Paradoxically, the microfil casts indicated less vascularization for matrices with islets than for those without. This data clearly did not correlate with what was observed in the previous study macroscopically and histologically. The microfil injection procedure is somewhat tenuous and exhibits significant variability in the quality of the perfusion from one

animal to the next. Based on this contradictory evidence we were forced to conclude that the reliability of the microCT data may be questionable. A positive indication from the microCT tomograms is that the vessels at the implant site at 4 weeks were not permeable to the microfil supporting the lectin staining data. Some publications have previously reported leakiness and microfil "pooling" in the vicinity of growth-factor induced vasculature [284].

Conclusions

We have successfully delivered islets to the small bowel mesentery in syngeneic Lewis rats using VEGF-containing PEG-MAL hydrogels. These hydrogel vehicles promoted potent vascularization of the hydrogel and islets. Transplanted islets showed high levels of engraftment, were connected to the host vasculature (demonstrated by lectin injected into host vasculature), and continued to produce insulin. These results demonstrate the significant potential of these engineered hydrogels for islet engraftment and function

Methods

Hydrogel

As described in Chp. 4, PEG-4MAL 20,000 MW was purchased from Laysan Bio. The peptide crosslinker GCRDVPMSMRGGDRCG (VPM) and adhesive ligand GRGDSPC were custom synthesized by AAPPTEC. Michael-type addition PEG hydrogels were formed by first reacting PEG-4MAL with the cell-adhesion peptide GRGDSPC and VEGF for 1 hour in 4 mM TEA in PBS. The precursor solution was cross-linked with the cysteine-flanked and protease degradable peptide VPM at stoichiometrically balanced 1:1 cysteine to remaining maleimide reactive group molar ratio.

VEGF labeling

Human VEGF$_{165}$ (Invitrogen) was solubilized at 1 mg/mL in PBS. VivoTag-S 750 (Perkin Elmer) was solubilized in DMSO. 50 molar excess of VivoTag-S 750 was added to the VEGF and incubated at room temperature for 1 hour to make VEGF-750. Labeled protein was purified from excess dye by 3 successive purification rounds on Zeba Spin Desalting Columns 7,000 MWCO (Pierce). Dye concentration in the purified conjugated protein sample was measured on a NanoDrop 1000 system using dye extinction coefficient of 240,000 M^{-1}cm^{-1}, absorbance of 750 ± 5 nm, and MW of 1183 g/mol. VEGF was conjugated to PEG-4MAL by incubation for 1 hour in 10% (wt/vol) PEG-4MAL in PBS + 4 mM TEA prior to addition to gels. To confirm protein labeling and ability of labeled VEGF to react with PEG-4MAL, 100 ng of labeled VEGF-750 was run on a NuPAGE Novex 4-12% Bis-Tris SDS-PAGE gel along with PEG-4MAL conjugated VEGF-750 unlabeled VEGF and free dye samples. VEGF was confirmed to be labeled and free of excess dye as well as conjugated to PEG-4MAL by imaging the gel on a LI-CORE Odyssey infrared imaging system.

In vitro VEGF release

PEG-4MAL gels containing 10 ug/mL of VEGF-750 cross-linked by VPM peptide were pre-cast in 9 mm x 1 mm cylindrical silicon molds. Gels were floated in baths of PBS and incubated at 37°C for 24 hours to fully swell. At 24 hours, a final concentration of 0.1 mg/mL of Type I Collagenase was added to half the samples were. For sampling of VEGF released to the media, 5 µL samples of the media bath were taken every 2 hours during the first day. Media samples were measured for VEGF content by ELISA using the human VEGF ELISA kit (invitrogen) and compared to standard samples of diluted VEGF in PBS equivalent to a fully degraded gel releasing all of the loaded VEGF. Samples were also imaged daily on an a 700 series Xenogen IVIS machine at 710 nm excitation, 780 nm emission and 60 s exposure time. Images were quantified for background subtracted average photon counts per ROI.

In vivo fluorescence imaging

PEG-4MAL hydrogels (100 uL) with 10 ug/mL VEGF cross-linked by VPM were adhered to the small bowel mesentery of Lewis rats fed a low-alfalfa diet to minimize tissue auto-fluorescence. Anesthetized rats were imaged at 710 nm excitation, 780 nm emission, and 60 s exposure time in a 700 series Xenogen IVIS machine a 0, 2, and 7 days post-transplant. Images were analyzed for background-subtracted average photon counts within an ROI gated over the implant site.

Islet isolation

Modified from [285], rats were anesthetized with isoflurane and euthanized by exsanguination by severing the vena cava. The distal common bile duct was clamped at the insertion point into the small intestine. Ten mL of ice cold Liberase TL collagenase

(0.2 mg/mL) in HBSS^{++} was injected into the proximal common bile duct through a catheter pulled from PE-50 polyethylene tubing attached to a 10 mL syringe. The inflated pancreas was dissected from surrounding tissue and placed in a container on ice. Vials containing pancreases were incubated for 17 minutes in a 37°C water bath. Tissue was broken up by pipetting up and down and then incubated for a further 7 minutes. Collagenase action was halted by addition of 40 mL ice cold HBSS^{++} + 10% FBS. Each sample was filtered through a mesh sink strainer to remove undigested tissue. Cells were collected into a pellet by centrifugation at 800 rpm for 2 minutes followed by two more rounds of washing / centrifugation with ice cold HBSS^{++} + 10% FBS. Cells were resuspended in 12 mL of Ficoll density 1.108 followed by layering of 7 mL Ficoll density 1.096 and 5 mL Ficoll density 1.037. The density gradients were centrifuged at 1100 rpm for 30 minutes to separate islets. Separated islets were picked from between the 1.096 and 1.037 layers with a sterile transfer pipette and washed 3 times in HBSS^{++}. Islets were cultured in RPMI-1640 + 10% FBS + 1% Penicillin-Streptomycin in a 37°C, 5% CO$_2$ incubator. Isolated islets were examined for purity by dithizone staining and counting with a macro-photography setup.

Islet culture and in vitro assays

For *in vitro* studies, islets were isolated the day before and allowed to recover for 12-24 hours before encapsulation in hydrogel. Fifty microliter gels of 4% PEG-4MAL + 2 mM RGD and with or without 10 µg/mL VEGF were cast in the bottom of 8 well Lab-Tek Chambered Coverglasses (Nunc). Approximately 25-50 islets were encapsulated per 50 µL gel. Gels were cultured with 500 µL media (RPMI-1640 + 10% FBS + 1% Penicillin-Streptomycin) changed daily. PEG-DA gels were formed similarly but were cured by a 10 min exposure to 10 mW/cm^2 365 nm UV light. Collagen I gels (3 mg/mL) were formed from dilution and pH stabilization of 10 mg/mL solubilized rat tail Collagen I (BD). Islets were examined daily and observations such as sprouting were recorded.

Samples were Live/Dead stained with PBS containing 2 μM calcein AM and 4 μM TOTO-3 iodide and imaged with a 20X objective on a Nikon-C1 laser scanning confocal microscope.

Insulin release to the media from encapsulated islets was measured by ELISA using the High Range Rat Insulin ELISA kit (Mercodia). Media was changed every day, therefore each data point represents total release from the hydrogel over a 24 hour period.

Histology

Explanted samples from FITC-lectin perfused rats containing hydrogel, islets, and tissue were fixed overnight in 10% neutral buffered formalin at 4°C. Samples were pre-stained (whole mount) for insulin by overnight permeabilization / blocking in 1% HD-BSA with 0.1% Triton-X 100 in PBS, wash with PBS + 0.1% TWEEN 20, overnight incubation with chicken anti-insulin primary antibody (Abcam) in PBS, 3 x 12 hours wash with PBS + 0.1% TWEEN 20, overnight incubation with Alexa Fluor 555 goat anti-chicken secondary antibody (Invitrogen) in PBS, and finally 3 x 12 hours wash with PBS + 0.1% TWEEN 20. Whole mount stains were imaged on a Zeiss fluorescent stereoscope for insulin staining before embedding for histology sections. Samples were then dehydrated in successive changes of 70%, 95%, 99%, and 3 x 100% ethanol under vacuum at 4°C. Dehydrated samples were infiltrated with three successive changes of activated Immuno-Bed (Polysciences) under vacuum at 4°C followed by a final embedding step in polyethylene molds. After 48 hours further curing of the blocks at room temperature, Immuno-Bed blocks were sectioned at 2 μm thickness. The sections were floated on an ultrapure water bath at room temperature and picked up with positively-charged glass slides and dried for 24 hours. Sections were deplasticized with a solvent exchange routine of xylene, acetone, ethanol, and water before further staining. Routine hematoxylene and eosin, trichrome, and immunostaining procedures were performed on the deplasticized sections.

Microfil perfusion and MicroCT Imaging

After sacrifice by CO_2 inhalation, rats were perfused with 0.9% saline + 4 mg/mL papaverine hydrocholoride (Sigma), followed by 0.9% saline, and 10% neutral buffered formalin. After fixation, 30 mL of 80% (v/v) diluted MV-122 Microfil (Flowtec) was injected into the aorta with a syringe and allowed to polymerize overnight before implant retrieval. Explants were scanned at 16 µm resolution with a Scanco µCT-40 microCT machine. Contour lines were drawn by hand to define the volume extent of the tissue sample and 3D renderings and analysis were performed based on the bone trabecular morphometry algorithm set.

CHAPTER 6

TRANSPLANTATION OF HYDROGEL-ENCAPSULATED PANCREATIC ISLETS IN A RAT MODEL OF TYPE-1 DIABETES

Summary

Polyethylene glycol maleimide (PEG-4MAL) hydrogel matrices incorporating sites for cell adhesion and vascular endothelial growth factor (VEGF) have been previously shown to induce an angiogenic response and support pancreatic islet engraftment and re-vascularization in healthy rats. We investigated the same transplantation model to alleviate hyperglycemia and weight loss in an STZ model of diabetes. In three independent trials transplants of 1500 islets failed to reverse hyperglycemia although moderate differences were observed in weight gain, fasting blood glucose levels, and response to a glucose challenge test. From this information we conclude that the animal model represented too severe of a case for the mass of islets transplanted to significantly alter the course of the disease state and that impaired angiogenic function and lack of an immuno-protective barrier added to the negative outcome.

Introduction

After the establishment of the Edmonton Protocol [286], successful transplantation of pancreatic islets in humans is performed at select clinics around the world with an estimated 750 patients having undergone intraportal islet-alone transplantation in the past 10 years [287]. The improvements in islet transplantation therapy following the Edmonton Protocol are largely related to transplantation of freshly isolated islets from multiple donors and administration of a glucocorticoid-free immunosuppressive regimen. Islet transplantation therapy has as its primary objective,

elimination of severe episodes of hypoglycemia which is recurrent in approximately 15% of patients with type 1 diabetes [287]. Islet transplantation has the secondary benefit of freedom from exogenous insulin injections which is an extremely attractive quality of life benefit to patients. While still in its infancy as a therapeutic option, and only a handful of centers possessing the skill and equipment to carry out the procedure, islet transplantation offers a much less invasive alternative to whole pancreas transplantation with similar clinical outcomes. It is estimated that 60% to 80% of transplanted islet mass is lost in the first hours to days following intra-portal vein infusion due to instant-blood mediated inflammatory reaction, ischemia, apoptosis, and a myriad of other factors. Because of the high numbers of islets that are lost in the procedure, as many as 5,000 islet equivalents (IEQ) or more per kg of body weight are required in human patients, which can require two to four donor pancreases depending on the quality of the isolations. A major challenge in the development of islet transplantation therapy is to improve the survival rate of the transplanted cells. Researchers are working on this problem from all angles including improvements to the isolation process, drugs to improve graft acceptance, protective materials to encapsulate the islets, and strategies to improve islet engraftment, and vascularization.

Several animal models of Type 1 diabetes are used in islet transplantation research [288]. Non-surgical methods of inducing hyperglycemia include administration of the toxins streptozotocin (STZ) and alloxan. Streptozotocin toxin is derived from the soil microbe *Streptomyces achromogenes*. It is a powerful alkylating agent that causes double-stranded damage to DNA. Structurally, streptozotocin is similar enough to glucose to be transported into cells by the glucose transport protein GLUT2, but is not recognized by other glucose transporters. Streptozotocin is preferentially uptaken by pancreatic beta cells which have relatively high levels of GLUT2 compared to other cells. GLUT2 is also found in the cellular membranes of liver cells, and the brush border

membrane of the small intestine. Diabetes can be induced in rodents with a single large dose or multiple low doses of streptozotocin.

For this study STZ-induced Lewis rats were chosen as the animal model. Rats were preferable over mice for their larger size to aid in islet isolation procedures. The Lewis rat was chosen as a syngenic inbred stain as both an islet donor and recipient to minimize complications from immune rejection of transplanted tissue. In STZ-induced rodent models of diabetes, islets have been transplanted with or without immuno-protective capsules subcutaneously, into the epididymal fat pad, under the renal capsule [289], intra-peritoneally, intra-muscularly [290], into the omentum [137], and infused via the portal vein into the liver. The number of islets in transplantation models which successfully reverses diabetic hyperglycemia in ranges from 500 to 4000 islets [291].

Because one of the most significant detrimental factors to islet grafting and function is poor vascular perfusion we hypothesized that we could improve the physiological outcomes in a diabetic animal model by promoting vascularization of transplanted islets. We hypothesized that we would see significant physiological improvements in islets transplanted via engineered vascular-inductive PEG-4MAL matrices over islets transplanted via the more traditional hepatic portal vein in measurements of hyperglycemia, weight gain, circulating insulin levels, c-peptide, and response to glucose challenge. This hypothesis is based in the idea that islets transplanted in a provascular matrix would avoid islet loss due to instant-blood mediated inflammatory reaction and have improve survival and function through increased vascularization. We have previously shown that these PEG-4MAL matrices incorporating peptides for cell adhesion and the growth factor VEGF are functional delivery vehicles to successfully graft and revascularize islets to the small bowel mesentery in healthy rats.

Results

Male Lewis rats weighing between 200-250 g were made diabetic by a single intravenous injection of STZ in citrate buffer (120 mg/kg). Daily monitoring of blood glucose levels by tail tip bleeding indicated an immediate jump in blood glucose levels to approximately 400 mg / dL within 24 hours of STZ injection for all test subjects. Twenty-four hours after STZ injection, test subjects began a supplemental insulin regime. Diabetic animals received daily injections of 2-4U subcutaneous human glargine (Lantus), a long-acting human insulin analog. The expected lifetime of the glargine insulin *in vivo* is ~18 hours, therefore glargine was administered daily immediately following the blood glucose check to minimize interference with daily readings. One week after STZ injection, rats underwent surgery to receive islet transplants. Islets were freshly isolated from healthy male Lewis rats using the methods described previously. Islets were isolated 24 hours prior to transplantation and cultured overnight in RPMI 1640 media supplemented with 10% FBS and 1% Penicillin-Streptomycin.

For islet transplants, diabetic subjects received 1500 islets (approximately 2 donor pancreases) as either an infusion to the hepatic portal system or in a 4% PEG-4MAL hydrogel + 2 mM RGD and 10 µg/mL $VEGF_{165}$ cross-linked with VPM peptide to the small bowel mesentery. Hydrogels were delivered as precursor solutions and cross-linked directly onto the tissue so that no suturing was required and a direct hydrogel to tissue bond was formed. Islets were delivered dispersed in the bulk of the hydrogel during cross-lining. Animals were followed daily for 4 weeks after the transplants for weight gain and blood glucose level and compared to control animals which underwent a sham surgery but received no islets.

Three independent trials were conducted to examine the effects of islet transplantation augmented by PEG-4MAL matrix delivery in diabetic subjects. In Trial 1 supplemental glargine dosing was continued throughout the 4 week post-transplant period. Animals receiving islets delivered in gels had lower blood glucose levels on

average compared to hepatic and sham. However reduction in blood sugar was only moderate not enough to reverse hyperglycemia. Animals receiving islets in hydrogel also gained weight at a greater rate than the sham or hepatic although they were receiving supplemental insulin. Notably these two trends of lower blood sugar and increased weight gain only emerged in the time period following islet transplantation indicating some positive effect of the islets delivered in hydrogel.

In Trial 2 supplemental glargine dosing was discontinued 3 weeks after the transplant and animals were followed for 1 week without supplemental insulin at the end of the trial. In the time period following islet transplant, both hepatic and hydrogel delivered groups had lower blood sugar than sham but were still hyperglycemic although hepatic delivery performed better than hydrogel. Notably animals receiving islets with hydrogel delivery dropped below 200 mg / dL for 2 days in the first week following transplantation but jumped back up into high range quickly thereafter. Coinciding with the moderately reduced blood sugar, the hepatically delivered islet group gained weight more rapidly than either gel delivered or sham. After insulin withdrawal during the last week, the blood glucose of sham animals skyrocketed to 600 mg / dL and several sham animals became immediately ketotic and had to be euthanized. In the week after insulin withdrawal weight gain continued in the hepatic group without supplemental insulin but at a lower rate while it plateaued in the gel group. There was not a significantly different trend in blood glucose levels for gel or hepatic groups between before and after withdrawal of insulin treatment.

In Trial 3 supplemental insulin dosing was discontinued at 1 week after the transplant and animals were followed for 3 weeks without supplemental insulin. Insulin was only given during the first week to help the animals recover from the surgery. Sham animals continued to receive supplemental insulin (2 U / day) so that they would not have to be euthanized as our previous experience predicted that they would die within 24 to 48 hours. Healthy animals were also included as a reference for blood glucose levels but did

not undergo surgery. After insulin withdrawal, blood glucose increased approximately 100 mg / dL across the board for all 3 groups. Weight gain was relatively stagnant for all 3 groups after insulin withdrawal while it had been rising moderately in the week before. While animals receiving islets in hydrogel maintained a higher body weight average than the other groups of the course of the study, the difference in weight gain only occurred during the first week with insulin supplementation and then plateaued.

At the end of trial 3, animals underwent a glucose tolerance test. Test animals were fasted 8 hours overnight prior to the test at which point the received a body weight-standardized bolus dose of 50% glucose solution by IP injection. Subsequent blood sugar monitoring revealed minor differences in glucose response between groups with the sham animals' blood sugar peaking almost 100 mg / dL higher than the gel group.

When the transplant sites were examined for islet survival and vascularization it was readily apparent that there was very little response to the transplant compared to experiments in healthy animals and there were no signs of islets surviving at the implant site macroscopically or histologically in any of the trials. Serum samples were collected at 4 weeks post-transplant in trial 3 and analyzed for circulating levels of insulin and c-peptide by ELISA. Animals receiving islets in gels or hepatically did not have detectable plasma insulin levels. Sham animals had circulating insulin due to supplemental dosing. All diabetic groups had c-peptide below the lowest standard in the kit indicating they were producing minimal or no insulin natively.
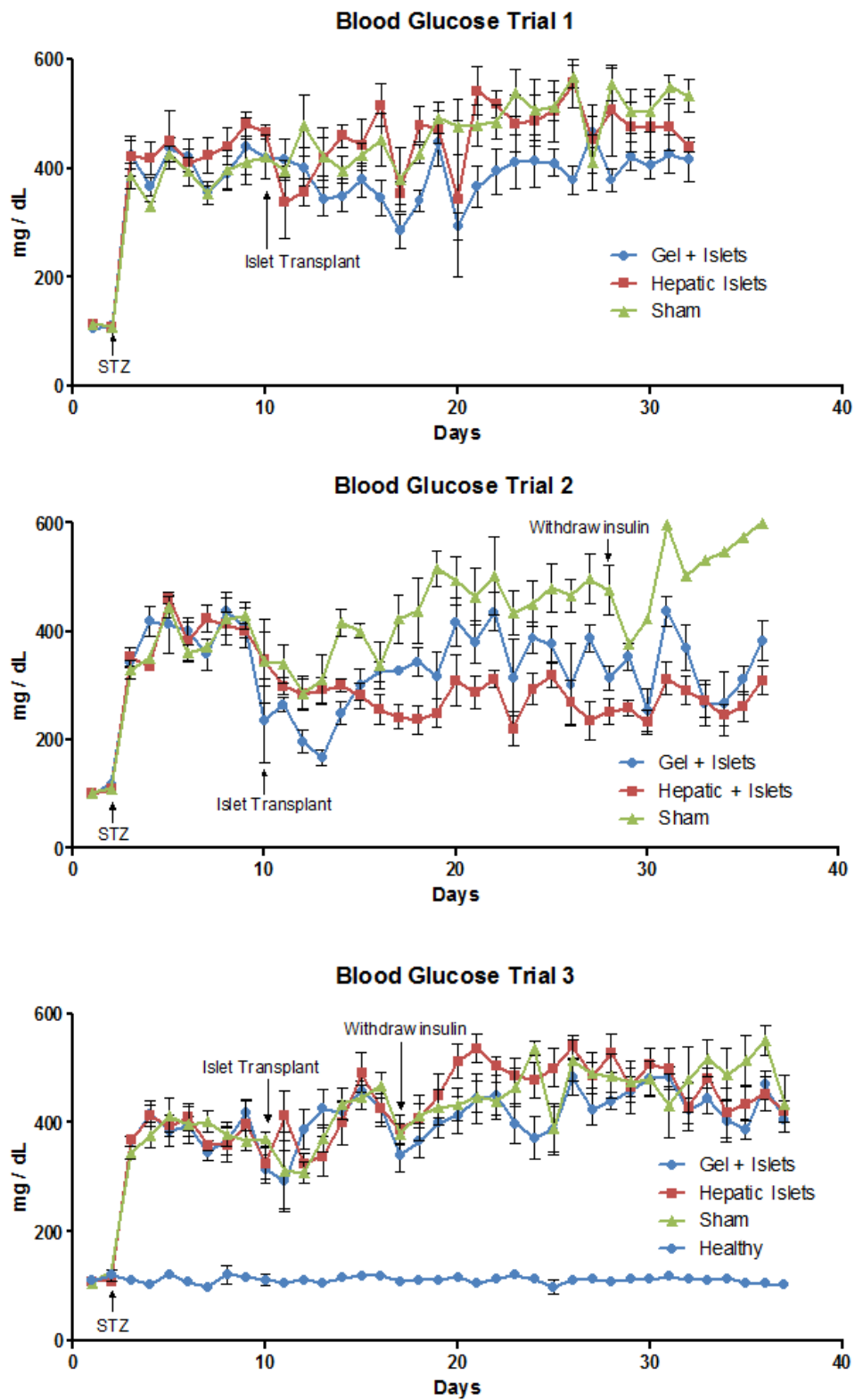
Figure 6.1 Daily blood glucose measurements for diabetic rats in three trials.
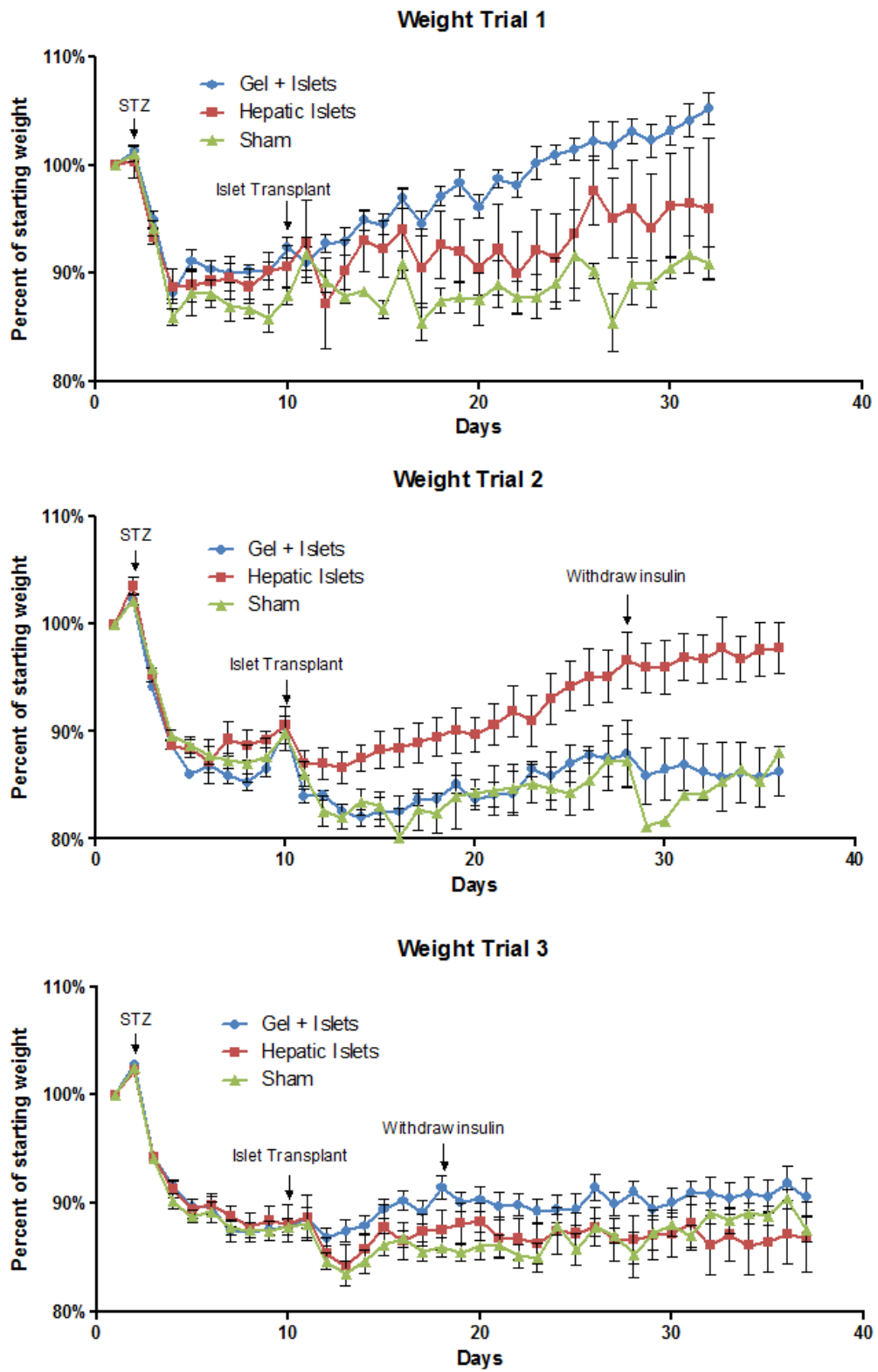
Figure 6.2 Daily weight measurements for diabetic rats in three trials

118
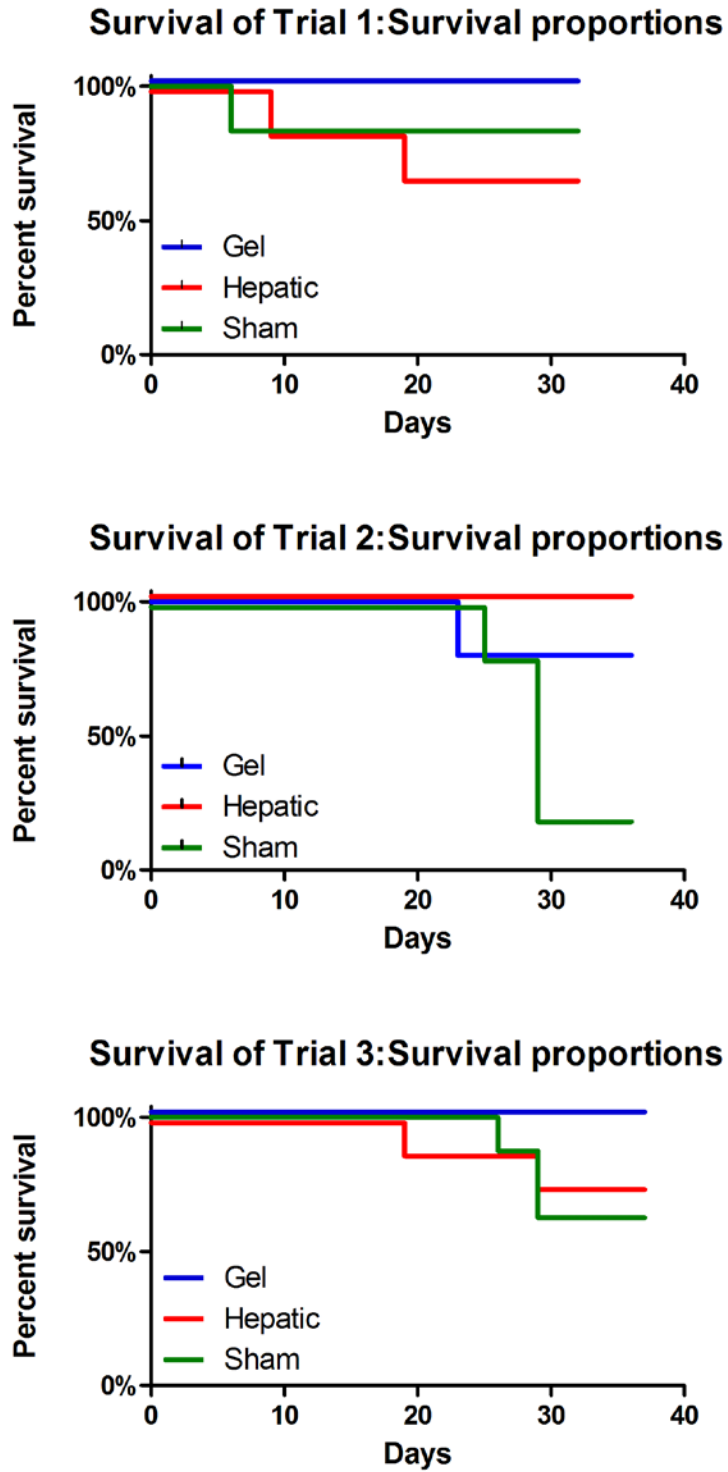
Figure 6.3 Survival curves for diabetic rats in three trials
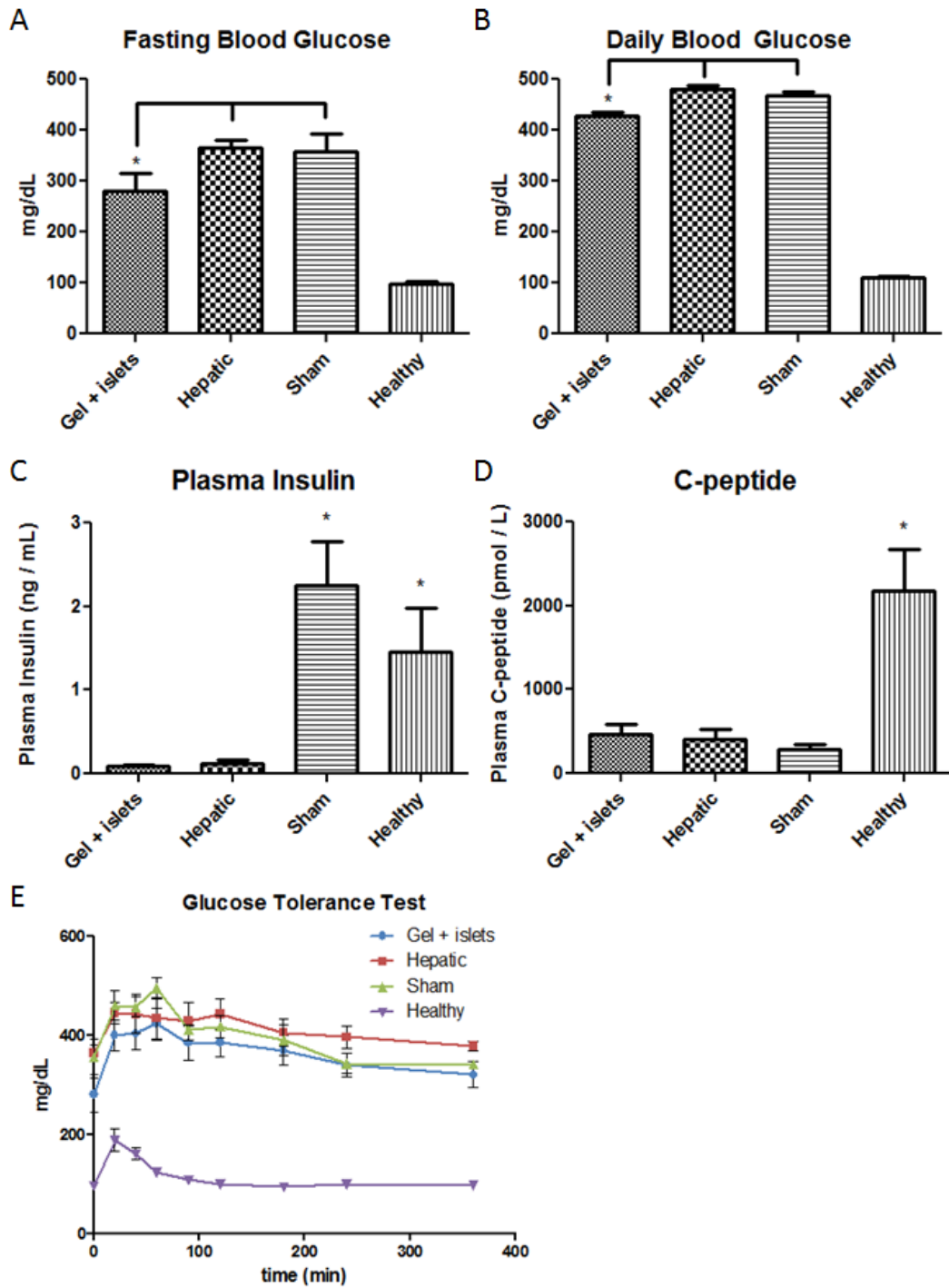
Figure 6.4 Physiological measurements for diabetic rats at the endpoint of trial 3. (A) Blood glucose after 8 hour fasting period. (B) Average of random daily blood glucose over 3 week period without supplemental insulin. (C) Plasma insulin levels 4 weeks after islet transplantation procedure. (D) C-peptide levels 4 weeks after islet transplantation procedure. (E) Glucose tolerance test curves.
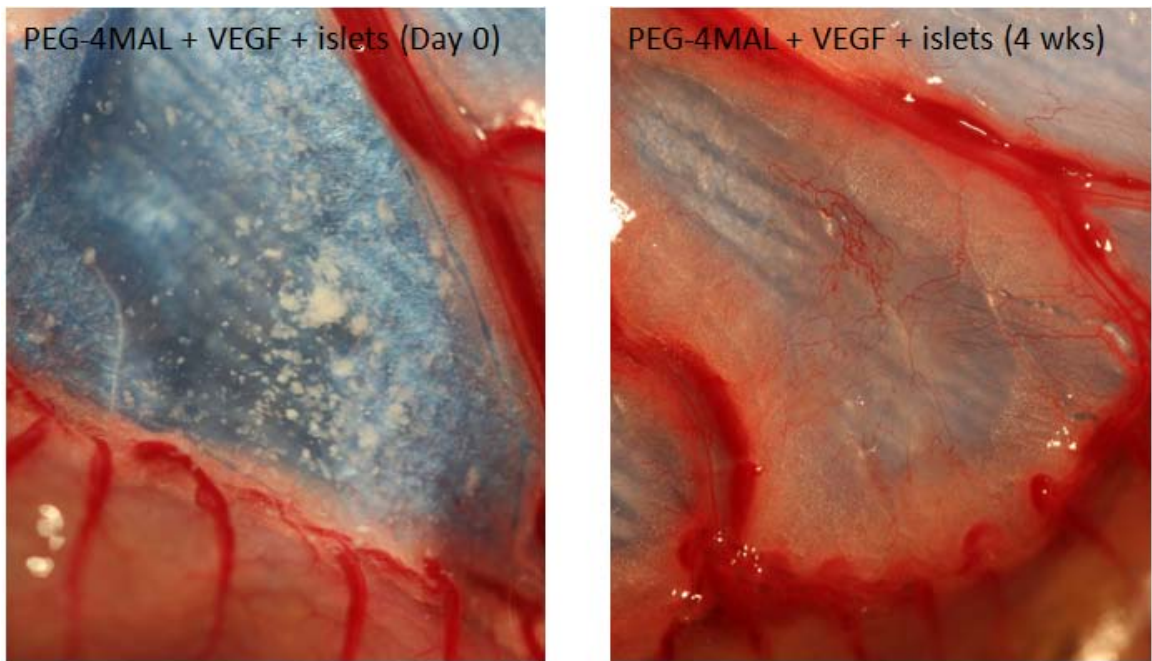
Figure 6.5 Macroscopic vascular response of diabetic rats to islets transplanted in PEG-4MAL

Discussion

Taken together the data indicate that the islet grafts failed to function as expected in the diabetic model with either hepatic portal delivery or gel delivery. The best response was observed in the hepatic delivery group in trial 2 where moderate weight gain was correlated with a lower but still hyperglycemic blood glucose level. Overall, the lack of significant improvements in either weight gain or hyperglycemia in 3 separate trials, no detectable circulating insulin or c-peptide, and no signs of surviving islets at the transplant site points to the conclusion that the islets failed to graft.

Macroscopically it was evident that the vascularization response to the matrices was diminished in diabetic animals compared to the healthy grafts. Complications from diabetic pathology could have resulted in poorer than expected vascularization and grafting response in the diabetic animals. Elevated glucose levels have been shown to inhibit angiogenesis and vascular density in pancreatic islets [279, 292]. In *in vitro* studies angiogenesis assays of HUVECS in the presence of high glucose revealed resulted in a decrease in tubulogenesis [292]. It is not unlikely that the extremely high blood glucose levels in the animals impaired vascularization response to the VEGF in the gel.

It is interesting that the animals had no detectable response to the islet graft during the first 24-48 hours after the transplant for either hepatic or gel delivery and is an indication that the animal model may be too severe for the islet mass delivered. A review of the islet transplantation literature indicates that the most commonly administered dose of STZ in rats ranges from 50-65 mg / kg [293]while we administered 120 mg / kg. High doses of STZ have additional non-specific cyto-toxicity on secondary organs such as the liver, kidneys, and intestine. STZ doses of 75, 150, and 200 mg /kg in mice [294] and 60 mg/kg in rats [295] have been shown to cause liver toxicity, acute kidney damage, and development of hyperglycemic nephropathy superimposed on STZ-related renal cytotoxicity which can significantly complicate interpretation of results. STZ doses of

100 and 150 mg / kg have been associated with high mortality, reduced glycogen processing, and reduced responsiveness to insulin therapy[296]. Moderately induced STZ diabetic animals should be able to survive for several weeks without supplemental insulin dosing while the sham animals in our experiments died within 24-48 hours of insulin withdrawal. While less toxic to secondary systems, a single lower dose of STZ may not result in full-blown diabetes with total elimination of beta cells. A multiple low-dose administration regime is often employed, especially in mice which are more resistant to STZ, but this method results in higher variance between test subjects. It is likely that were this study to be repeated with a lower STZ dose, the diabetic state would be less severe but potentially greater benefits from the islet transplants could be observed.

Lastly, a third possibility is that the total mass of islets delivered was insufficient to generate a detectable response in the animals. Because the animals that did receive islets were able to survive without supplemental insulin better than the sham animals, it is an indication that there was some benefit from the islet transplant. Since the islets were not found at the transplant site, it is possible that the transplanted islets were dislodged from the mesentery and grafted elsewhere in the IP cavity, although the survival rate must have been extremely low to not generate detectable levels of serum insulin. Our estimated delivery of 1500 islets per animal is in agreement with previous reports of successful reversal of STZ-induced diabetes [291, 297]. It is unlikely that the gel-encapsulation process itself is the primary mode of failure as islets were previously observed to be viable up to at least one week post-encapsulation, and surviving islets using the same gel formulation were successfully grafted in healthy animals. Additionally un-encapsulated islets delivered to the portal vein were also unsuccessful at reversing hyperglycemia.

Conclusions

From the outcomes of these studies we concluded that the diabetic state induced in the animals was overly severe for the number of islets being transplanted. Additionally we conclude that the success rate of islet grafting was too low to have a significant impact. We postulate that future iterations of this experiment should incorporate the following changes: Induce a more moderate but still fully hyperglycemic diabetic disease state with a lower dose of STZ. Deliver a larger and more concentrated mass of 6,000 islets instead of 1,500. Incorporate further refinements in the gel design such as an immuno-protective coating for islets and incorporate different or additional cytokines such as FGF, HGF, and glucagon-like peptide-1 to improve survival rates and vascularization.

Materials and Methods

Induction of diabetes in rats with streptozotocin

Streptozotocin was solubilized at 88.89 mg / mL in citrate buffer (20 mg / mL citric acid, 30 mg / mL sodium citrate, 55 mg / mL D-glucose, pH 4.5) by vortexing at 37°C for 60 sec, sterile filtered, and then immediately placed on ice. Under general anesthesia rats were injected with 120 mg / kg of STZ in citrate buffer through the penile vein using an insulin syringe.

Management of STZ-induced diabetes

The overall diabetic state was monitored daily by body weight, blood glucose, and urine ketone level. Daily blood glucose checks were taken by pricking the tail tip with a 30G ½ inch beveled needle and milking a single blood drop onto a handheld glucose meter test strip (Accu-Chek Aviva). In studies 1 and 2, animals were given a daily dose of Glargine Insulin (Lantus) according to their daily blood glucose in mg/dL between 2-5

U. In Study 3 all animals received the same insulin injection dosing of 2 U Glargine per day until 7 days post-transplant at which point insulin was withdrawn from all animals receiving islets. Diabetic animals received fresh water and cage changes daily to account for excessive urination. Animals were euthanized if they lost more than 20% of their initial body weight and did not recover, became severely ketotic, or appeared to be in pain or distress and did not respond to insulin or rehydration therapy.

Serum insulin and c-peptide ELISA

300 uL of blood was collected in heparinized microhematocrit tubes by tail tip bleeding. Plasma was separated by microhematocrit centrifugation, extracted from the capillary tube, and stored at -80°C. Serum insulin and c-peptide were measured with ultra-sensitive rat insulin and c-peptide ELISA kits (Mercodia).

Glucose tolerance test

Rats were fasted for 8 hours prior to the test. 2 grams / kg of 50% D-glucose in PBS diluted to a standard volume of 2 mL was delivered via IP injection in animals that are gently restrained in the head down position with their head covered by a towel to minimize stress. At specified time intervals, glucose levels were determined by tail prick blood on a test strip in a hand-held meter. During the test, food was withheld.

CHAPTER 7

SUMMARY OF CONCLUSIONS

The objective of this dissertation was to develop an engineered synthetic matrix material that would function to enhance islet transplantation through induced vascularization. This objective was proposed to be accomplished through three specific aims. 1: Engineering of bio-functionalized hydrogels to support pancreatic islet encapsulation. 2: Evaluate the in vivo vascularization potential of the engineered hydrogel and islet grafting in healthy rats. 3: Evaluate transplantation of hydrogel-encapsulated pancreatic islets in a rat model of type-1 diabetes.

The initial approach to engineer the hydrogel matrix was based on the photo-cross-linked PEG-DA platform. PEG-DA achieved the primary design criteria for modularity including enzyme-cleavable cross-links, cell adhesion site, and growth factor delivery. PEG-DA includes the additional benefit of photo-patterning capability which we envisioned could eventually be useful to guide angiogenic morphogenesis into specific vascular tree patterns. While we achieved initial success in inducing angiogenesis *in vivo* with PEG-DA hydrogels, the platform ultimately proved incompatible for islet encapsulation and transplantation due to poor islet viability in the encapsulation process and poor tissue / vascular infiltration into the bulk of the material at the small bowel mesentery implant site. These failure modes were attributed to islet sensitivity to the UV light and free radical cross-linking process and the high bulk polymer density and low swelling ratio of the PEG-DA matrix. We found PEG-DA to be extremely unwieldy for *in situ* delivery due to the low viscosity of the precursor solution and UV light requirement for cross-linking.

We sought to address these issues by designing a PEG-based hydrogel with milder cross-linking chemistry, faster degradation kinetics, and a less dense bulk polymer

matrix. We decided to investigate PEG-4MAL as a hydrogel platform due to the commercial availability of the macromer and favorable reaction kinetics of the maleimide to thiol cross-linking reaction. As there were no previous reports of PEG-4MAL hydrogel in the tissue engineering literature, we conducted studies to compare the characteristics of PEG-4MAL to similar molecules including PEG-4A and PEG-4VS which have been widely employed. Our results were very promising, indicating the PEG-4MAL performed better than the established Michael addition hydrogel chemistries in many of our criteria, including lower-modulus matrices, cell viability, reaction efficiency, and *in situ* deliverability.

PEG-4MAL hydrogels proved to be effective matrices for encapsulation of isolated pancreatic islets, preserving viability, insulin expression, and with the addition of VEGF, encouraging endothelial sprouting from intra-islet endothelial cells. Islets delivered in PEG-4MAL were successfully grafted in the small bowel mesentery of healthy animals and were stably connected to the host vascular system by 4 weeks.

We have begun investigate the performance of islets delivered in PEG-4MAL in an STZ animal model of Type 1 diabetes. Unfortunately our first several attempts failed to show significantly favorable improvements in several physiological indicators, ultimately leading to the conclusion that too few islets were surviving the engraftment process in the diabetic animals. This result has lead us to refine our delivery strategy to account for more immuno-protection for the islets with a dual-layered approach for future work as outlined in the next chapter.

CHAPTER 8

FUTURE DIRECTIONS

Introduction

The PEG-4MAL platform developed as the bio-artificial matrix component of this dissertation is a significant leap forward in engineered matrix technology. The introduction of maleimide end groups significantly improves reactive efficiency and decreases cross-linking time by an order of magnitude. Because the improved maleimide-based cross-linking results in predictable ligand tethering at near 1:1 stoichiometric ratios, the PEG-4MAL platform more successfully fulfills the engineering design requirement for controlled and predictable incorporation of bioactive signals than the alternative chemistries PEG-4VS and PEG-4A. Cross-linking speeds on the order of one minute solves a significant *in situ* delivery problem where the gel must set up quickly to maintain shape and position. Importantly the maleimide group's high-affinity to form covalent bonds with thiols allows the PEG-4MAL gel to bond itself to thiols present in tissue, opening up a huge repertoire of potential future directions.

Islet transplantation model

While the islet transplantation efforts on this project to date have not rescued diabetic rats from STZ-induced hyperglycemia, the design flexibility of the material allows for future modifications to improve transplant acceptance and test new ideas. In a new design variation, dual-layer engineered polyethylene glycol maleimide (PEG-4MAL) hydrogels are designed to shield transplanted cells from the host immune system

and enhance engraftment and vascularization of the shielded islets with a vascular-inductive PEG-4MAL matrix as the transplantation vehicle (Fig. 8.1). We hypothesize that micro-bead encapsulated islets transplanted within vascular-inductive bulk PEG-4MAL matrices will lead to improved vascularization in the vicinity of the micro-capsules which in turn will hinder immune rejection responses to the islets themselves.
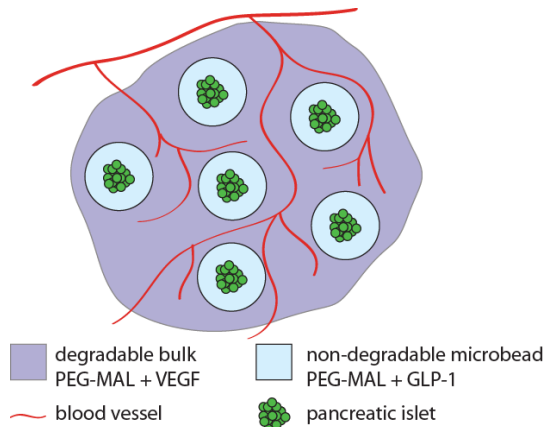
Fig. 8.1: Schematic of dual-layered hydrogels for islet engraftment and function

This approach is entirely different from other encapsulation vehicles that attempt to achieve immuno-isolation alone and serve as simple delivery vehicles (e.g., alginate). Furthermore, we expect that immunoprotection can be achieved in outbred animals without immune suppression or co-stimulatory blockade while simultaneously enhancing islet survival and vascularization. Micro-encapsulation of islets will be achieved by flowing a precursor solution of islets and PEG-4MAL through an air jet encapsulation needle where droplets fall into a bath of dilute di-thiol non-degradable cross-linker. By varying reaction conditions, the thickness and structure of the hydrogel coating can be controlled. Because PEG-4MAL hydrogels are nano-porous, they provide an effective barrier to host immune cells but allow for transport of nutrients/waste and insulin. We hypothesize that these materials will support encapsulated islet survival and endocrine function *in vitro* as measured by viability assays, insulin/glucagon production, and

glucose challenge responsiveness. In addition we will assess the effects of tethering glucagon-like peptide-1 to the PEG-4MAL micro-capsules, a factor known to enhance the function of PEG-encapsulated islets [268].

Tissue Engineering

Outside of islet transplantation, PEG-4MAL shows promise in a variety of tissue engineering models. Our lab is developing materials-based applications in bone repair and regeneration where PEG-4MAL matrices incorporate the adhesive ligands GFOGER [298] and FNIII7-10 [299] to target osteo-specific integrin receptors and subsequently initiate bone repair signaling [300, 301]. Tubular scaffolds are designed to bridge non-healing long-bone fractures and are filled with osteo-inductive hydrogel.

We are also developing models employing PEG-4MAL hydrogel for post-myocardial infarction repair and regeneration. We are experimenting with synergistically delivering growth factors VEGF and HGF bound to PEG-4MAL matrices cross-linked intra-myocardially. Preliminary data shows improved vascularization in the infarct area and improved left ventricular ejection fraction after treatment. In a similar study of infarct regeneration, we are using PEG-4MAL matrices to deliver alginate-encapsulated bone-marrow stromal cells to the surface of infarcted myocardium. The encapsulated stromal cells, which produce regenerative growth factors and cytokines, have much higher viability and are retained at the injury site longer when delivered using PEG-4MAL than alginate-encapsulated cells or cells delivered alone. Lastly we are in the beginning stages of using PEG-4MAL delivery of RNAi to repair aortic aneurisms and delivery of cells and growth factors to treat chronic limb ischemia. All of these models were developed with rapid prototyping due to the plug and play nature of the PEG-4MAL matrix.

Basic Science

PEG-4MAL hydrogel is very useful for basic scientific studies. The intrinsically non-adhesive background of the bulk PEG material provides an environment where the interactions between cells and ligands at specific densities can be studied in three dimensions. Material degradation and elastic modulus can be independently altered and examined. We are currently investigating the use of PEG-4MAL matrices to direct stem cell differentiation through the controlled presentation of integrin-specific ligands. We are also employing PEG-4MAL hydrogels as synthetic microenvironments for epithelial morphogenesis. Epithelial cells encapsulated in PEG-4MAL, under the right matrix formulations, recapitulate the cyst-structure formation seen in natural matrices [131]. Incorporation of bioactive motifs such as degradable cross-linking sequences and cell-adhesion ligands, as well as hydrogel material density (polymer weight / volume percentage) have significant impact on cyst formation.

Smart Materials

Finally, we are investigating PEG-4MAL matrices for the fabrication of dynamic materials. In one project, we are working to develop a contractile cellular machine combining skeletal myocytes with nerve cell networks, using PEG-4MAL hydrogel as a highly-defined and engineered extracellular matrix material. We are also investigating the use of PEG-4MAL in materials with dynamic cell-adhesion ligands. We are working with an RGD peptide with a photo-labile masking group [302] to dynamically present adhesive ligands with the ability to turn adhesion on and off with temporal and special control to modulate such factors as inflammatory response and cell-differentiation timing.

VITA

EDWARD A. PHELPS

PHELPS was born in Oak Ridge, Tennessee. His father was a civil engineer and his mother a special education teacher. Having lived in Virginia, California, and the UK as a boy, he returned to Oak Ridge, Tennessee at age 12. As a young man Phelps competed in men's crew, was active in Boy Scouts achieving the rank of Eagle, and earned his high school diploma from Oak Ridge High School in 2002. After graduating, Phelps attended Georgia Tech and earned a B.S. in Biomedical Engineering with a Minor in International Affairs in 2006. During his undergraduate years Phelps participated on the Georgia Tech Sailing Club race team and studied abroad in Brussels, Belgium where he met his future wife, Amanda Books, now an attorney. In 2006 Phelps continued his studies at Georgia Tech to pursue a Doctorate in Bioengineering with Minor in Chemical Engineering. Phelps is passionate about the great outdoors and adventure sports. He enjoys traveling with his wife, rock climbing, and hiking with his two dogs Beau and Annie.

REFERENCES

1. Lu, C., et al., *Effect of age on vascularization during fracture repair.* J Orthop Res, 2008.

2. Takeshita, S., et al., *Therapeutic angiogenesis. A single intraarterial bolus of vascular endothelial growth factor augments revascularization in a rabbit ischemic hind limb model.* J Clin Invest, 1994. **93**(2): p. 662-70.

3. van Weel, V., et al., *Vascular growth in ischemic limbs: a review of mechanisms and possible therapeutic stimulation.* Ann Vasc Surg, 2008. **22**(4): p. 582-97.

4. Simons, M. and J.A. Ware, *Therapeutic angiogenesis in cardiovascular disease.* Nat Rev Drug Discov, 2003. **2**(11): p. 863-71.

5. Renault, M.A. and D.W. Losordo, *Therapeutic myocardial angiogenesis.* Microvasc Res, 2007. **74**(2-3): p. 159-71.

6. Tongers, J., J.G. Roncalli, and D.W. Losordo, *Therapeutic angiogenesis for critical limb ischemia: microvascular therapies coming of age.* Circulation, 2008. **118**(1): p. 9-16.

7. Jacobs, J., *Combating cardiovascular disease with angiogenic therapy.* Drug Discov Today, 2007. **12**(23-24): p. 1040-5.

8. Tse, H.F. and C.P. Lau, *Therapeutic angiogenesis with bone marrow--derived stem cells.* J Cardiovasc Pharmacol Ther, 2007. **12**(2): p. 89-97.

9. Kuhlmann, M.T., R. Klocke, and S. Nikol, *Therapeutic angiogenesis for peripheral artery disease: cytokine therapy.* Vasa, 2007. **36**(4): p. 253-60.

10. Lachmann, N. and S. Nikol, *Therapeutic angiogenesis for peripheral artery disease: stem cell therapy.* Vasa, 2007. **36**(4): p. 241-51.

11. Simons, M., *Angiogenesis: where do we stand now?* Circulation, 2005. **111**(12): p. 1556-66.

12. Carmeliet, P., *Angiogenesis in health and disease.* Nat Med, 2003. **9**(6): p. 653-60.

13.   Carmeliet, P., *Mechanisms of angiogenesis and arteriogenesis.* Nat Med, 2000. **6**(4): p. 389-95.

14.   Adams, R.H. and K. Alitalo, *Molecular regulation of angiogenesis and lymphangiogenesis.* Nat Rev Mol Cell Biol, 2007. **8**(6): p. 464-78.

15.   Potente, M., H. Gerhardt, and P. Carmeliet, *Basic and Therapeutic Aspects of Angiogenesis.* Cell, 2011. **146**(6): p. 873-887.

16.   Davies, N., et al., *The dosage dependence of VEGF stimulation on scaffold neovascularisation.* Biomaterials, 2008. **29**(26): p. 3531-8.

17.   Djonov, V., O. Baum, and P.H. Burri, *Vascular remodeling by intussusceptive angiogenesis.* Cell Tissue Res, 2003. **314**(1): p. 107-17.

18.   le Noble, F., et al., *Neural guidance molecules, tip cells, and mechanical factors in vascular development.* Cardiovasc Res, 2008. **78**(2): p. 232-41.

19.   Wilson, B.D., et al., *Netrins promote developmental and therapeutic angiogenesis.* Science, 2006. **313**(5787): p. 640-4.

20.   Luttun, A., M. Tjwa, and P. Carmeliet, *Placental growth factor (PlGF) and its receptor Flt-1 (VEGFR-1): novel therapeutic targets for angiogenic disorders.* Ann N Y Acad Sci, 2002. **979**: p. 80-93.

21.   Khurana, R. and M. Simons, *Insights from angiogenesis trials using fibroblast growth factor for advanced arteriosclerotic disease.* Trends Cardiovasc Med, 2003. **13**(3): p. 116-22.

22.   Hao, X., et al., *Angiogenic effects of sequential release of VEGF-A165 and PDGF-BB with alginate hydrogels after myocardial infarction.* Cardiovasc Res, 2007. **75**(1): p. 178-85.

23.   Pipp, F., et al., *Elevated fluid shear stress enhances postocclusive collateral artery growth and gene expression in the pig hind limb.* Arterioscler Thromb Vasc Biol, 2004. **24**(9): p. 1664-8.

24.   Cai, W. and W. Schaper, *Mechanisms of arteriogenesis.* Acta Biochim Biophys Sin (Shanghai), 2008. **40**(8): p. 681-92.

25.   Murray, C.D., *The Physiological Principle of Minimum Work: I. The Vascular System and the Cost of Blood Volume.* Proc Natl Acad Sci U S A, 1926. **12**(3): p. 207-14.

26.   Purhonen, S., et al., *Bone marrow-derived circulating endothelial precursors do not contribute to vascular endothelium and are not needed for tumor growth.* Proc Natl Acad Sci U S A, 2008. **105**(18): p. 6620-5.

27.   Kocher, A.A., et al., *Neovascularization of ischemic myocardium by human bone-marrow-derived angioblasts prevents cardiomyocyte apoptosis, reduces remodeling and improves cardiac function.* Nat Med, 2001. **7**(4): p. 430-6.

28.   Stamm, C., et al., *Autologous bone-marrow stem-cell transplantation for myocardial regeneration.* Lancet, 2003. **361**(9351): p. 45-6.

29.   Beeres, S.L., et al., *Intramyocardial injection of autologous bone marrow mononuclear cells in patients with chronic myocardial infarction and severe left ventricular dysfunction.* Am J Cardiol, 2007. **100**(7): p. 1094-8.

30.   Asahara, T. and A. Kawamoto, *Endothelial progenitor cells for postnatal vasculogenesis.* Am J Physiol Cell Physiol, 2004. **287**(3): p. C572-9.

31.   Carmeliet, P., *VEGF gene therapy: stimulating angiogenesis or angioma-genesis?* Nat Med, 2000. **6**(10): p. 1102-3.

32.   Sun, Q., et al., *Sustained vascular endothelial growth factor delivery enhances angiogenesis and perfusion in ischemic hind limb.* Pharm Res, 2005. **22**(7): p. 1110-6.

33.   Simons, M., et al., *Clinical trials in coronary angiogenesis: issues, problems, consensus: An expert panel summary.* Circulation, 2000. **102**(11): p. E73-86.

34.   Ennett, A.B., D. Kaigler, and D.J. Mooney, *Temporally regulated delivery of VEGF in vitro and in vivo.* J Biomed Mater Res A, 2006. **79**(1): p. 176-84.

35.   Dietrich, F. and P.I. Lelkes, *Fine-tuning of a three-dimensional microcarrier-based angiogenesis assay for the analysis of endothelial-mesenchymal cell co-cultures in fibrin and collagen gels.* Angiogenesis, 2006. **9**(3): p. 111-25.

36.   Nehls, V. and D. Drenckhahn, *A novel, microcarrier-based in vitro assay for rapid and reliable quantification of three-dimensional cell migration and angiogenesis.* Microvasc Res, 1995. **50**(3): p. 311-22.

37.   Chen, R.R., et al., *Integrated approach to designing growth factor delivery systems.* Faseb J, 2007. **21**(14): p. 3896-903.

38.   Gerhardt, H., et al., *VEGF guides angiogenic sprouting utilizing endothelial tip cell filopodia.* J Cell Biol, 2003. **161**(6): p. 1163-77.

39.   Fleury, M.E., K.C. Boardman, and M.A. Swartz, *Autologous morphogen gradients by subtle interstitial flow and matrix interactions.* Biophys J, 2006. **91**(1): p. 113-21.

40.   Helm, C.L., et al., *Synergy between interstitial flow and VEGF directs capillary morphogenesis in vitro through a gradient amplification mechanism.* Proc Natl Acad Sci U S A, 2005. **102**(44): p. 15779-84.

41.   Semino, C.E., R.D. Kamm, and D.A. Lauffenburger, *Autocrine EGF receptor activation mediates endothelial cell migration and vascular morphogenesis induced by VEGF under interstitial flow.* Exp Cell Res, 2006. **312**(3): p. 289-98.

42.   Luttun, A., et al., *Revascularization of ischemic tissues by PlGF treatment, and inhibition of tumor angiogenesis, arthritis and atherosclerosis by anti-Flt1.* Nat Med, 2002. **8**(8): p. 831-40.

43.   Carmeliet, P., et al., *Synergism between vascular endothelial growth factor and placental growth factor contributes to angiogenesis and plasma extravasation in pathological conditions.* Nat Med, 2001. **7**(5): p. 575-83.

44.   van Royen, N., et al., *Stimulation of arteriogenesis; a new concept for the treatment of arterial occlusive disease.* Cardiovasc Res, 2001. **49**(3): p. 543-53.

45.   Silva, E.A. and D.J. Mooney, *Spatiotemporal control of vascular endothelial growth factor delivery from injectable hydrogels enhances angiogenesis.* J Thromb Haemost, 2007. **5**(3): p. 590-8.

46.   Hopkins, S.P., et al., *Controlled delivery of vascular endothelial growth factor promotes neovascularization and maintains limb function in a rabbit model of ischemia.* J Vasc Surg, 1998. **27**(5): p. 886-94; discussion 895.

47.   Jain, R.K., *Molecular regulation of vessel maturation.* Nat Med, 2003. **9**(6): p. 685-93.

48.   Dellian, M., et al., *Quantitation and physiological characterization of angiogenic vessels in mice: effect of basic fibroblast growth factor, vascular endothelial growth factor/vascular permeability factor, and host microenvironment.* Am J Pathol, 1996. **149**(1): p. 59-71.

49.   Chen, R.R., et al., *Spatio-temporal VEGF and PDGF delivery patterns blood vessel formation and maturation.* Pharm Res, 2007. **24**(2): p. 258-64.

50.   Richardson, T.P., et al., *Polymeric system for dual growth factor delivery.* Nat Biotechnol, 2001. **19**(11): p. 1029-34.

51.   Marui, A., et al., *Simultaneous application of basic fibroblast growth factor and hepatocyte growth factor to enhance the blood vessels formation.* J Vasc Surg, 2005. **41**(1): p. 82-90.

52.   Shyu, K.G., H. Chang, and J.M. Isner, *Synergistic effect of angiopoietin-1 and vascular endothelial growth factor on neoangiogenesis in hypercholesterolemic rabbit model with acute hindlimb ischemia.* Life Sci, 2003. **73**(5): p. 563-79.

53.   Zohlnhofer, D., et al., *Stem cell mobilization by granulocyte colony-stimulating factor in patients with acute myocardial infarction: a randomized controlled trial.* Jama, 2006. **295**(9): p. 1003-10.

54.   Horowitz, A. and M. Simons, *Branching morphogenesis.* Circ Res, 2008. **103**(8): p. 784-95.

55.   Vincent, K.A., et al., *Angiogenesis is induced in a rabbit model of hindlimb ischemia by naked DNA encoding an HIF-1alpha/VP16 hybrid transcription factor.* Circulation, 2000. **102**(18): p. 2255-61.

56.   Shyu, K.G., et al., *Intramyocardial injection of naked DNA encoding HIF-1alpha/VP16 hybrid to enhance angiogenesis in an acute myocardial infarction model in the rat.* Cardiovasc Res, 2002. **54**(3): p. 576-83.

57.   Rajagopalan, S., et al., *Use of a constitutively active hypoxia-inducible factor-1alpha transgene as a therapeutic strategy in no-option critical limb ischemia patients: phase I dose-escalation experience.* Circulation, 2007. **115**(10): p. 1234-43.

58.   Elson, D.A., et al., *Induction of hypervascularity without leakage or inflammation in transgenic mice overexpressing hypoxia-inducible factor-1alpha.* Genes Dev, 2001. **15**(19): p. 2520-32.

59.   Liu, L., et al., *Age-dependent impairment of HIF-1alpha expression in diabetic mice: Correction with electroporation-facilitated gene therapy increases wound healing, angiogenesis, and circulating angiogenic cells.* J Cell Physiol, 2008.

60.   Wang, R., et al., *Gene transfer of vascular endothelial growth factor plasmid/liposome complexes in glioma cells in vitro: the implication for the treatment of cerebral ischemic diseases.* Clin Hemorheol Microcirc, 2000. **23**(2-4): p. 303-6.

61.   Xie, D., et al., *An engineered vascular endothelial growth factor-activating transcription factor induces therapeutic angiogenesis in ApoE knockout mice with hindlimb ischemia.* J Vasc Surg, 2006. **44**(1): p. 166-75.

62.   Dai, Q., et al., *Engineered zinc finger-activating vascular endothelial growth factor transcription factor plasmid DNA induces therapeutic angiogenesis in rabbits with hindlimb ischemia.* Circulation, 2004. **110**(16): p. 2467-75.

63.   Fuchs, S., et al., *Transendocardial delivery of autologous bone marrow enhances collateral perfusion and regional function in pigs with chronic experimental myocardial ischemia.* J Am Coll Cardiol, 2001. **37**(6): p. 1726-32.

64.   Gavira, J.J., et al., *Autologous skeletal myoblast transplantation in patients with nonacute myocardial infarction: 1-year follow-up.* J Thorac Cardiovasc Surg, 2006. **131**(4): p. 799-804.

65.   Menasche, P., et al., *The Myoblast Autologous Grafting in Ischemic Cardiomyopathy (MAGIC) trial: first randomized placebo-controlled study of myoblast transplantation.* Circulation, 2008. **117**(9): p. 1189-200.

66.   Menasche, P., et al., *Autologous skeletal myoblast transplantation for severe postinfarction left ventricular dysfunction.* J Am Coll Cardiol, 2003. **41**(7): p. 1078-83.

67.   Kalka, C., et al., *Transplantation of ex vivo expanded endothelial progenitor cells for therapeutic neovascularization.* Proc Natl Acad Sci U S A, 2000. **97**(7): p. 3422-7.

68.   Tateishi-Yuyama, E., et al., *Therapeutic angiogenesis for patients with limb ischaemia by autologous transplantation of bone-marrow cells: a pilot study and a randomised controlled trial.* Lancet, 2002. **360**(9331): p. 427-35.

69.   Jujo, K., M. Ii, and D.W. Losordo, *Endothelial progenitor cells in neovascularization of infarcted myocardium.* J Mol Cell Cardiol, 2008. **45**(4): p. 530-44.

70.   Kawamoto, A., T. Asahara, and D.W. Losordo, *Transplantation of endothelial progenitor cells for therapeutic neovascularization.* Cardiovasc Radiat Med, 2002. **3**(3-4): p. 221-5.

71.   Wu, Y., et al., *Mesenchymal stem cells enhance wound healing through differentiation and angiogenesis.* Stem Cells, 2007. **25**(10): p. 2648-59.

72.   Matsumoto, T., et al., *Circulating endothelial/skeletal progenitor cells for bone regeneration and healing.* Bone, 2008.

73.   Asahara, T., et al., *Isolation of putative progenitor endothelial cells for angiogenesis.* Science, 1997. **275**(5302): p. 964-7.

74.   Kawamoto, A., et al., *CD34-positive cells exhibit increased potency and safety for therapeutic neovascularization after myocardial infarction compared with total mononuclear cells.* Circulation, 2006. **114**(20): p. 2163-9.

75.   Losordo, D.W., et al., *Intramyocardial transplantation of autologous CD34+ stem cells for intractable angina: a phase I/IIa double-blind, randomized controlled trial.* Circulation, 2007. **115**(25): p. 3165-72.

76.   Kawamoto, A., et al., *Intramuscular transplantation of G-CSF-mobilized CD34(+) cells in patients with critical limb ischemia: a phase I/IIa, multicenter, single-blinded, dose-escalation clinical trial.* Stem Cells, 2009. **27**(11): p. 2857-64.

77.   Van't Hof, W., et al., *Direct delivery of syngeneic and allogeneic large-scale expanded multipotent adult progenitor cells improves cardiac function after myocardial infarct.* Cytotherapy, 2007. **9**(5): p. 477-87.

78.   Avci-Adali, M., G. Ziemer, and H.P. Wendel, *Induction of EPC homing on biofunctionalized vascular grafts for rapid in vivo self-endothelialization--a review of current strategies.* Biotechnol Adv, 2010. **28**(1): p. 119-29.

79.   Zampetaki, A., J.P. Kirton, and Q. Xu, *Vascular repair by endothelial progenitor cells.* Cardiovasc Res, 2008. **78**(3): p. 413-21.

80.   Penn, M.S. and M.K. Khalil, *Exploitation of stem cell homing for gene delivery.* Expert Opin Biol Ther, 2008. **8**(1): p. 17-30.

81.   Korbling, M. and Z. Estrov, *Adult stem cells for tissue repair - a new therapeutic concept?* N Engl J Med, 2003. **349**(6): p. 570-82.

82.   Mathur, A. and J.F. Martin, *Stem cells and repair of the heart.* Lancet, 2004. **364**(9429): p. 183-92.

83.   Wang, Y., et al., *Effect of mobilization of bone marrow stem cells by granulocyte colony stimulating factor on clinical symptoms, left ventricular perfusion and function in patients with severe chronic ischemic heart disease.* Int J Cardiol, 2005. **100**(3): p. 477-83.

84.   Engelmann, M.G., et al., *Autologous bone marrow stem cell mobilization induced by granulocyte colony-stimulating factor after subacute ST-segment elevation myocardial infarction undergoing late revascularization: final results from the G-CSF-STEMI (Granulocyte Colony-Stimulating Factor ST-Segment Elevation Myocardial Infarction) trial.* J Am Coll Cardiol, 2006. **48**(8): p. 1712-21.

85.   Ripa, R.S., et al., *Intramyocardial injection of vascular endothelial growth factor-A165 plasmid followed by granulocyte-colony stimulating factor to induce angiogenesis in patients with severe chronic ischaemic heart disease.* Eur Heart J, 2006. **27**(15): p. 1785-92.

86.   Qin, G., et al., *Functional disruption of alpha4 integrin mobilizes bone marrow-derived endothelial progenitors and augments ischemic neovascularization.* J Exp Med, 2006. **203**(1): p. 153-63.

87.   Prosper, F., et al., *Mobilization and homing of peripheral blood progenitors is related to reversible downregulation of alpha4 beta1 integrin expression and function.* J Clin Invest, 1998. **101**(11): p. 2456-67.

88.   Wagers, A.J., R.C. Allsopp, and I.L. Weissman, *Changes in integrin expression are associated with altered homing properties of Lin(-/lo)Thy1.1(lo)Sca-1(+)c-kit(+) hematopoietic stem cells following mobilization by cyclophosphamide/granulocyte colony-stimulating factor.* Exp Hematol, 2002. **30**(2): p. 176-85.

89.   Kwon, S.M., et al., *Specific Jagged-1 signal from bone marrow microenvironment is required for endothelial progenitor cell development for neovascularization.* Circulation, 2008. **118**(2): p. 157-65.

90.   Kawamoto, A. and T. Asahara, *Role of progenitor endothelial cells in cardiovascular disease and upcoming therapies.* Catheter Cardiovasc Interv, 2007. **70**(4): p. 477-84.

91.   Askari, A., et al., *Cellular, but not direct, adenoviral delivery of vascular endothelial growth factor results in improved left ventricular function and*

neovascularization in dilated ischemic cardiomyopathy. J Am Coll Cardiol, 2004. **43**(10): p. 1908-14.

92.   Bian, J., et al., *Engineered cell therapy for sustained local myocardial delivery of nonsecreted proteins.* Cell Transplant, 2006. **15**(1): p. 67-74.

93.   Penn, M.S., *Cell-based gene therapy for the prevention and treatment of cardiac dysfunction.* Nat Clin Pract Cardiovasc Med, 2007. **4 Suppl 1**: p. S83-8.

94.   Jabbarzadeh, E., et al., *Induction of angiogenesis in tissue-engineered scaffolds designed for bone repair: a combined gene therapy-cell transplantation approach.* Proc Natl Acad Sci U S A, 2008. **105**(32): p. 11099-104.

95.   Koike, N., et al., *Tissue engineering: creation of long-lasting blood vessels.* Nature, 2004. **428**(6979): p. 138-9.

96.   Kobayashi, H., et al., *Fibroblast sheets co-cultured with endothelial progenitor cells improve cardiac function of infarcted hearts.* J Artif Organs, 2008. **11**(3): p. 141-7.

97.   Levenberg, S., et al., *Engineering vascularized skeletal muscle tissue.* Nat Biotechnol, 2005. **23**(7): p. 879-84.

98.   Rizzi, S.C., et al., *Recombinant protein-co-PEG networks as cell-adhesive and proteolytically degradable hydrogel matrixes. Part II: biofunctional characteristics.* Biomacromolecules, 2006. **7**(11): p. 3019-29.

99.   Ehrbar, M., et al., *The role of actively released fibrin-conjugated VEGF for VEGF receptor 2 gene activation and the enhancement of angiogenesis.* Biomaterials, 2008. **29**(11): p. 1720-9.

100.   Dye, J., et al., *Distinct patterns of microvascular endothelial cell morphology are determined by extracellular matrix composition.* Endothelium, 2004. **11**(3-4): p. 151-67.

101.   Stupack, D.G. and D.A. Cheresh, *Integrins and angiogenesis.* Curr Top Dev Biol, 2004. **64**: p. 207-38.

102.   Serini, G., et al., *Besides adhesion: new perspectives of integrin functions in angiogenesis.* Cardiovasc Res, 2008. **78**(2): p. 213-22.

103.   Clark, R.A., *Synergistic signaling from extracellular matrix-growth factor complexes.* J Invest Dermatol, 2008. **128**(6): p. 1354-5.

104. Ehrbar, M., et al., *Cell-demanded liberation of VEGF121 from fibrin implants induces local and controlled blood vessel growth.* Circ Res, 2004. **94**(8): p. 1124-32.

105. Zisch, A.H., et al., *Cell-demanded release of VEGF from synthetic, biointeractive cell ingrowth matrices for vascularized tissue growth.* Faseb J, 2003. **17**(15): p. 2260-2.

106. Zisch, A.H., M.P. Lutolf, and J.A. Hubbell, *Biopolymeric delivery matrices for angiogenic growth factors.* Cardiovasc Pathol, 2003. **12**(6): p. 295-310.

107. Gobin, A.S. and J.L. West, *Effects of epidermal growth factor on fibroblast migration through biomimetic hydrogels.* Biotechnol Prog, 2003. **19**(6): p. 1781-5.

108. Moon, J.J., S.H. Lee, and J.L. West, *Synthetic biomimetic hydrogels incorporated with ephrin-A1 for therapeutic angiogenesis.* Biomacromolecules, 2007. **8**(1): p. 42-9.

109. Hahn, M.S., et al., *Photolithographic patterning of polyethylene glycol hydrogels.* Biomaterials, 2006. **27**(12): p. 2519-2524.

110. Polizzotti, B.D., B.D. Fairbanks, and K.S. Anseth, *Three-dimensional biochemical patterning of click-based composite hydrogels via thiolene photopolymerization.* Biomacromolecules, 2008. **9**(4): p. 1084-7.

111. Lee, S.H., J.J. Moon, and J.L. West, *Three-dimensional micropatterning of bioactive hydrogels via two-photon laser scanning photolithography for guided 3D cell migration.* Biomaterials, 2008. **29**(20): p. 2962-8.

112. Dike, L.E., et al., *Geometric control of switching between growth, apoptosis, and differentiation during angiogenesis using micropatterned substrates.* In Vitro Cell Dev Biol Anim, 1999. **35**(8): p. 441-8.

113. Mancuso, M.R., et al., *Rapid vascular regrowth in tumors after reversal of VEGF inhibition.* J Clin Invest, 2006. **116**(10): p. 2610-21.

114. Kamba, T., et al., *VEGF-dependent plasticity of fenestrated capillaries in the normal adult microvasculature.* Am J Physiol Heart Circ Physiol, 2006. **290**(2): p. H560-76.

115. Fournier, A.E. and S.M. Strittmatter, *Regenerating nerves follow the road more traveled.* Nat Neurosci, 2002. **5**(9): p. 821-2.

116. Baffert, F., et al., *Cellular changes in normal blood capillaries undergoing regression after inhibition of VEGF signaling.* Am J Physiol Heart Circ Physiol, 2006. **290**(2): p. H547-59.

117. Vracko, R. and E.P. Benditt, *Basal lamina: the scaffold for orderly cell replacement. Observations on regeneration of injured skeletal muscle fibers and capillaries.* J Cell Biol, 1972. **55**(2): p. 406-19.

118. Cheng, D. and M.V. Sefton, *Dual delivery of placental growth factor and vascular endothelial growth factor from poly(hydroxyethyl methacrylate-co-methyl methacrylate) microcapsules containing doubly transfected luciferase-expressing L929 cells.* Tissue Eng Part A, 2009. **15**(8): p. 1929-39.

119. Sarkar, K., et al., *Adenoviral transfer of HIF-1alpha enhances vascular responses to critical limb ischemia in diabetic mice.* Proc Natl Acad Sci U S A, 2009. **106**(44): p. 18769-74.

120. Sun, L., Y. Bai, and G. Du, *Endothelial dysfunction--an obstacle of therapeutic angiogenesis.* Ageing Res Rev, 2009. **8**(4): p. 306-13.

121. Yang, F., et al., *Genetic engineering of human stem cells for enhanced angiogenesis using biodegradable polymeric nanoparticles.* Proc Natl Acad Sci U S A, 2010. **107**(8): p. 3317-22.

122. Melero-Martin, J.M., et al., *Engineering robust and functional vascular networks in vivo with human adult and cord blood-derived progenitor cells.* Circ Res, 2008. **103**(2): p. 194-202.

123. Loffredo, F. and R.T. Lee, *Therapeutic vasculogenesis: it takes two.* Circ Res, 2008. **103**(2): p. 128-30.

124. Kraehenbuehl, T.P., et al., *Cell-responsive hydrogel for encapsulation of vascular cells.* Biomaterials, 2009. **30**(26): p. 4318-24.

125. Moon, J.J., et al., *Biomimetic hydrogels with pro-angiogenic properties.* Biomaterials, 2010. **31**(14): p. 3840-7.

126. Leslie-Barbick, J.E., J.J. Moon, and J.L. West, *Covalently-immobilized vascular endothelial growth factor promotes endothelial cell tubulogenesis in poly(ethylene glycol) diacrylate hydrogels.* J Biomater Sci Polym Ed, 2009. **20**(12): p. 1763-79.

127.   Phelps, E.A., et al., *Bioartificial matrices for therapeutic vascularization.* Proc Natl Acad Sci USA, 2010. **107**(8): p. 3323-8.

128.   Ghanaati, S., et al., *Dynamic in vivo biocompatibility of angiogenic peptide amphiphile nanofibers.* Biomaterials, 2009. **30**(31): p. 6202-12.

129.   Kraehenbuehl, T.P., et al., *Three-dimensional extracellular matrix-directed cardioprogenitor differentiation: systematic modulation of a synthetic cell-responsive PEG-hydrogel.* Biomaterials, 2008. **29**(18): p. 2757-66.

130.   Weber, L.M. and K.S. Anseth, *Hydrogel encapsulation environments functionalized with extracellular matrix interactions increase islet insulin secretion.* Matrix Biol, 2008. **27**(8): p. 667-73.

131.   Chung, I.M., et al., *Bioadhesive hydrogel microenvironments to modulate epithelial morphogenesis.* Biomaterials, 2008. **29**(17): p. 2637-45.

132.   Gupta, R., N. Van Rooijen, and M.V. Sefton, *Fate of endothelialized modular constructs implanted in an omental pouch in nude rats.* Tissue Eng Part A, 2009. **15**(10): p. 2875-87.

133.   Kelm, J.M., et al., *A novel concept for scaffold-free vessel tissue engineering: Self-assembly of microtissue building blocks.* J Biotechnol, 2010.

134.   Sasagawa, T., et al., *Design of prevascularized three-dimensional cell-dense tissues using a cell sheet stacking manipulation technology.* Biomaterials, 2010. **31**(7): p. 1646-54.

135.   Su, D., et al., *Angiopoietin-1 production in islets improves islet engraftment and protects islets from cytokine-induced apoptosis.* Diabetes, 2007. **56**(9): p. 2274-83.

136.   Cheng, Y., et al., *Elevation of vascular endothelial growth factor production and its effect on revascularization and function of graft islets in diabetic rats.* World J Gastroenterol., 2007. **13**(20): p. 2862-2866.

137.   Hussey, A.J., et al., *Seeding of pancreatic islets into prevascularized tissue engineering chambers.* Tissue Eng Part A, 2009. **15**(12): p. 3823-33.

138.   Hiscox, A.M., et al., *An islet-stabilizing implant constructed using a preformed vasculature.* Tissue Eng Part A, 2008. **14**(3): p. 433-40.

139.   Stevens, K.R., et al., *Scaffold-free human cardiac tissue patch created from embryonic stem cells.* Tissue Eng Part A, 2009. **15**(6): p. 1211-22.

140.   Lesman, A., et al., *Transplantation of a tissue-engineered human vascularized cardiac muscle.* Tissue Eng Part A, 2010. **16**(1): p. 115-25.

141.   Dvir, T., et al., *Prevascularization of cardiac patch on the omentum improves its therapeutic outcome.* Proc Natl Acad Sci U S A, 2009. **106**(35): p. 14990-5.

142.   Shepherd, B.R., J.B. Hoying, and S.K. Williams, *Microvascular transplantation after acute myocardial infarction.* Tissue Eng, 2007. **13**(12): p. 2871-9.

143.   Mironov, V., et al., *Organ printing: promises and challenges.* Regen Med, 2008. **3**(1): p. 93-103.

144.   Visconti, R.P., et al., *Towards organ printing: engineering an intra-organ branched vascular tree.* Expert Opin Biol Ther, 2010. **10**(3): p. 409-20.

145.   Moon, J.J., et al., *Micropatterning of Poly(Ethylene Glycol) Diacrylate Hydrogels with Biomolecules to Regulate and Guide Endothelial Morphogenesis.* Tissue Engineering Part A, 2009. **15**(3): p. 579-585.

146.   Kloxin, A.M., et al., *Tunable Hydrogels for External Manipulation of Cellular Microenvironments through Controlled Photodegradation.* Advanced Materials, 2010. **22**(1): p. 61-66.

147.   Chung, S., et al., *Surface-Treatment-Induced Three-Dimensional Capillary Morphogenesis in a Microfluidic Platform.* Advanced Materials, 2009. **21**(47): p. 4863-4867.

148.   Murohara, T., et al., *Nitric oxide synthase modulates angiogenesis in response to tissue ischemia.* J Clin Invest, 1998. **101**(11): p. 2567-78.

149.   Benest, A.V., et al., *Arteriolar genesis and angiogenesis induced by endothelial nitric oxide synthase overexpression results in a mature vasculature.* Arterioscler Thromb Vasc Biol, 2008. **28**(8): p. 1462-8.

150.   Yu, J., et al., *Endothelial nitric oxide synthase is critical for ischemic remodeling, mural cell recruitment, and blood flow reserve.* Proc Natl Acad Sci U S A, 2005. **102**(31): p. 10999-1004.

151.	Kumar, D., et al., *Chronic sodium nitrite therapy augments ischemia-induced angiogenesis and arteriogenesis.* Proc Natl Acad Sci U S A, 2008. **105**(21): p. 7540-5.

152.	Carmeliet, P. and M. Baes, *Metabolism and therapeutic angiogenesis.* N Engl J Med, 2008. **358**(23): p. 2511-2.

153.	Arany, Z., et al., *HIF-independent regulation of VEGF and angiogenesis by the transcriptional coactivator PGC-1alpha.* Nature, 2008. **451**(7181): p. 1008-12.

154.	Aragones, J., et al., *Deficiency or inhibition of oxygen sensor Phd1 induces hypoxia tolerance by reprogramming basal metabolism.* Nat Genet, 2008. **40**(2): p. 170-80.

155.	Papandreou, I., et al., *HIF-1 mediates adaptation to hypoxia by actively downregulating mitochondrial oxygen consumption.* Cell Metab, 2006. **3**(3): p. 187-97.

156.	Murry, C.E., R.B. Jennings, and K.A. Reimer, *Preconditioning with ischemia: a delay of lethal cell injury in ischemic myocardium.* Circulation, 1986. **74**(5): p. 1124-36.

157.	Eckle, T., et al., *Hypoxia-inducible factor-1 is central to cardioprotection: a new paradigm for ischemic preconditioning.* Circulation, 2008. **118**(2): p. 166-75.

158.	Staton, C.A., M.W. Reed, and N.J. Brown, *A critical analysis of current in vitro and in vivo angiogenesis assays.* Int J Exp Pathol, 2009. **90**(3): p. 195-221.

159.	Duvall, C.L., et al., *The role of osteopontin in recovery from hind limb ischemia.* Arterioscler Thromb Vasc Biol, 2008. **28**(2): p. 290-5.

160.	Duvall, C.L., et al., *Quantitative microcomputed tomography analysis of collateral vessel development after ischemic injury.* Am J Physiol Heart Circ Physiol, 2004. **287**(1): p. H302-10.

161.	Jay, S.M., et al., *Engineering of multifunctional gels integrating highly efficient growth factor delivery with endothelial cell transplantation.* Faseb J, 2008. **22**(8): p. 2949-56.

162.	*National Diabetes Fact Sheet.* Centers for Disease Control and Prevention, 2005.

163.	Azzi, J., et al., *Immunological aspects of pancreatic islet cell transplantation.* Expert Rev Clin Immunol, 2010. **6**(1): p. 111-24.

164. *Type 1 Diabetes Facts*. 2010 Dec 2010 [cited 2011 Sept 5 2011]; Available from: http://www.jdrf.org/index.cfm?page_id=102585.

165. Yu, B., et al., *Use of hydrogel coating to improve the performance of implanted glucose sensors.* Biosens Bioelectron, 2008. **23**(8): p. 1278-84.

166. Close, N.C., B.J. Hering, and T.L. Eggerman, *Results From the Inaugural Year of the Collaborative Islet Transplant Registry.* Transplantation Proceedings, 2005. **37**(2): p. 1305-1308.

167. Rickels, M.R., et al., *Islet cell hormonal responses to hypoglycemia after human islet transplantation for type 1 diabetes.* Diabetes, 2005. **54**(11): p. 3205-11.

168. Robertson, R.P., *Islet transplantation as a treatment for diabetes - a work in progress.* N Engl J Med, 2004. **350**(7): p. 694-705.

169. Ryan, E.A., et al., *Successful islet transplantation: continued insulin reserve provides long-term glycemic control.* Diabetes, 2002. **51**(7): p. 2148-57.

170. Ryan, E.A., et al., *Clinical outcomes and insulin secretion after islet transplantation with the Edmonton protocol.* Diabetes, 2001. **50**(4): p. 710-9.

171. Lakey, J.R., M. Mirbolooki, and A.M. Shapiro, *Current status of clinical islet cell transplantation.* Methods Mol Biol, 2006. **333**: p. 47-104.

172. Vaithilingam, V., G. Sundaram, and B.E. Tuch, *Islet cell transplantation.* Curr Opin Organ Transplant, 2008. **13**(6): p. 633-8.

173. Chow, L.W., et al., *Self-assembling nanostructures to deliver angiogenic factors to pancreatic islets.* Biomaterials, 2010.

174. Gupta, R. and M.V. Sefton, *Application of an endothelialized modular construct for islet transplantation in syngeneic and allogeneic immunosuppressed rat models.* Tissue Eng Part A, 2011. **17**(15-16): p. 2005-15.

175. Ballian, N. and F.C. Brunicardi, *Islet vasculature as a regulator of endocrine pancreas function.* World J Surg, 2007. **31**(4): p. 705-14.

176. Brissova, M. and A.C. Powers, *Revascularization of transplanted islets: can it be improved?* Diabetes, 2008. **57**(9): p. 2269-71.

177. Brissova, M., et al., *Pancreatic islet production of vascular endothelial growth factor--a is essential for islet vascularization, revascularization, and function.* Diabetes, 2006. **55**(11): p. 2974-85.

178. Brissova, M., et al., *Intraislet endothelial cells contribute to revascularization of transplanted pancreatic islets.* Diabetes, 2004. **53**(5): p. 1318-25.

179. Carlsson, P.O., et al., *Markedly decreased oxygen tension in transplanted rat pancreatic islets irrespective of the implantation site.* Diabetes, 2001. **50**(3): p. 489-95.

180. Mattsson, G., L. Jansson, and P.O. Carlsson, *Decreased vascular density in mouse pancreatic islets after transplantation.* Diabetes, 2002. **51**(5): p. 1362-6.

181. Shimoda, M., et al., *In vivo non-viral gene delivery of human vascular endothelial growth factor improves revascularisation and restoration of euglycaemia after human islet transplantation into mouse liver.* Diabetologia, 2010.

182. Cheng, K., et al., *Adenovirus-based vascular endothelial growth factor gene delivery to human pancreatic islets.* Gene Ther., 2004. **11**(14): p. 1105-1116.

183. Narang, A.S., et al., *Vascular endothelial growth factor gene delivery for revascularization in transplanted human islets.* Pharm Res, 2004. **21**(1): p. 15-25.

184. Zhang, N., et al., *Elevated vascular endothelial growth factor production in islets improves islet graft vascularization.* Diabetes, 2004. **53**(4): p. 963-70.

185. Barshes, N.R., S. Wyllie, and J.A. Goss, *Inflammation-mediated dysfunction and apoptosis in pancreatic islet transplantation: implications for intrahepatic grafts.* J Leukoc.Biol, 2005. **77**(5): p. 587-597.

186. Emamaullee, J.A. and A.M. Shapiro, *Factors influencing the loss of beta-cell mass in islet transplantation.* Cell Transplant., 2007. **16**(1): p. 1-8.

187. Linn, T., et al., *Ischaemia is linked to inflammation and induction of angiogenesis in pancreatic islets.* Clin.Exp.Immunol., 2006. **144**(2): p. 179-187.

188. Sigrist, S., et al., *Influence of VEGF on the viability of encapsulated pancreatic rat islets after transplantation in diabetic mice.* Cell Transplant., 2003. **12**(6): p. 627-635.

189. Stendahl, J.C., et al., *Growth factor delivery from self-assembling nanofibers to facilitate islet transplantation.* Transplantation, 2008. **86**(3): p. 478-81.

190.   Olerud, J., et al., *Improved vascular engraftment and graft function after inhibition of the angiostatic factor thrombospondin-1 in mouse pancreatic islets.* Diabetes, 2008. **57**(7): p. 1870-7.

191.   Konstantinova, I. and E. Lammert, *Microvascular development: learning from pancreatic islets.* BioEssays, 2004. **26**(10): p. 1069-75.

192.   Cruise, G.M., D.S. Scharp, and J.A. Hubbell, *Characterization of permeability and network structure of interfacially photopolymerized poly(ethylene glycol) diacrylate hydrogels.* Biomaterials, 1998. **19**(14): p. 1287-94.

193.   Moon, J.J., et al., *Micropatterning of poly(ethylene glycol) diacrylate hydrogels with biomolecules to regulate and guide endothelial morphogenesis.* Tissue Eng Part A, 2009. **15**(3): p. 579-85.

194.   Petrie, T.A., et al., *Integrin specificity and enhanced cellular activities associated with surfaces presenting a recombinant fibronectin fragment compared to RGD supports.* Biomaterials, 2006. **27**(31): p. 5459-5470.

195.   Eliceiri, B.P. and D.A. Cheresh, *The role of alpha v integrins during angiogenesis: insights into potential mechanisms of action and clinical development.* Journal of Clinical Investigation, 1999. **103**(9): p. 1227-1230.

196.   Reyes, C.D., et al., *Biomolecular surface coating to enhance orthopaedic tissue healing and integration.* Biomaterials, 2007. **28**(21): p. 3228-35.

197.   Stendahl, J.C., D.B. Kaufman, and S.I. Stupp, *Extracellular matrix in pancreatic islets: relevance to scaffold design and transplantation.* Cell Transplant, 2009. **18**(1): p. 1-12.

198.   *Peripheral artery disease quick facts.* American Heart Association, 2009.

199.   *Heart Disease & Stroke Statistics -- 2009 Update.* American Heart Association, 2009.

200.   van Weel, V., et al., *Vascular growth in ischemic limbs: A review of mechanisms and possible therapeutic stimulation.* Annals of Vascular Surgery, 2008. **22**(4): p. 582-597.

201.   Hummers, L.K., et al., *Evidence for abnormal angiogenesis in scleroderma patients.* Arthritis and Rheumatism, 2004. **50**(9): p. S630-S631.

202. Annex, B.H. and M. Simons, *Growth factor-induced therapeutic angiogenesis in the heart: protein therapy.* Cardiovascular Research, 2005. **65**(3): p. 649-655.

203. Simons, M., *Angiogenesis - Where do we stand now?* Circulation, 2005. **111**(12): p. 1556-1566.

204. Tongers, J., J.G. Roncalli, and D.W. Losordo, *Therapeutic angiogenesis for critical limb ischemia - Microvascular therapies coming of age.* Circulation, 2008. **118**(1): p. 9-16.

205. Tse, H.F. and C.P. Lau, *Therapeutic angiogenesis with bone marrow-derived stem cells.* Journal of Cardiovascular Pharmacology and Therapeutics, 2007. **12**(2): p. 89-97.

206. Simons, M. and J.A. Ware, *Therapeutic angiogenesis in cardiovascular disease.* Nature Reviews Drug Discovery, 2003. **2**(11): p. 863-871.

207. Phelps, E.A. and A.J. Garcia, *Update on therapeutic vascularization strategies.* Regenerative Medicine, 2009. **4**(1): p. 65-80.

208. Zisch, A.H., M.P. Lutolf, and J.A. Hubbell, *Biopolymeric delivery matrices for angiogenic growth factors.* Cardiovascular Pathology, 2003. **12**(6): p. 295-310.

209. Lutolf, M.P. and J.A. Hubbell, *Synthetic biomaterials as instructive extracellular microenvironments for morphogenesis in tissue engineering.* Nature Biotechnology, 2005. **23**(1): p. 47-55.

210. Lutolf, M.P., et al., *Synthetic matrix metalloproteinase-sensitive hydrogels for the conduction of tissue regeneration: Engineering cell-invasion characteristics.* Proceedings of the National Academy of Sciences of the United States of America, 2003. **100**(9): p. 5413-5418.

211. Zisch, A.H., et al., *Cell-demanded release of VEGF from synthetic, biointeractive cell-ingrowth matrices for vascularized tissue growth.* Faseb Journal, 2003. **17**(13): p. 2260-+.

212. Raeber, G.P., M.P. Lutolf, and J.A. Hubbell, *Molecularly engineered PEG hydrogels: a novel model system for proteolytically mediated cell migration.* Biophys J, 2005. **89**(2): p. 1374-88.

213. Lee, S.H., et al., *Proteolytically degradable hydrogels with a fluorogenic substrate for studies of cellular proteolytic activity and migration.* Biotechnology Progress, 2005. **21**(6): p. 1736-1741.

214.   Gobin, A.S. and J.L. West, *Cell migration through defined, synthetic extracellular matrix analogues.* Faseb Journal, 2002. **16**(3): p. 751-+.

215.   Duvall, C.L., et al., *Quantitative microcomputed tomography analysis of collateral vessel development after ischemic injury.* American Journal of Physiology-Heart and Circulatory Physiology, 2004. **287**(1): p. H302-H310.

216.   Tressel, S.L., et al., *Angiopoietin-2 stimulates blood flow recovery after femoral artery occlusion by inducing inflammation and arteriogenesis.* Arterioscler Thromb Vasc Biol, 2008. **28**(11): p. 1989-95.

217.   Couffinhal, T., et al., *Mouse model of angiogenesis.* Am J Pathol, 1998. **152**(6): p. 1667-79.

218.   Rocha, F.G., et al., *The efffect of sustained delivery of vascular endothelial growth factor on angiogenesis in tissue-engineered intestine.* Biomaterials, 2008. **29**(19): p. 2884-2890.

219.   Sun, Q.H., et al., *Sustained vascular endothelial growth factor delivery enhances angiogenesis and perfusion in ischemic hind limb.* Pharmaceutical Research, 2005. **22**(7): p. 1110-1116.

220.   Ehrbar, M., et al., *Cell-demanded liberation of VEGF(121) from fibrin implants induces local and controlled blood vessel growth.* Circulation Research, 2004. **94**(8): p. 1124-1132.

221.   Cazalis, C.S., et al., *C-terminal site-specific PEGylation of a truncated thrombomodulin mutant with retention of full bioactivity.* Bioconjugate Chemistry, 2004. **15**(5): p. 1005-1009.

222.   Lutolf, M.P., et al., *Synthetic matrix metalloproteinase-sensitive hydrogels for the conduction of tissue regeneration: engineering cell-invasion characteristics.* Proc Natl Acad Sci U S A, 2003. **100**(9): p. 5413-8.

223.   Kloxin, A.M., et al., *Mechanical properties of cellularly responsive hydrogels and their experimental determination.* Advanced Materials, 2010. **22**(31): p. 3484-94.

224.   Zhu, J., *Bioactive modification of poly(ethylene glycol) hydrogels for tissue engineering.* Biomaterials, 2010. **31**(17): p. 4639-56.

225.   Hou, Y., et al., *Photo-cross-linked PDMSstar-PEG hydrogels: synthesis, characterization, and potential application for tissue engineering scaffolds.* Biomacromolecules, 2010. **11**(3): p. 648-56.

226.	Munoz-Pinto, D.J., A.S. Bulick, and M.S. Hahn, *Uncoupled investigation of scaffold modulus and mesh size on smooth muscle cell behavior.* Journal of biomedical materials research. Part A, 2009. **90**(1): p. 303-16.

227.	Zieris, A., et al., *FGF-2 and VEGF functionalization of starPEG-heparin hydrogels to modulate biomolecular and physical cues of angiogenesis.* Biomaterials, 2010. **31**(31): p. 7985-94.

228.	Hermanson, G.T., *Bioconjugate techniques*1996, San Diego: Academic Press. xxv, 785 p.

229.	Hahn, M.S., J.S. Miller, and J.L. West, *Three-dimensional biochemical and biomechanical patterning of hydrogels for guiding cell behavior.* Advanced Materials, 2006. **18**(20): p. 2679-+.

230.	Nemir, S., H.N. Hayenga, and J.L. West, *PEGDA hydrogels with patterned elasticity: Novel tools for the study of cell response to substrate rigidity.* Biotechnol Bioeng, 2010. **105**(3): p. 636-44.

231.	Kloxin, A.M., M.W. Tibbitt, and K.S. Anseth, *Synthesis of photodegradable hydrogels as dynamically tunable cell culture platforms.* Nature protocols, 2010. **5**(12): p. 1867-87.

232.	Rizzi, S.C. and J.A. Hubbell, *Recombinant protein-co-PEG networks as cell-adhesive and proteolytically degradable hydrogel matrixes. Part I: Development and physicochemical characteristics.* Biomacromolecules, 2005. **6**(3): p. 1226-38.

233.	Elbert, D.L. and J.A. Hubbell, *Conjugate addition reactions combined with free-radical cross-linking for the design of materials for tissue engineering.* Biomacromolecules, 2001. **2**(2): p. 430-41.

234.	Fu, Y. and W.J. Kao, *In situ forming poly(ethylene glycol)-based hydrogels via thiol-maleimide Michael-type addition.* Journal of biomedical materials research. Part A, 2011.

235.	Metters, A. and J. Hubbell, *Network formation and degradation behavior of hydrogels formed by Michael-type addition reactions.* Biomacromolecules, 2005. **6**(1): p. 290-301.

236.	Lutolf, M.P. and J.A. Hubbell, *Synthesis and physicochemical characterization of end-linked poly(ethylene glycol)-co-peptide hydrogels formed by Michael-type addition.* Biomacromolecules, 2003. **4**(3): p. 713-22.

237.	Seliktar, D., et al., *MMP-2 sensitive, VEGF-bearing bioactive hydrogels for promotion of vascular healing.* J Biomed Mater Res A, 2004. **68**(4): p. 704-16.

238.	Kim, J., B.K. Wacker, and D.L. Elbert, *Thin polymer layers formed using multiarm poly(ethylene glycol) vinylsulfone by a covalent layer-by-layer method.* Biomacromolecules, 2007. **8**(11): p. 3682-6.

239.	Hiemstra, C., et al., *Novel in Situ Forming, Degradable Dextran Hydrogels by Michael Addition Chemistry: Synthesis, Rheology, and Degradation.* Macromolecules, 2007. **40**(4): p. 1165-1173.

240.	Yu, H., et al., *Synthesis and characterization of three-dimensional crosslinked networks based on self-assembly of α-cyclodextrins with thiolated 4-arm PEG using a three-step oxidation.* Soft Matter, 2006. **2**(4): p. 343.

241.	Hiemstra, C., et al., *Rapidly in Situ-Forming Degradable Hydrogels from Dextran Thiols through Michael Addition.* Biomacromolecules, 2007. **8**(5): p. 1548-1556.

242.	Hu, B.-H., J. Su, and P.B. Messersmith, *Hydrogels Cross-Linked by Native Chemical Ligation.* Biomacromolecules, 2009. **10**(8): p. 2194-2200.

243.	Su, J., et al., *Anti-inflammatory peptide-functionalized hydrogels for insulin-secreting cell encapsulation.* Biomaterials, 2010. **31**(2): p. 308-314.

244.	Mather, B.D., et al., *Michael addition reactions in macromolecular design for emerging technologies.* Progress in Polymer Science, 2006. **31**(5): p. 487-531.

245.	Pratt, A.B., et al., *Synthetic extracellular matrices for in situ tissue engineering.* Biotechnology and bioengineering, 2004. **86**(1): p. 27-36.

246.	Shikanov, A., et al., *Hydrogel network design using multifunctional macromers to coordinate tissue maturation in ovarian follicle culture.* Biomaterials, 2011. **32**(10): p. 2524-31.

247.	Bott, K., et al., *The effect of matrix characteristics on fibroblast proliferation in 3D gels.* Biomaterials, 2010. **31**(32): p. 8454-64.

248.	Patterson, J. and J.A. Hubbell, *Enhanced proteolytic degradation of molecularly engineered PEG hydrogels in response to MMP-1 and MMP-2.* Biomaterials, 2010. **31**(30): p. 7836-45.

249.	Phelps, E.A., et al., *Bioartificial matrices for therapeutic vascularization.* Proc Natl Acad Sci U S A, 2010. **107**(8): p. 3323-8.

250. Zisch, A.H., et al., *Cell-demanded release of VEGF from synthetic, biointeractive cell ingrowth matrices for vascularized tissue growth.* The FASEB journal : official publication of the Federation of American Societies for Experimental Biology, 2003. **17**(15): p. 2260-2.

251. Adelow, C., et al., *The effect of enzymatically degradable poly(ethylene glycol) hydrogels on smooth muscle cell phenotype.* Biomaterials, 2008. **29**(3): p. 314-26.

252. Wacker, B.K., et al., *Endothelial cell migration on RGD-peptide-containing PEG hydrogels in the presence of sphingosine 1-phosphate.* Biophysical journal, 2008. **94**(1): p. 273-85.

253. Peppas, N.A., et al., *Physicochemical, foundations and structural design of hydrogels in medicine and biology.* Annual Review of Biomedical Engineering, 2000. **2**: p. 9-29.

254. Canal, T. and N.A. Peppas, *Correlation between Mesh Size and Equilibrium Degree of Swelling of Polymeric Networks.* Journal of Biomedical Materials Research, 1989. **23**(10): p. 1183-1193.

255. Lu, S.X. and K.S. Anseth, *Release behavior of high molecular weight solutes from poly(ethylene glycol)-based degradable networks.* Macromolecules, 2000. **33**(7): p. 2509-2515.

256. Lutolf, M.P., et al., *Cell-responsive synthetic hydrogels.* Advanced Materials, 2003. **15**(11): p. 888-+.

257. Patterson, J. and J.A. Hubbell, *SPARC-derived protease substrates to enhance the plasmin sensitivity of molecularly engineered PEG hydrogels.* Biomaterials, 2011. **32**(5): p. 1301-10.

258. Lévy, R. and M. Maaloum, *Measuring the spring constant of atomic force microscope cantilevers: thermal fluctuations and other methods.* Nanotechnology, 2002. **13**(1): p. 33-37.

259. Sabass, B., et al., *High Resolution Traction Force Microscopy Based on Experimental and Computational Advances ☆.* Biophysical Journal, 2008. **94**(1): p. 207-220.

260. Tan, J.L., *From the Cover: Cells lying on a bed of microneedles: An approach to isolate mechanical force.* Proceedings of the National Academy of Sciences, 2003. **100**(4): p. 1484-1489.

261. Ouasti, S., et al., *Network connectivity, mechanical properties and cell adhesion for hyaluronic acid/PEG hydrogels.* Biomaterials, 2011. **32**(27): p. 6456-6470.

262. Tibbitt, M.W. and K.S. Anseth, *Hydrogels as extracellular matrix mimics for 3D cell culture.* Biotechnol Bioeng, 2009. **103**(4): p. 655-63.

263. Lin, C.C. and K.S. Anseth, *PEG hydrogels for the controlled release of biomolecules in regenerative medicine.* Pharm Res, 2009. **26**(3): p. 631-43.

264. Fairbanks, B.D., et al., *Photoinitiated polymerization of PEG-diacrylate with lithium phenyl-2,4,6-trimethylbenzoylphosphinate: polymerization rate and cytocompatibility.* Biomaterials, 2009. **30**(35): p. 6702-7.

265. Davis, K.A., J.A. Burdick, and K.S. Anseth, *Photoinitiated crosslinked degradable copolymer networks for tissue engineering applications.* Biomaterials, 2003. **24**(14): p. 2485-95.

266. Nguyen, K.T. and J.L. West, *Photopolymerizable hydrogels for tissue engineering applications.* Biomaterials, 2002. **23**(22): p. 4307-14.

267. Cruise, G.M., et al., *A sensitivity study of the key parameters in the interfacial photopolymerization of poly(ethylene glycol) diacrylate upon porcine islets.* Biotechnol Bioeng, 1998. **57**(6): p. 655-65.

268. Lin, C.C. and K.S. Anseth, *Glucagon-like peptide-1 functionalized PEG hydrogels promote survival and function of encapsulated pancreatic beta-cells.* Biomacromolecules, 2009. **10**(9): p. 2460-7.

269. Weber, L.M., K.N. Hayda, and K.S. Anseth, *Cell-matrix interactions improve beta-cell survival and insulin secretion in three-dimensional culture.* Tissue Eng Part A, 2008. **14**(12): p. 1959-68.

270. Weber, L.M., et al., *PEG-based hydrogels as an in vitro encapsulation platform for testing controlled beta-cell microenvironments.* Acta Biomater, 2006. **2**(1): p. 1-8.

271. Weber, L.M., C.G. Lopez, and K.S. Anseth, *Effects of PEG hydrogel crosslinking density on protein diffusion and encapsulated islet survival and function.* J Biomed Mater Res A, 2009. **90**(3): p. 720-9.

272. Weber, L.M., C.Y. Cheung, and K.S. Anseth, *Multifunctional pancreatic islet encapsulation barriers achieved via multilayer PEG hydrogels.* Cell Transplant, 2008. **16**(10): p. 1049-57.

273.	Narang, A.S. and R.I. Mahato, *Biological and biomaterial approaches for improved islet transplantation.* Pharmacol.Rev, 2006. **58**(2): p. 194-243.

274.	Yun, L.D., N.J. Hee, and Y. Byun, *Functional and histological evaluation of transplanted pancreatic islets immunoprotected by PEGylation and cyclosporine for 1 year.* Biomaterials, 2007. **28**(11): p. 1957-1966.

275.	Wilson, J.T., W. Cui, and E.L. Chaikof, *Layer-by-layer assembly of a conformal nanothin PEG coating for intraportal islet transplantation.* Nano Lett, 2008. **8**(7): p. 1940-8.

276.	Merani, S., et al., *Optimal implantation site for pancreatic islet transplantation.* Br J Surg, 2008. **95**(12): p. 1449-61.

277.	van der Windt, D.J., et al., *The choice of anatomical site for islet transplantation.* Cell Transplant, 2008. **17**(9): p. 1005-14.

278.	Watada, H., *Role of VEGF-A in pancreatic beta cells.* Endocr J, 2010. **57**(3): p. 185-91.

279.	Akirav, E.M., et al., *Glucose and inflammation control islet vascular density and beta-cell function in NOD mice: control of islet vasculature and vascular endothelial growth factor by glucose.* Diabetes, 2011. **60**(3): p. 876-83.

280.	Langlois, A., et al., *Overexpression of vascular endothelial growth factor in vitro using deferoxamine: a new drug to increase islet vascularization during transplantation.* Transplant Proc, 2008. **40**(2): p. 473-6.

281.	Lin, C.C. and K.S. Anseth, *Cell-cell communication mimicry with poly(ethylene glycol) hydrogels for enhancing beta-cell function.* Proc Natl Acad Sci U S A, 2011. **108**(16): p. 6380-5.

282.	Nyqvist, D., et al., *Donor Islet Endothelial Cells in Pancreatic Islet Revascularization.* Diabetes, 2011.

283.	Nyqvist, D., et al., *Donor islet endothelial cells participate in formation of functional vessels within pancreatic islet grafts.* Diabetes, 2005. **54**(8): p. 2287-93.

284.	Chamberlain, M.D., R. Gupta, and M.V. Sefton, *Chimeric vessel tissue engineering driven by endothelialized modules in immunosuppressed Sprague-Dawley rats.* Tissue Eng Part A, 2011. **17**(1-2): p. 151-60.

285.   Szot, G.L., P. Koudria, and J.A. Bluestone, *Murine Pancreatic Islet Isolation.* Journal of Visualized Experiments, 2007(7).

286.   Shapiro, A.M., et al., *Islet transplantation in seven patients with type 1 diabetes mellitus using a glucocorticoid-free immunosuppressive regimen.* N Engl J Med, 2000. **343**(4): p. 230-8.

287.   Shapiro, A.M., *State of the art of clinical islet transplantation and novel protocols of immunosuppression.* Curr Diab Rep, 2011. **11**(5): p. 345-54.

288.   Rees, D.A. and J.C. Alcolado, *Animal models of diabetes mellitus.* Diabet Med, 2005. **22**(4): p. 359-70.

289.   Lim, J.Y., et al., *A fibrin gel carrier system for islet transplantation into kidney subcapsule.* Acta Diabetologica, 2009. **46**(3): p. 243-248.

290.   Christoffersson, G., et al., *Clinical and experimental pancreatic islet transplantation to striated muscle: establishment of a vascular system similar to that in native islets.* Diabetes, 2010. **59**(10): p. 2569-78.

291.   de Souza, Y.E., et al., *Islet transplantation in rodents. Do encapsulated islets really work?* Arq Gastroenterol, 2011. **48**(2): p. 146-52.

292.   Dubois, S., et al., *Glucose inhibits angiogenesis of isolated human pancreatic islets.* J Mol Endocrinol, 2010. **45**(2): p. 99-105.

293.   Tesch, G.H. and T.J. Allen, *Rodent models of streptozotocin-induced diabetic nephropathy.* Nephrology (Carlton), 2007. **12**(3): p. 261-6.

294.   Tay, Y.C., et al., *Can murine diabetic nephropathy be separated from superimposed acute renal failure?* Kidney Int, 2005. **68**(1): p. 391-8.

295.   Kraynak, A.R., et al., *Extent and persistence of streptozotocin-induced DNA damage and cell proliferation in rat kidney as determined by in vivo alkaline elution and BrdUrd labeling assays.* Toxicol Appl Pharmacol, 1995. **135**(2): p. 279-86.

296.   Chen, V. and C.D. Ianuzzo, *Dosage effect of streptozotocin on rat tissue enzyme activities and glycogen concentration.* Can J Physiol Pharmacol, 1982. **60**(10): p. 1251-6.

297.   Hara, Y., et al., *Influence of the numbers of islets on the models of rat syngeneic-islet and allogeneic-islet transplantations.* Transplant Proc, 2006. **38**(8): p. 2726-8.

298.   Wojtowicz, A.M., et al., *Coating of biomaterial scaffolds with the collagen-mimetic peptide GFOGER for bone defect repair.* Biomaterials, 2010. **31**(9): p. 2574-82.

299.   Petrie, T.A., et al., *Multivalent integrin-specific ligands enhance tissue healing and biomaterial integration.* Sci Transl Med, 2010. **2**(45): p. 45ra60.

300.   Shekaran, A. and A.J. Garcia, *Extracellular matrix-mimetic adhesive biomaterials for bone repair.* J Biomed Mater Res A, 2011. **96**(1): p. 261-72.

301.   Shekaran, A. and A.J. Garcia, *Nanoscale engineering of extracellular matrix-mimetic bioadhesive surfaces and implants for tissue engineering.* Biochim Biophys Acta, 2011. **1810**(3): p. 350-60.

302.   Wirkner, M., et al., *Triggered cell release from materials using bioadhesive photocleavable linkers.* Adv Mater, 2011. **23**(34): p. 3907-10.